LABORATORY INVESTIGATION OF DENSE NON-AQUEOUS PHASE LIQUID (DNAPL) PARTIAL SOURCE ZONE REMEDIATION USING COSOLVENTS

By

ANDREW JOSEPH KAYE

A THESIS PRESENTED TO THE GRADUATE SCHOOL
OF THE UNIVERSITY OF FLORIDA IN PARTIAL FULFILLMENT
OF THE REQUIREMENTS FOR THE DEGREE OF
MASTER OF ENGINEERING

UNIVERSITY OF FLORIDA

2006

ACKNOWLEDGMENTS

Primary thanks go to my advisor, Dr. Mike Annable, and committee member Dr. Jim Jawitz for their support, encouragement, and guidance during the many months of laboratory experiments and for thinking of me when they had extra football or basketball tickets. Additional thanks go to my third committee member, Dr. Joe Delfino, for his helpful edits and comments while writing my thesis. Finally, I would especially like to thank Dr. Jaehyun Cho for his endless assistance, his positive attitude, and for being fun to work with during my countless hours in the lab.

TABLE OF CONTENTS

page

LIST OF TABLES

LIST OF FIGURES

LIST OF ABBREVIATIONS

DNAPL	Dense non-aqueous phase liquid
NAPL	Non-aqueous phase liquid
PCE	Tetrachloroethylene
TCE	Trichloroethylene
MCL	Maximum contaminant levels
PITT	Partitioning tracer test
BTC	Breakthrough curve
LTV	Light transmission visualization
GC	Gas chromatography
RA	Reagent alcohol
EL	Ethyl-lactate
ND	Neutral density
SF	Single-flushing
MF	Multiple-flushing
PV	Pore volume
DI	Distilled ionized
MeOH	Methanol
TBA	Tert butyl alcohol
2,4 DMP	2,4 dimethyl 3 pentanol
S_N	NAPL saturation
η	Porosity
SSA	Solubility scaled approach

MR	Mass reduction
FR	Flux reduction

Abstract of Thesis Presented to the Graduate School
of the University of Florida in Partial Fulfillment of the
Requirements for the Degree of Master of Engineering

LABORATORY INVESTIGATION OF DENSE NON-AQUEOUS PHASE LIQUID (DNAPL) PARTIAL SOURCE ZONE REMEDIATION USING COSOLVENTS

By

Andrew Joseph Kaye

December 2006

Chair: Michael D. Annable
Major Department: Environmental Engineering Sciences

There are hundreds of thousands of commercial, military, and industrial sites across the country where chemical wastes cause contamination to groundwater. Some of the more challenging sites to clean up contain contaminants as dense non-aqueous phase liquids (DNAPLs). There is currently no consensus in the academic, technical and regulatory communities on the ecological or environmental impacts of DNAPL source zone treatment. While many in-situ technologies have shown the ability to remove a significant portion of the contaminant mass, none are able to remove all of it from the source zone.

This study investigates the benefits of partial source zone removal using cosolvent flushing. The benefits were assessed by characterizing the relationship between reductions in DNAPL mass and the corresponding reduction in contaminant mass discharge in several laboratory scale experiments. Also, the effects of fluid override and underride associated with cosolvent flushing on the mass reduction (MR) vs. flux reduction (FR) relationship were investigated. The results indicate a model with $\beta > 1$ may be a good approximation of the MR vs. FR relationship using enhanced dissolution by the cosolvents in systems with similar degrees DNAPL and media heterogeneity. Also, the override and underride associated with cosolvents did not significantly affect their remediation.

CHAPTER 1
BACKGROUND AND INTRODUCTION

Introduction

The objective of this work is to develop a scientifically defensible approach for assessing the long-term environmental impacts (benefits) of dense non-aqueous phase liquid (DNAPL) partial source zone remediation compared to no source removal. Six controlled laboratory experiments were performed to characterize the functional relationship between DNAPL architecture, mass removal and contaminant mass flux under well-defined heterogeneous aquifer conditions by quantifying the reduction in contaminant flux due to partial removal of DNAPL source zones.

The type of DNAPL source zone remediation technology utilized in these experiments was cosolvent solubilization or cosolvent flushing. Three unique cosolvent mixtures were each tested in two different experiments in a two-dimensional heterogeneous aquifer model. Accounting for spatial heterogeneity of both media and DNAPL saturation is critical to the study of source zone removal. Two-dimensional flow chamber experiments allow for the emplacement of heterogeneous distributions of porous media and contaminants as opposed to a simplified combination of homogeneous media and homogeneous DNAPL that is much less representative of more complex field conditions. Tetrachloroethylene (PCE) was used as a model compound because of its ubiquity as an environmental contaminant and its relatively low aqueous solubility compared to other DNAPL contaminants. A lower-solubility DNAPL is preferred for enhanced dissolution laboratory experiments to minimize source zone depletion during water flow.

Research Motivation

On a global scale, over 90% of available potable fresh water is located as groundwater. Prior to the environmental awareness movement that occurred in the United States in the 1970s,

there was little regard for the disposal of chemicals and organic compounds in the ground or on the ground surface. This type of pollution is much less common now that people have become aware of the public health issues related to groundwater contamination. Still, large amounts of contaminants that were disposed in the past act as a source for groundwater contamination plumes that have spread with time. There are hundreds of thousands of commercial, military, and industrial sites across the country where chemical wastes cause contamination to subsurface materials including groundwater (National Research Council, 2004). Although many hazardous waste sites have been cleaned up since the enactment of the Superfund regulations of the 1980s, many sites contain contaminants that pose significant challenges to site remediation and long term site management. Some of the more challenging sites contain chlorinated solvents that are present as DNAPLs. Today, chlorinated solvents are by far the most prevalent organic contaminants in groundwater and one of the most difficult to clean up (Stroo et al., 2003). Chlorinated hydrocarbons, such as trichlorethylene (TCE) and PCE, are found at approximately 80% of all Superfund sites with groundwater contamination and more than 3000 Department of Defense sites in the United States (U.S. Environmental Protection Agency, 1997).

Non-aqueous phase liquids (NAPLs) below the ground surface slowly dissolve into groundwater and contaminate it for years or even decades as the water slowly flows by. Locating these NAPL sources of pollution is difficult since even a small amount of NAPL can contaminate comparatively very large volumes of water (Pope, Jin, Varadarajan, Rouse, and Sepehrnoori, 1994).

These chemicals have low water solubility and tend to remain in the subsurface as a separate liquid phase. The distribution of DNAPL in the subsurface is typically sparse and highly heterogeneous. They are denser than water and tend to migrate downward through the

soil and groundwater and collect on less permeable layers where they spread out until connecting with courser media and continuing downward (MacKay and Cherry, 1989). The groundwater region in which DNAPL is present as a separate phase, either as randomly distributed sub-zones at residual saturations or "pools" of accumulation above confining units is defined as the source zone (MacKay and Cherry, 1989; Feenstra, Cherry, and Parker, 1996). DNAPL source zones serve as long-term sources of contamination to groundwater and can result in significant down gradient dissolved plumes of contamination.

Aquifer contamination by DNAPLs poses risks to both humans and the environment. The approaches for managing risk at DNAPL contaminated sites can be generalized as plume management approaches and source-zone remediation (Fure, Jawitz, and Annable, 2006). The plume management approach, in which the risk is mitigated by management or containment of the dissolved plume, has been utilized at many DNAPL sites. However, because of the persistence of the source zone, maintenance and operational costs associated with this approach can be tremendous. Therefore, the second approach, removal of the source zone, is an attractive alternative.

It has been demonstrated that ~65–90% of the NAPL mass can be removed from source zones by implementing aggressive in-situ remediation technologies, such as surfactant or cosolvent flooding (Rao et al., 1997; Jawitz, Annable, Rao, and Rhue, 1998b; Jawitz, Sillan, Annable, Rao, and Warner, 2000; Brooks et al., 2004). These studies have shown that while a significant fraction of the DNAPL mass can be removed in a short period, the efficiency of DNAPL extraction often decays exponentially with increasing mass removal (U.S. EPA, 2003). Unfortunately, due to the complex entrapment architecture and challenging aspects of source zone characterization, complete removal of the source zone by in-situ technologies is not yet an

option (Soga, Page, and Illangasekare, 2004). This poses the question: What are the benefits of partial source zone remediation?

There is currently no consensus in the academic, technical and regulatory communities on the ecological or environmental impacts of DNAPL source zone treatment (U.S. EPA, 2003). Assessing the performance of a particular source zone remediation technology should not be limited to meeting certain regulatory goals such as maximum contaminant levels (MCLs). Achieving MCLs in the source zone is beyond the capabilities of current available in-situ technologies in most geologic settings (U.S. EPA, 2003). Also, measurements within the source zone would not allow for a mixing or buffer zone as in surface water MCL regulations. Therefore, a more realistic regulatory approach that considers alternate or intermediate performance goals and phased remedial action approaches to cleanup contaminated sites would be appropriate (U.S. EPA, 2003). This would encourage stake holders to seek alternatives to plume management at sites where source zone remediation is deemed to be a more efficient approach. The reduction in DNAPL source zone mass is expected to provide the following benefits: a reduction in risk; a decrease in source longevity; lower operation and maintenance costs due to a decrease in the need for site monitoring and care; shorter time for plume management; and an increase in natural attenuation (Sale and McWhorter, 2001). Recent modeling studies have predicted decreases in mass flux, source longevity, and associated maintenance costs with partial source removal (Falta, Rao, and Basu, 2005a; Falta, Basu, and Rao, 2005b; Jawitz, Fure, Demmy, Berglund, and Rao, 2005).

Site Characterization

Before a remediation technology can be implemented at a particular site, the source zone and down gradient contaminant plume must be well-characterized. NAPL site characterization

involves determining the NAPL location, volume or mass, composition, and mass discharge. Characterization is essential for safe, efficient, and cost effective clean up (Pope et al., 1994).

Source Zone Assessment by Partitioning Inter-Well Tracer Test

Traditional methods for characterizing the NAPL in the subsurface are invasive, requiring soil cores or other disturbance of the subsurface. These offer only a point measurement and require interpolation to estimate NAPL characteristics. An attractive alternative for successful NAPL characterization is the use of partitioning inter-well tracer tests (PITTs) which sample much larger volumes of the subsurface. Adapted from technology developed in the oil industry, PITTs provide an integrated measure of the NAPL in the flow field and are seen as non-invasive because less soil coring is required. The selected tracers partition into the NAPL phase with predictable or measurable relationships. From these measurements, it is possible to determine the NAPL quantity present in the tracer flow field (Annable et al., 1998).

The partitioning tracer method is based on liquid-liquid partitioning theory. This theory was first established in the chromatography field in 1941 (Brusseau, Nelson, and Costanza-Robinson, 2003). Tracers are chemicals that can be added to fluids at small but measurable concentrations and follow the fluid pathways while not affecting the fluid properties. The PITT consists of the simultaneous injection of several tracers into injection wells and the measurement of tracer concentrations as they discharge through production wells. Typically, one non-partitioning tracer and several partitioning tracers with differing partitioning coefficients are injected and measured. Partitioning refers to the distribution of tracer between the water phase and the NAPL phase. The water phase is considered the mobile phase because the tracer flows with the same velocity as the water. When the tracer is in the residual NAPL phase, it remains stationary. The net result is that the partitioning tracer lags behind the non-partitioning tracer.

The separation between the non-partitioning tracer and partitioning tracer breakthrough curves (BTCs) can be related to the amount of NAPL in the flow field.

Jin et al. (1995) described in detail the theory of moments used to obtain a characterization of the NAPL. The partitioning coefficient describes how a particular tracer will behave in the subsurface. Tracers with higher partitioning coefficients will partition more into the NAPL phase and will lag further behind the non-partitioning tracer. The simplest approach to describe a tracer partitioning is a linear relationship:

$$K_{Nw} = \frac{C_N}{C_w} \tag{1-1}$$

where C_N is the tracer concentration in the NAPL phase, C_w is the tracer concentration in the aqueous phase, and K_{Nw} is the NAPL-water partitioning coefficient. Values of K_{Nw} for particular tracers are typically calculated in laboratory tests. The average travel times are calculated from the method of moments (Jin et al., 1995; Annable et al., 1998; Jawitz, Annable, Demmy, and Rao, 2003). The *N*th absolute moment (M_N) of a distribution is described by:

$$M_N = \int_0^\infty t_N C(t) dt \tag{1-2}$$

The first normalized moment (μ_1) is determined by dividing M_1 by M_o:

$$\mu_1 = \frac{\int_0^\infty tC(t)dt}{\int_0^\infty C(t)dt} \tag{1-3}$$

One half of the tracer pulse duration (t_o) was subtracted from the first normalized moment to get the *i*th tracer mean arrival time, τ_i:

$$\tau_i = \mu_1 - \frac{t_0}{2} \tag{1-4}$$

The retardation factor *(R)* is used to determine the average NAPL saturation in the flow field of a well. It is calculated as the ratio of average travel times for the partitioning tracer pulse (τ_p) and the non-partitioning tracer pulse *(τ_n)*.

$$R = 1 + \frac{K_{Nw} S_N}{(1 - S_N)} = \frac{\tau_p}{\tau_n} \tag{1-5}$$

Equation 1-5 can be rearranged to solve for the average NAPL saturation percent *(S_N)* in the tracer flow field:

$$S_N = \frac{R - 1}{(R - 1) + K_{Nw}} \tag{1-6}$$

The effective pore volume *(V_e)* swept by the tracers can be calculated for an individual pumping well using the first temporal moment or average travel time of the non-partitioning tracer, $t_{n,i}$.

$$V_{e,i} = Q_i t_{n,i} \tag{1-7}$$

where Q_i is the pumping rate from pumping well, *i*. Finally, the total NAPL volume in the swept zone or flow field of each pumping well is calculated by:

$$V_{N,i} = \frac{S_N V_{e,i}}{1 - S_N} \tag{1-8}$$

Partitioning tracers should be chosen so that the separation between their BTC peaks is measurable. Annable et al. (1998) stated other desirable tracer characteristics, including: non-hazardous, non-toxic, non-degrading, low volatility, reasonable cost and availability, and easily quantifiable especially in the presence of numerous NAPL constituents. Typically, alcohols act as good tracers because they can meet these criteria. Longer chain alcohols results in a larger retardation. Methanol acts as a non-partitioning tracer that stays in the groundwater mobile

phase. Higher chain alcohols such as hexanol, 2,4-dimethyl-3-pentanol, and 2-octanol behave as good partitioning tracers, particularly for PCE contaminated sites.

Contaminant Mass Discharge

Proper site characterization is important to determine the risks posed by a specific DNAPL source zone. The risk to a down-gradient receptor has less to do with the mass of DNAPL in the source zone than with the amount of contamination leaving the site. This contaminant flux is highly dependent upon the hydrogeologic conditions. One of the alternative metrics for judging the performance of source zone remediation is contaminant mass discharge. Unlike simple point measurements from groundwater wells, it is the summation at a point in time of multiple point values of contaminant mass flux (mass per time per area) along a vertical control plane encompassing the plume and perpendicular to the mean groundwater flow direction at a location down-gradient of the DNAPL source zone (U.S. EPA, 2003). There have been several new technologies recently developed for assessing the in-situ mass flux and applied at the field scale level. These include the passive flux meter technology (Hatfield, Annable, Cho, Rao, and Klammler, 2004; Annable et al., 2005; Basu, Rao, Poyer, Annable, and Hatfield, 2006) and the integral pump test method (Bockelmann, Ptak, and Teutsch, 2001). Measurement of contaminant mass flux before and after a remediation technology has been applied in the source zone can be a useful metric for judging the technology performance.

Mass Reduction Versus Flux Reduction

The relationship of mass reduction and flux reduction in DNAPL contaminated sites has been modeled by many researchers recently (Rao and Jawitz, 2003; Parker and Park, 2004; Jawitz et al., 2005; Falta et al., 2005a,b; Enfield et al., 2005; Wood et al., 2005; Basu et al., 2006). This relationship is described in Equation 1-9, and shown in Figure 1-1 where fractional mass reduction (1-M/Mo) is plotted against fractional flux reduction (1-C/Co).

$$\left(1-\frac{C}{C_o}\right)=\left[1-\frac{M}{M_o}\right]^{1/\beta} \tag{1-9}$$

Conditions where very large mass reductions are required to create significant flux reduction ($\beta<<1$) are considered unfavorable and were obtained in a theoretical homogeneous aquifer (Sale and McWhorter, 2001). In 2-D heterogeneous physical models, aqueous dissolution experiments determined that NAPL architecture was the primary control of the mass reduction, flux response relationship and showed that a heterogeneous DNAPL contamination in heterogeneous medium lead to a near 1:1 mass reduction vs. flux reduction relationship (Fure et al., 2006).

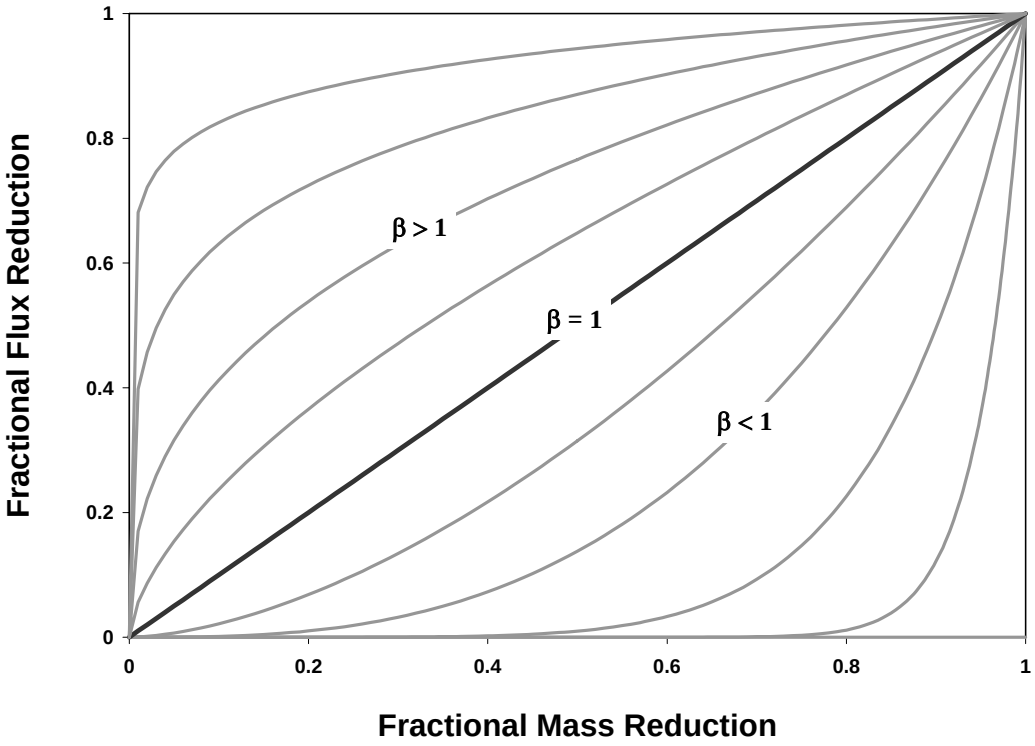

Figure 1-1. Fractional mass reduction versus fractional flux reduction relationship described by Equation 1-9 with different β values.

CHAPTER 2
MATERIALS AND METHODS

Materials

Six cosolvent solubilization experiments were conducted in a two-dimensional flow chamber packed with porous media and contaminated by tetrachloroethylene (PCE) (ACRŌS spectrophotometric grade, 99+%). PCE was used in all of the experiments because of its ubiquity as an environmental contaminant and its relatively low aqueous solubility compared to other common dense non-aqueous phase liquid (DNAPL) contaminants.

Flow Chamber

The design of the flow chamber was similar to that used in previous studies (Jawitz, Annable, and Rao, 1998a; Fure et al., 2006). The chambers were constructed using two 5.5 mm thick glass sheets set around a 41 cm high by 61 cm long frame of 1.3 cm square aluminum tubing. The frame enclosed the chamber on three sides with the top remaining open. The two vertical sections at either end acted as integrated injection and extraction wells and were slotted to a width of 0.03 cm at a frequency of 4 slots per cm. The aluminum tubing was attached with epoxy to one of the glass plates and 0.95 cm wide weather stripping was placed on the tubing. The second glass sheet was placed onto the weather stripped frame and secured using 13 large 1" capacity binder clips. The epoxy and weather stripping increased the total width of the chamber to 1.5 cm. Glass sheets were used on both sides of the chamber so that light transmission visualization (LTV, e.g., Niemet and Selker, 2001) could be utilized.

The integrated injection and extraction wells were each constructed with three ports located 3 cm, 17 cm, and 31 cm from the bottom of the vertical section (i.e., the top of the bottom piece of tubing). On each well, these ports were connected via 0.32 cm Teflon tubing to a series of valves that allowed for injection to or extraction from any single port alone, any two

ports simultaneously, or all three ports simultaneously. On the injection end, Teflon tubing connected the valves to a constant head reservoir. The reservoir used during water injection was a 20 L Marriott bottle. A 1 L and 4 L Marriott bottle served as the reservoirs during tracer and cosolvent injection. On the extraction end, Teflon tubing connected the valves to a piston pump (Fluid Metering Corp. "Q" Pump) which continuously extracted effluent from the chamber. Effluent samples were analyzed for eluted PCE and alcohol tracers using a Gas Chromatography (GC, Perkin-Elmer Autosystem) in-line sampling method (Jawitz, Annable, Clark, and Puranik, 2002). A flame-ionization detector (FID) was used in the analysis for all effluent samples. The GC column used for this study was a 30 meter × 0.530 mm, 3 um fixed phase, DB-624 column (J&W Scientific). Figure 2-1 shows a schematic of the experimental setup.

Porous Media

As with similar studies performed by our group, Accusand (Unimin Minnesota Corp.), a translucent porous media, was used for all of the experiments (Fure et al., 2006). All of the media originated from the Ottawa Plant in Lesueur, MN. The sizes of media used in these experiments were 20/30, 40/50, and 50/70. The particle diameter (d_{50}), the saturated hydraulic conductivity (K_{SAT}), and intrinsic permeability (k_i) of the 20/30 and 40/50 mesh sand are located in Table 2-1. The domain estimated value is based on the assumption that 90% of the flow field was in the 20/30 sand and 10% was in the 40/50.

Cosolvents

The cosolvents used in the experiments were reagent alcohol (RA) (Fisher Scientific; 90.5% Ethanol, 4.5% Methanol, 5.0% Iso Propyl Alcohol) and ethyl-lactate (EL) (VertecBio 99%). Three different cosolvent mixtures (50% RA/50% Distilled Ionized (DI) water; 40% EL/60% DI water; and 18% RA/26% EL/56% DI water) were used in two separate experiments, for a total of six experiments. The cosolvent mixtures were volume based. The three mixtures

will be referred to as 50% RA, 40% EL and Neutral Density (ND) respectively. The physical and chemical properties of these cosolvent mixtures are presented in Table 2-2. The densities and the PCE solubility of the fluid mixtures were measured in the lab. The mixtures were chosen because they have similar PCE solubility, but significantly different densities. The resulting buoyancy effects were expected to be reflected by different horizontal flooding behavior.

Flow and Contaminant Visualization

To help visualize fluid flow in the chamber, either the displacing fluid or resident fluid was dyed. The dye used should have low sorption to the media, have a low toxicity, and for studies investigating density effects, must be clearly visible at concentrations low enough that the density of the fluid is not significantly altered (Jawitz et al. 1998a). Similar to Jawitz et al. (1998a), Erioglaucine A (Fluka) or brilliant Blue dye was used because it met all of the criteria. However, concentrations used in these studies were lower than those used by Jawitz et al. (1998a) because the use of light transmission visualization (LTV) aided in the visualization of less intense colors.

The PCE was also dyed to aid visualization. Prior to injection, it was dyed using Oil Red O (FisherBiotech, Electrophoresis Grade) at a concentration of approximately 50 mg/L.

Tracers

Partitioning inter-well tracer tests (PITTs) were performed after the PCE was spilled in the flow chamber. Both partitioning and non-partitioning tracers were used. The non-partitioning tracers were methanol (MeOH) (Fisher Scientific HPLC Grade 99.9%) and tert-butyl alcohol (TBA) (ACRŌS, 99.5%). The partitioning tracers were hexyl alcohol (hexanol) (ACRŌS, 98%), 2,4 dimethyl-3-pentanol (2,4 DMP) (Aldrich, 99%) and 2-octanol (ACRŌS, 98%).

Experimental Methods

Porous Media Packing

Sand was introduced into the flow chamber using a funnel connected to a rigid plastic tube. Approximately 5 cm of standing water was maintained as the sand was introduced. A 1.5 cm layer of 50/70 sand was placed at the bottom of the chamber in direct contact with the aluminum tubing. This layer was emplaced to prevent contact between the separate phase PCE and the aluminum tubing or the weather-stripping. It was feared that contact with the aluminum tubing could somehow change the PCE properties. Also, free phase PCE could partition into the weather-stripping, or could dissolve the epoxy and cause leaks in the chamber. A metal rod was used to agitate the sand to remove any trapped air and to shape the bottom layer to ensure that it had a very slight slope away from each well. Above the 50/70 layer, the chamber was packed with discrete layers of 40/50 sand inserted into otherwise homogeneous 20/30 sand. As the sand built up, the metal rod was again used to shape and agitate the 20/30 sand to maintain its homogeneity. The rod was used to shape the 40/50 layers and tapping of the glass helped to smooth and settle the 40/50 layers before more 20/30 sand was placed above.

When the height of the packed sand reached approximately 28 cm, a deflected point non-coring septum penetration needle (Popper & Sons Inc.) was mounted onto a frame that held the chamber and positioned so that the tip was just into the sand and centered between the two glass plates. Then the sand was packed above the needle to a height of about 33 cm. An electric massager was pressed against the glass and moved around to vibrate the chamber and tightly pack the sand. The porosity within the flow chamber based upon the non-reactive tracers was approximately 0.35. The porosities of the 20/30 and 40/50 measured by Schroth, Ahearn, Sekler, and Istok, (1996) ranged from 0.33 to 0.35.

A strip of one-inch wide Teflon tape was placed along the top of the sand and along the portion of the screened wells that were exposed above the sand. Approximately 5 cm of Benseal grouting bentonite clay was packed on top of the tape. The purpose of the Teflon tape was to minimize the contact between the flushing solution (cosolvents and tracers) in the porous media or the wells and the clay layer which helped to prevent or minimize any volatile losses of PCE. Note that over the course of this study, the flow chamber was disassembled, cleaned, and re-packed several times. Each time the chamber was re-packed, care was taken to replicate the layering in the first pack.

Pre-Contaminant Spill Flushing

Nearly identical steady-state flow conditions were established prior to initiating each experiment. The constant head reservoir at the inlet was fixed to maintain a steady water level in the well. The pump at the effluent end was used to establish steady-state conditions by pumping at a constant rate for several hours. This rate was maintained at approximately 5.5 mL/min or a Darcy flow of 1.6 m/day. While this is approximately an order of magnitude higher than most natural systems, these rates were deemed necessary to conduct several experiments with a range of fluid properties. Issues of non-equilibrium partitioning were considered. An experiment was conducted in which the flowrate with a newly contaminated chamber was varied from approximately 0.7 mL/min to approximately 12 mL/min, a range of about 0.2 m/d to 3.5 m/d, for 10 pore volumes (PVs) at each flowrate. The data from this experiment, Figure A-1 in the Appendix, suggests that the PCE concentration was approximately 20% higher for at the lowest flow rate (0.7 mL/min) compared to the concentration at the highest flow rate (12 mL/min). The concentration at 0.7 mL/min was only about 10% higher than the concentration at 6 mL/min. Therefore, a flowrate close to 6 mL/min was assumed to have minimal non-equilibrium issues and it would allow the set of experiments to be completed within a reasonable amount of time.

The flowrate was monitored at the effluent by measuring the volume of water collected in a 25 mL graduated cylinder over a period of time, usually 3 or 4 minutes and adjusted accordingly. After the chamber was packed, more than five PVs of water were flushed through the chamber to establish steady conditions before beginning the experiment.

Dye Tracer Displacement Experiment

A dye tracer experiment, in which dyed water was used to displace colorless water, was performed to determine if the flow within the system was uniform. As expected, the flow through the less permeable lenses was slower than the water flow through the courser background sand, but due to the nature of the permeability distributions in the chamber and to a degree, mixing of stream tubes, the overall flow through the chamber was nearly plug flow. These tests were mainly performed to confirm the absence or presence of dead zones, where the water was not flowing. If dead zones existed, the box was disassembled, cleaned, and repacked. Dead zones only occurred in situations where several weeks had elapsed between solvent floods and bio-films or mineral deposits may have clogged the slots of the influent well. The dye tracer tests were also performed to ensure that there were no significant high flow areas. The major area of concern was between the top of the sand and the Teflon tape.

Cosolvent Flushing Experiments

Two types of flushing experiments were performed with each cosolvent mixture: (1) a single flushing of cosolvent designed to remove approximately 90% of the initial PCE mass; and (2) multiple flushing of cosolvent intended develop a functional relationship between mass reduction and flux reduction. In the multiple-flushing experiments a pulse of cosolvent was injected that was intended to remove only a portion of PCE mass and was followed by several pore volumes of water. Then, more pulses of cosolvent and water were injected until approximately 90% of the mass was removed.

Other than the type of flushing (single or multiple), the overall experimental procedure was similar for all experiments. First, the NAPL was injected. Then, a PITT was performed. Aqueous steady-state flow conditions were established. Then, the cosolvent mixture was injected either a single or multiple times. Steady-state flow conditions were established after cosolvent flushing. Then, the remaining PCE in the chamber was removed to complete a mass balance. The following sections describe in more detail the procedures used in each step towards completion of an experiment.

Non-aqueous phase liquid (NAPL) injection

A 20 mL, gas tight syringe was filled with 10 mL of Oil-Red-O dyed PCE and connected via a Teflon tube to the injection needle already positioned in the 20/30 sand. A syringe pump (Harvard Apparatus Syringe Infusion Pump 22) was used to inject the PCE at a rate of 0.5 mL/min. Based on experiments in similar systems, it was expected that the NAPL migration and distribution would be exclusive to the 20/30 sand and that pools would form above the 40/50 lenses and the 50/70 layer (Oostrom, Hofstee, Walker, and Dane, 1999; Taylor, Pennell, Abriola, and Dane, 2001, Fure et al., 2006). The Darcy velocity during PCE injection was about 1.6 m/day. There was no noticeable effect on the NAPL distribution due to the water flow. The slopes of the top of the 40/50 sand lenses were the greatest factors in determining the DNAPL distributions.

Effluent monitoring

The flow chamber effluent continuously flowed to a modified GC sampling tray (Jawitz et al., 2002). A 0.5 μL sub-sample was injected to the GC at a user defined interval. The time between samples was the time required for the GC to analyze an individual sample (17 to 18 minutes). This time was chosen because it was important to closely monitor the PCE concentration to best estimate contaminate mass removal and contaminant flux reduction. The

inline system was used during cosolvent flushing, aqueous flushing, and during the PITT. The effluent from the inline system dripped through an activated carbon filter and was collected in 10 L hazardous waste containers for disposal by University of Florida Environmental Health and Safety.

Partitioning inter-well tracer tests (PITTs)

After the PCE was spilled, but before the PITT began, several PVs of DI water were flushed through the chamber to establish steady-state flow conditions. The tracer mixture was prepared and thoroughly mixed overnight and was transferred to a 1 L Marriott bottle which served as the tracer mixture reservoir. The NAPL water partitioning coefficients (K_{NW}) of the partitioning tracers and the approximate concentration of each tracer in the tracer mixture are located in Table 2-3. Before the tracer was injected, three sub-samples of the mixture were analyzed in the GC to measure the initial concentrations (Co) of the individual tracers in the mixture. To inject the tracer mixture, the influent was switched to the tracer reservoir with the same constant head as the water reservoir. While the tracer was being injected, the chamber effluent was collected and the volume was measured. This volume was assumed to be equivalent to the injected tracer volume. In each PITT, approximately 200–250 mL of tracer mixture were injected, followed by 6–8 PVs of DI water. The flowrate during the PITT was maintained at approximately 5.5 mL/min, or a Darcy velocity of 1.6 m/day.

Aqueous dissolution

During aqueous dissolution, steady-state conditions were established by maintaining a flow rate of approximately 5.5 mL/min for several PVs. It was important to have the same steady-state flow rate and pore-water velocity during all aqueous flow experiments so that the relative PCE concentrations could be used to estimate the flux reduction.

Prior to flushing the chamber with cosolvent, the initial aqueous PCE concentration was determined. These measurements were taken towards the end of each PITT following multiple PVs of water flooding. During the PITT, the PCE concentrations tended to increase for the first two to three PVs because of its increased solubility in the tracer mixture.

After flushing with cosolvent, at least 10 PVs of DI water were flushed through the chamber before the aqueous PCE concentrations were measured.

Single-flushing experiments

In the single-flushing experiments, the cosolvent mixture was continuously flushed through the contaminated flow chamber to achieve more than 90% mass removal. The Darcy velocity during cosolvent flushing was approximately 1.3 m/d. Steady-state aqueous concentrations and mass fluxes were measured both before and after the source zone removal. After aqueous flushing, the remaining mass was removed to complete a mass balance. After all of the contaminate mass had been removed from the chamber, the flow characteristics were tested using a dye tracer. If the characteristics were favorable (i.e., no dead zones) PCE was injected into the media and a new experiment was started; If they were unfavorable, the chamber was taken apart, cleaned, and repacked.

Multiple-flushing experiments

In the multiple-flushing experiments, the cosolvent flushing duration was limited so that only a portion of mass was removed. The remaining DNAPL source zone spatial distribution and corresponding integrated down-gradient contaminant mass flux were measured under steady-state aqueous conditions. Then, additional cosolvent was injected to further reduce the contaminant mass, and again, the steady-state aqueous contaminant mass flux was measured. This process was repeated until approximately 90% of the total mass was removed or the initial mass flux was reduced by more than 90%. The goal was to have either four or five consecutive

injections that would achieve approximately 20%, 40%, 60%, 80%, and above 90% total contaminant mass removal and to measure the aqueous steady-state contaminant mass flux at each step. After the initial mass or flux was reduced by more than 90%, the remaining mass was removed to complete a mass balance.

Fluid injection and extraction

Because of buoyancy effects, displacing ethanol (in this case, RA) solutions tend to override water during horizontal flooding (Jawitz et al., 1998a). Due to the same effects, displacing EL solutions tend to underride water during horizontal flooding. Therefore, it was important to strategically inject and extract the cosolvent mixtures to ensure there was no stratification within the wells or the chamber during flushing.

For example, to minimize override effects the 50% RA cosolvent mixture was injected in the bottom port only, and during its injection, the resident water was only extracted from the bottom extraction well port. This limited the override of the 50% RA and is similar to practices in the field (Jawitz et al., 2000). The same procedure was used to limit water override of resident 40% EL cosolvent. It was noted that the 40% EL cosolvent would remain in the flow chamber for a longer period of time if other extraction ports were also open.

To minimize underride effects of a more dense fluid displacing a less dense fluid, the more dense fluid was injected in the top port and the resident fluid was extracted from the top and middle ports. Examples of this include water displacing 50% RA cosolvent and 40% EL cosolvent displacing water. Once a displacing fluid (either water or cosolvent) occupied approximately 95% of the pore space, both the influent and effluent ports were all opened until a different fluid was introduced. The ND cosolvent mixture was neutrally buoyant with water, so it was injected to and extracted from all open ports.

Residual mass removal

The PCE that remained in the chamber after the cosolvent flushing phase of the experiment was removed using a 50% EL / 50% DI water cosolvent mixture. This mixture was chosen because the majority of the remaining PCE was usually in pools at the bottom of the flow chamber. This mixture is denser than water and has a higher PCE solubility (approximately 25,000 mg/L) than the mixtures used in the flushing experiments. A spacer was placed in the influent and effluent well between the top port and the middle port. Several PVs of 50% EL were injected in the middle and bottom port and DI water was injected in the top port. The effluent was extracted from the bottom port only. Within the flow chamber, a layer of DI water stayed above the cosolvent which flowed underneath. This focused the cosolvent on the contaminated area only (the bottom pools), and minimized the waste of flushing through areas that were already clean (Jawitz et al., 2000). Instead of being pumped to the GC, the effluent was collected in a 4 L or 20 L glass container. The 4 L container was used in the beginning when concentrations were expected to be high. The 20 L container was used to collect a larger volume. The openings of the containers were sealed using Teflon tape and Parafilm ® to minimize PCE volatile losses. The total volume collected was measured and five sub-samples were taken from the well-mixed effluent and analyzed in the GC to estimate the residual mass that had been removed.

Image Processing

Digital images were taken during the experiments using a mounted Canon PowerShot S200 Digital Elph, a 2.0 mega-pixel digital camera. The images were 1200 x 1600 resolution. For the purposes of this thesis, the images provide qualitative information of the NAPL distribution before, during and after cosolvent flushing. Also, they showed the displacing fluid front for semi-quantitative analysis of the fluid override and underride. The images were

processed using Adobe Photoshop to increase the color differential between the dyed PCE or dyed fluid and the translucent porous media. The processing involved two main steps in Photoshop: First, a copy of the image was transferred to black and white. Then, the dyed fluid of interest, either the Oil Red O dyed PCE or a Brilliant Blue dyed displacing fluid was selected from the color image and copied onto the black and white image as a separate layer. In the resulting image, the contrast between the dyed fluid and the translucent media was enhanced and thus was more visually apparent.

Table 2-1. Porous media properties

	20/30	40/50	Domain estimated
d_{50} (mm)[a]	0.713 ± 0.023	0.359 ± 0.010	
K_{SAT} (cm/min)[a]	15.02	4.33	13.95
k_i (cm^2)	2.28E-06	6.58E-07	2.12E-06

[a] Schroth et al., 1996

Table 2-2. Fluid properties

	Water	50% RA	40% EL	ND mixture
Density, ρ (g/cm^3)	1.000	0.89	1.014	1.001
Viscosity (cp),	0.895[b]	2.386[a,b]	2.238	2.369
PCE Solubility, C_{MAX} (mg/L)	150[b]	10,003	8,881	8,850

[a] Van Valkenberg, 1999
[b] Lide, D.R. and Frederikse, H.P.R., 1996

Table 2-3. Tracer properties

	MeOH	TBA	n-hexanol	2,4 DMP	2-octanol
K_{NW}	-	-	6.7	26	110
Conc. (mg/L)	1560	1120	800	800	320

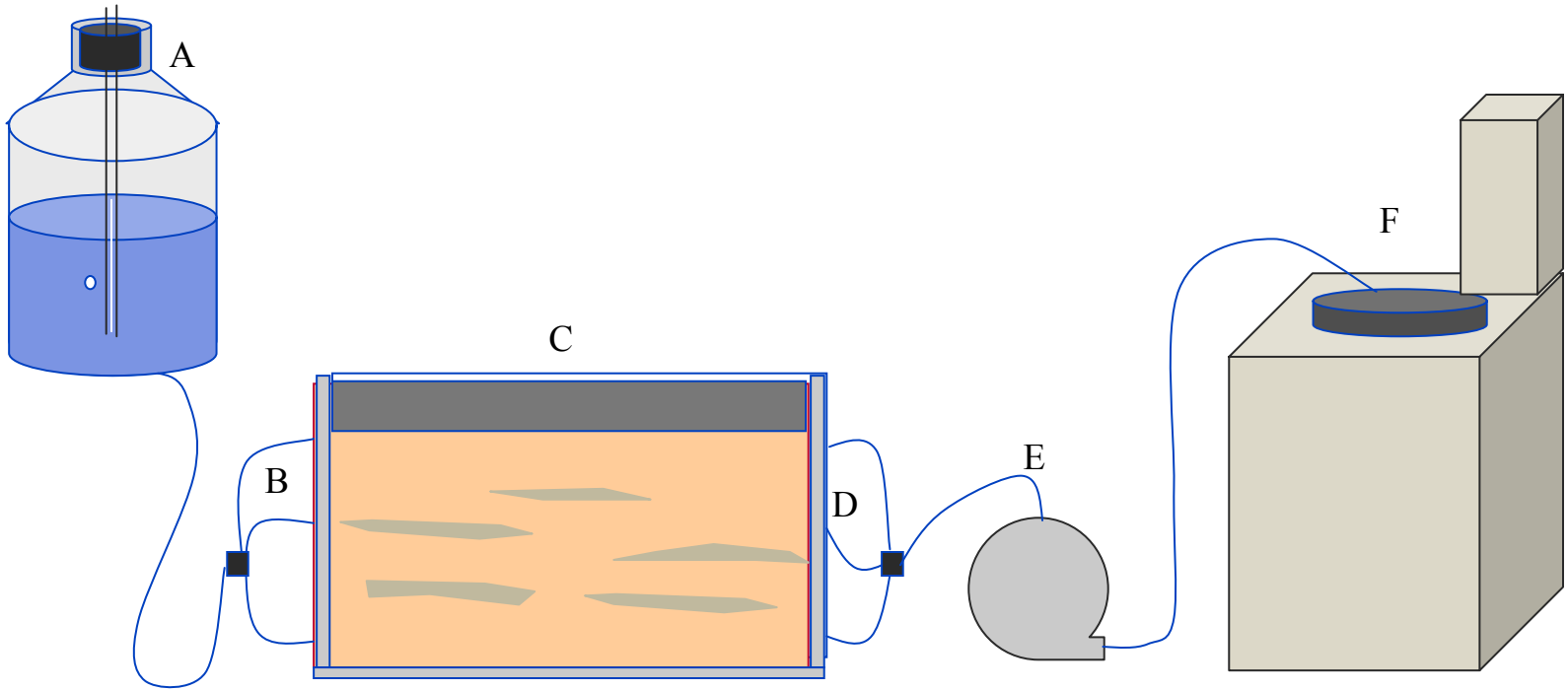

Figure 2-1. Schematic of the experimental setup. The process flow is from left to right. A) Constant head reservoir. B) Tubing, valves and influent well. C) 2-dimensional flow chamber. D) Effluent well, valves, and tubing. E) Piston pump. F) In-line gas chromatography.

CHAPTER 3
EXPERIMENTAL RESULTS AND DISCUSSION

Results

Dense Non-Aqueous Phase Liquid (DNAPL) Spill

Figure 3-1 provides a series of pictures depicting a typical dense non-aqueous phase liquid (DNAPL) spill in the two-dimensional flow chamber. Because it has a higher density (1.62 g/cm^3) than water, the tetrachloroethylene (PCE), which was dyed red, migrated downward through the saturated media. As it migrated, entrapped residual DNAPL was held in pore spaces by capillary forces or as films coating the media (Bradford, Rathfelder, Lang, and Abrioal, 2003). When the infiltrating DNAPL encountered the less permeable lenses of 40/50 sand it tended to accumulate in pools and spread laterally due to contrasting capillary entry pressure (Bradford, Abriola, and Rathfelder, 1998). Thus, the DNAPL migration and distribution was exclusive to the higher permeability 20/30 sand. This was expected based observations reported in similar systems (Oostrom et al., 1999; Taylor et al., 2001, Fure et al., 2006). In an aged system, the DNAPL may slowly migrate into the less permeable zones through wetting property changes (Bradford et al., 2003), but these experiments were not designed to represent an aged system.

The results of the spill were a heterogeneous DNAPL distribution with both residual phase and pooled phases of PCE in the flow field. The last picture in the series, taken at approximately 50 minutes after beginning PCE injection, was a good representation of the initial DNAPL distribution for all of the experiments except ND-MF (Note: The 50% reagent alcohol (RA), 40% ethyl-lactate (EL), and neutral density (ND) cosolvent single-flushing experiments will be known as RA-SF, EL-SF, and ND-SF, respectively. The multiple-flushing experiments will be known as RA-MF, EL-MF, and ND-MF, respectively.)

The heterogeneous media was constructed to promote PCE flow over both sides of the top lens followed by a cascade down the other lenses finally forming a pool at the bottom of the chamber. However, as shown in Figure 3-2, during the ND-MF PCE spill, the PCE only flowed down one side of the top lens and formed a relatively larger pool at the bottom of the chamber since a smaller fraction of the DNAPL release volume was retained as residual above the lenses and as pools on the lenses. The implications of this will be discussed later.

Partitioning Inter-Well Tracer Test (PITT)

The partitioning inter-well tracer tests (PITTs) in these experiments had a different purpose than what they are typically used for in the field. In the field, PITTs are used to estimate the NAPL volume with the tracer flow field. However, in these experiments, the NAPL volume was already known. Instead, the PITTs were performed to predict the mass reduction (MR) vs. flux reduction (FR) relationship of the system using higher temporal moments (Jawitz et al., 2003). However, this analysis has yet to be performed and was mentioned as future work in Chapter 4. For comparison purposes and proof of concept, the results presented were the estimated NAPL volume, pore volume, and porosity.

The breakthrough curves (BTCs) of the PITTs of the RA-SF and RA-MF experiments that were measured by the in-line gas chromatography (GC) system (Jawitz et al., 2002) are shown in Figures 3-3 and 3-4 respectively. The BTCs of the PITTs of the other experiments are located in the Appendix as Figures A-2–A-5. The in-line measurements are indicated by the marker representing the specific tracer. The entire BTC was not measured using the in-line system because extensive tailing was expected for a heterogeneous media with non-uniform non-aqueous phase liquid (NAPL) distributions (Jawitz et al., 2000). Measurement of the tail would have taken another 10–15 PVs of fluid flow in which a significant portion of the initial PCE mass would have been removed. However, extrapolation of the tracer BTC tails was critical for

estimating the NAPL volume, so the BTC tails were extrapolated to 10^{-4} using a log-log relationship. On the figures, the lines through the respective data points of each tracer represent this extrapolation. Typically, the BTCs are extrapolated by a log-linear relationship (Annable et al., 1998; Jawitz et al., 2000; Brooks et al., 2002). However, the log-log extrapolation appeared to more closely fit the curvature of the in-line data and it produced better tracer mass recovery percentages. The mass recovery percentages based on the log-log extrapolated curves of the tracers in of all the experiments are located in Table 3-1.

The extrapolated BTCs of the non-partitioning tracers were analyzed using the method of moments to estimate the pore volume (PV) and the partitioning tracers were used to estimate the NAPL saturation (S_N) within the flow field. Together, the tubing and well volume was approximately 75 mL. This volume was subtracted from the estimate by the non-partitioning tracers to calculate the PV of the chamber. The calculated PV, S_N values, and NAPL volumes are presented in Table 3-2 and in Figures A-6, A-7, and A-8 in the Appendix. The results indicate that the PV and S_N estimates of the ND-MF experiment deviate from the other experiments where the PV and S_N estimations are relatively consistent. The average PV, S_N, and NAPL volume estimates were calculated both including and disregarding ND-MF which had a relatively higher PV and a lower S_N estimation.

Since the ND-MF PV estimation deviated from the other experiments (Figure A-6 in the Appendix) it was ignored for the porosity and NAPL volume estimations. Disregarding ND-MF, the average PV estimation by methanol (MeOH) and tert-butyl alcohol (TBA) were 1079 mL and 1071 mL respectively. Given the dimensions of the flow chamber (61 cm long, 33 cm high, and 1.5 cm wide) the porosity (η) can be estimated from Equation 3-1:

$$\eta = \frac{V_V}{V_T} \tag{3-1}$$

where V_T is the total volume including both solids and voids and V_V is the volume of the voids, or the PV. Taking the average of the MeOH and TBA PV estimation, the η of the flow chamber was approximately 0.356. This is a reasonable value considering the η of well sorted sand or gravel ranges from about 0.25–0.5 (Fetter, 2001) and the measured η of the 20/30 and 40/50 sand by Schroth et al., (1996) ranged from 0.33–0.35.

The average NAPL volume estimation by the partitioning tracers n-hexanol and 2,4 DMP, 12.9 mL and 10.9 mL respectively, were higher than the actual NAPL volume injected (10 mL), whereas the average NAPL volume estimation of 2-octanol was lower at 9.0 mL. A log-linear extrapolation of the tracer BTCs did not significantly (~5–10%) reduce the NAPL volume estimate of n-hexanol and 2,4 DMP, however, it did significantly reduce the NAPL volume estimation of 2-octanol by approximately 20%.

The NAPL volume estimations by tracers in ND-MF were significantly lower than in the other experiments. This was because the NAPL distribution formed a large pool at the bottom of the chamber with less NAPL mass as residual or pooled phase above the higher lenses. Therefore, the contact area between the NAPL and the flow field of the partitioning tracers was reduced, thus reducing the NAPL volume estimation. These results are similar to those observed in other 2-dimensional systems with relatively large fractions of the NAPL in pools (Jalbert, Dane, and Bahaminyakamwe, 2003).

Figures showing the individual tracer BTCs plotted as a function of volume of flow through the chamber for the different experiments are attached in the Appendix as Figures A-9–A-13. They show that the individual tracer BTCs of ND-MF tended to be different than the tracer BTCs of the other experiments. For example, the n-hexanol BTC of ND-MF in

Figure A-11 was significantly shorter than the rest of the experiments, indicating that the differing NAPL distribution had a significant impact on the tracer S_N prediction.

Miscible Fluid Displacement

Figures 3-5 and 3-6 show the behavior of the cosolvents displacing water and water displacing cosolvents, respectively. These figures were created by tracing the dyed fluid front, which was enhanced by the light transmission visualization (LTV) system, at different times.

Figure 3-5 shows how the cosolvent displacement of water differed for each mixture. The 50% RA tended to override the water, while the 40% EL tended to underride the water, and there was close to a plug flow displacement of water by the ND cosolvent. The mixing zone of the displacing front of all the cosolvents was approximately 2 cm. The 50% RA nearly reached the bottom of the chamber after 1.5 PVs. However, based on the effluent cosolvent concentrations, it is estimated that it did not completely displace the water at the bottom of the chamber until approximately 2 PVs had been injected. The 40% EL never completely displaced the resident water during the experiment; water remained in the top effluent corner of the chamber after almost 7 PVs of cosolvent had been injected. However, the 40% EL front reached all of the PCE contaminated areas, both residual and pooled, after only about 1.2 PVs. The angle from the horizontal of the 50% RA mixture override approached zero with continued cosolvent injection, while the angle from the horizontal made by the 40% EL mixture underride of the water stayed nearly constant from approximately 0.5 to 7 PVs.

Figure 3-6 shows the differences in the water displacement of the resident cosolvent mixtures. The water tended to underride the 50% RA, override the 40% EL, and exhibited significant fingering during the displacement of the ND cosolvent. The mixing zone of water displacing 50% RA and 40% EL was approximately 2 cm. The last measurement of the water underride of the 50% RA mixture was taken at just over 2 PVs but the 50% RA had not been

completely displaced. Based on the effluent data, there was less than 1% RA in the effluent after about 2.5 PVs of water had been injected indicating that the RA had been essentially displaced. However, because of the underride, water displaced the 50% RA near the bottom of the chamber after only 0.5 PVs and it had displaced the cosolvent within all of the initially PCE contaminated areas after approximately 1.5 PVs. Because water overrides the 40% EL and the DNAPL tends to pool at the bottom of the chamber, the 40% EL mixture remained in the contaminated zones much longer than the 50% RA after beginning water injection. Based on the effluent data, 4 PVs of water flowed through the chamber before there was less than 1% EL in the effluent.

Significant fingering due to viscosity differences occurred when water displaced the neutral density cosolvent mixture. This made it difficult to assess the mixing zone thickness. There was less than 1% of the ND cosolvent in the effluent after 3 PVs of water was injected. A probable explanation for the ND cosolvent remaining in the chamber longer than the 50% RA is that ND cosolvent in the 40/50 mesh lenses took longer to be displaced. The ND cosolvent displacement from the lenses by the water was horizontal and along the longest length of the lens rather than a semi vertical displacement of the 50% RA by water across a much shorter lens length caused by the water underride.

The fluid behavior during miscible displacement can also be predicted by the following set of equations. Similar to Jawitz et al. (1998a), the density (ρ) and dynamic viscosity (μ) of the flushing fluids can be used along with the media intrinsic permeability (k_i) to evaluate the miscible displacement of two fluids within the flow chamber. The ratio of the dynamic viscosities of the resident fluid (μ_r) and the displacing fluid (μ_d) fluids is known as the mobility ratio (M) (Slobod and Lestz, 1960; Jawitz et al., 1998a):

$$M = \frac{\mu_r}{\mu_d} \tag{3-2}$$

Viscous fingering is expected when the viscosity of the displacing fluid is less than that of the resident fluid (i.e., $M > 1$). In these experiments, M is greater than 1 when the water is used to displace the cosolvents as in Figure 3-6. Jawitz et al. (1998a) noted a study by Crane, Kendall, and Gardner (1963) in which miscible displacements where both the density and viscosity varied, showed that as the density differences between the fluids increases from zero, the displacement instabilities change from viscous fingering to override or underride in which gravity forces dominate. The density difference between the ND mixture and water is nearly zero, but the density contrast between the 50% RA and water and the 40% EL and water are larger (Table 2-2). The ratio of viscous to gravity forces is described by:

$$R_{v/g} = \left(\frac{q\mu_r}{k_i g \Delta\rho} \right) \left(\frac{L}{Z} \right) \tag{3-3}$$

where q is the Darcy flux, k_i is the media intrinsic permeability, g is the gravitational constant, $\Delta\rho$ is the density difference between the two fluids, L is the length of the system, and Z is the height. Jawitz et al. (1998a) also noted that the data presented by Crane et al. (1963) indicated that for relatively small mobility ratios (approximately $M < 10$), the ratio of viscous to gravity forces, must be very large (approximately $R_{v/g} > 100$) to produce displacements dominated by viscous forces. Therefore, viscous fingering dominated in the case of water displacing ND because the density difference was nearly zero and $R_{v/g}$ was very large. Density dominated instabilities occurred when the 50% RA or 40% EL was displaced by water because the density difference increased from zero and $R_{v/g}$ was below 100.

Jawitz et al. (1998a) goes on to describe a previously proposed theory to calculate the tilt angle of the interface between the two fluids of different densities in a two-dimensional flow system. In a horizontal displacement, the angle, β, between the fluid interface and the horizontal can be calculated from:

$$\tan \beta = \frac{q \Delta \mu}{kg \Delta \rho} \tag{3-4}$$

For fluid override, β will be between 0˚ and 90˚ and for fluid underride, β will be between 90˚ and 180˚. The calculated values for M, $R_{v/g}$, and β and measured values of β for the miscible fluid displacements during the single-flushing experiments are presented in Table 3-3. When the cosolvents are used to displace the resident water (Figure 3-5), $M < 1$ and there was no miscible fingering. The neutrally buoyant cosolvent mixture had approximately plug flow displacement of water with a slight override. However, there was differential advection during this displacement due to the presence of the less permeable lenses. In the experiments with either 50% RA or 40% EL cosolvents, the injected solution would tend to either override or underride the resident fluid because of density/buoyancy effects. Since $R_{v/g}$ was not very large (i.e., $R_{v/g} < 100$) the gravitational forces tended to dominate. However, $R_{v/g}$ is very large when water was used to displace the resident ND cosolvent, and viscous fingering occurred.

The measured values of β when cosolvent displaced water (Figure 3-5) were estimated at approximately 0.3 PV, 0.85 PV, and 0.4 PV for 50% RA, ND cosolvent, and 40% EL respectively. The measured values of β when water displaced cosolvent (Figure 3-6) were estimated at approximately 0.4 PV, 0.2 PV, and 0.4 PV for 50% RA, ND cosolvent, and 40% EL respectively. The measured values of β were similar to the calculated values for the 40% EL and ND cosolvent experiments. However, they were relatively less accurate for both of the 50% RA displacements and the water displacement of 40% EL. This was because the length of the flow chamber was not sufficient to allow the angle to reach a stable value and was similar to the observations of Jawitz et al. (1998a). The boundary conditions of the effluent well influenced the override or underride angle in the 50% RA experiments and in the water displacement of

40% EL. In an infinitely long chamber, the measured and calculated values of β would likely be the same.

In the single-flushing experiments, as described in Chapter 2, a cosolvent mixture was injected until approximately 90% of the mass was removed. However, in the multiple-flushing experiments, the amount of cosolvent injected was limited so that only a portion of the mass would be removed. Since pulses of the cosolvent were injected, the override and underride effects were magnified because the override and underride occurred each time the injection fluid was switched. For the multiple-flushing experiments, it was expected that this increased override and underride would have a negative effect on the PCE flux reduction (FR), in the sense that, for a given mass reduction (MR), the FR was expected to be lower for the multiple-flushing experiments than for the single-flushing experiments.

Cosolvent Experiments: Single-Flushing

In Figure 3-7, a single injection of 50% RA is used to remediate the PCE source zone. Only the 50% RA sequence is shown in this chapter; however, Figures A-18 and A-20 in the Appendix show the single-flushing experiments for the 40% EL and ND mixtures, respectively. On each image, the total volume of cosolvent injected into the chamber at the time the image was taken is displayed in the upper right hand corner. The first image (0 PV) is the initial distribution of PCE. After approximately 2.7 PVs of the cosolvent had been injected, most PCE mass that had been removed was from the residual portions above the lenses. Also, the cosolvent had just reached the bottom of the chamber because of override, so as of 2.7 PVs, the bottom pool and residual above the bottom pool appear relatively unchanged. However, at 3.3 PVs, the cosolvent had removed much of the residual above the bottom pool. Towards the end of the injection, only pools of PCE remained above the top lens and at the bottom of the chamber. The cosolvent

injected between 6.1 and 8.6 PVs removed most of the PCE above the top lens, however, removed relatively little from the bottom pool.

Figure 3-8 shows the accumulating fractional MR for a given amount of cosolvent injected in the single-flushing experiments. The solid line represents mass removed during cosolvent flushing and the dashed line represents mass removed during post-cosolvent water flushing when the cosolvent concentration in the effluent was < 1%. Approximately 8.6 PVs, 6.4 PVs, and 7.0 PVs of cosolvent were injected for RA-SF, EL-SF, and ND-SF respectively. Figure 3-9 shows the PCE and cosolvent BTCs of the single-flushing experiments. During the single injection of 40% EL, the mass was removed more quickly than the 50% RA or the ND cosolvent even through the PCE solubility was slightly lower in the 40% EL (Table 2-2). The 40% EL tended to underride the water. Therefore, it contacted the relatively larger pool of PCE containing a significant amount of the PCE mass at the bottom of the chamber after fewer PVs than the other cosolvent mixtures and removed the pooled mass more quickly. Figure A-18, located in the Appendix, shows that more of the PCE near the bottom of the chamber was removed after fewer PVs with 40% EL flushing than with 50% RA (Figure 3-7) or ND cosolvents (Figure A-20). The location of the PCE removal by the ND cosolvent was similar to the 50% RA experiments.

Cosolvent Experiments: Multiple-Flushing

Figure 3-11 is a sequence of images showing the PCE distribution during the 50% RA multiple-flushing experiment. Only the 50% RA sequence is shown in this chapter; however, Figures A-19 and A-21 in the Appendix show the multiple-flushing experiments for the 40% EL and ND mixtures, respectively. In Figure 3-11, the top image shows the initial distribution of PCE. The rest of the images show the PCE distribution after each cosolvent flood. The total PVs of cosolvent injected after each flood is located in the upper right hand corner of the

respective image. After the first and second floods, a majority of the residual PCE in the top half of the chamber had been removed and primarily pools remained. Similar to the single-flushing experiment with 50% RA, the residual PCE above the bottom pool was relatively unchanged. A little over 1 PV of 50% RA was injected in each the first and second flood, therefore, based on Figure 3-5, the cosolvent front never reached the bottom pool and may have just reached the residual PCE above the pool.

The PCE above the top lens was completely removed after the third flood, whereas it was never removed in the single-flushing experiment. This is because in the multiple-flushing experiments, the repeating cosolvent override and water underride behavior caused significantly more 50% RA cosolvent to flow through the upper half of the chamber than the bottom half. In contrast, because of the repeating cosolvent underride during the 40% EL multiple-flushing experiment, significantly more cosolvent flowed through the bottom half of the chamber than the top half.

Figure 3-12 shows the accumulating fractional mass removal during the multiple-flushing experiments. Five separate injections were performed with the 40% EL and the ND cosolvents, but there were only four injections of the 50% RA. When the slope of the accumulating mass removal line on the chart was steep (> 45˚), cosolvent was flushing through the chamber. The mass removal line flattened when water was flushing through the system because water has a low PCE solubility and thus, removes less fractional mass. In the first flushing of the RA-MF and ND-MF, about 1 PV of the respective cosolvent was injected, whereas, in the first injection of the EL-MF experiment, only about 0.5 PV of 40% EL was injected. Although the cosolvent mixtures had approximately the same PCE solubility, from Figure 3-12, the fractional mass removal by the first injection of 50% RA was significantly larger than the fractional mass

removal by the other flushing solutions. The fractional mass removed by the first 40% EL flush was lower because only about half as much cosolvent was injected. But why was the fractional mass removal so much less for the ND-MF experiment first injection if the cosolvent volume injected was nearly the same? Recall that in the ND-MF experiment, the DNAPL distribution differed by having a significant amount of PCE in pools at the bottom of the chamber, rather than distributed as residual above the lenses or as smaller pools on top of the lenses. Pools of PCE have significantly less surface area than residual ganglia (Totten, 2005), therefore, there is less contact and interaction with the cosolvent, reducing the ability of the cosolvent to solubilize the PCE and remove the mass. Also, recall that when the water displaced the resident ND cosolvent in the chamber, there was significant fingering. This could have reduced the strength of the ND cosolvent such that its PCE solubility was reduced.

After the first injection, the trends in the RA-MF and EL-MF fractional mass reduction look similar. The differences between their fractional mass remoavl at a given PV were mostly caused by differing amounts of cosolvent injected in each flush and differing amounts of water injected after each flush. Approximately 6.7, 5.0, and 8.8 total PVs of cosolvent were injected in RA-MF, EL-MF, and ND-MF respectively. The repeating underride during EL-MF allowed the mass at the bottom of the chamber to be removed with less fluid injected, and the repeating override during RA-MF helped remove the mass above the upper lenses more quickly, whereas the mass was removed more evenly during the ND-MF experiment.

Aqueous Flushing Results

The average aqueous PCE concentrations were calculated from the inline GC measurements. Before cosolvent flushing, the standard deviation of the inline aqueous PCE concentration data tended to be higher than after flushing. In the multiple-flushing experiments as the aqueous PCE concentrations declined the standard deviation tended to as well. Figure

3-13 is inline measurements taken during aqueous flushing for a single-flushing experiment, RA-SF, and Figure 3-14 is the aqueous PCE concentrations taken during a multiple-flushing experiment, RA-MF. Figures showing the inline aqueous PCE dissolution data for the 40% EL and ND cosolvent experiments can be found in Figures A-14–A-17 the Appendix.

The average aqueous concentrations were estimated from the solid data points only. The initial average aqueous PCE concentrations ranged from about 98–143 mg/L for the experiments with similar NAPL distribution. The initial aqueous concentration of ND-MF was lower at approximately 81 mg/L. The pre and post-cosolvent flushing average aqueous PCE concentrations are located in Table 3-4 for the single-flushing experiments and in Table 3-5 for the multiple-flushing experiments. The reported standard deviations (STDEV) were calculated only from the values used to estimate the averages.

Discussion

Estimating Mass Reduction (MR)

Because the injected mass was known, the fractional mass reduction (MR) during the experiments could be estimated by calculating the accumulated mass at any point in time. This accumulated mass was calculated from the effluent concentration data collected by the in-line system, knowing both the concentration and the time between sub-samples. The MR estimation was relative only to the mass present in the flow chamber just prior to initiating cosolvent flushing. So, in all of the experiments, the mass removed during pre-flushing aqueous dissolution and during the PITT were subtracted from the total mass obtained for the mass balance to estimate the mass in the chamber before flushing. This value was used as the total mass for estimating the fractional MR.

The inline system extracted sub-samples from the continuously flowing effluent every 17 to 18 minutes. For each time step, the average PCE concentration (mg/L) of the current sub-

sample (C_i) and the previous sub-sample (C_{i-1}) was multiplied by the volume of effluent (mL) between the samples. Thus the integrated mass (mg) of PCE removed during each time step was known. Accumulating the masses from all previous time steps gave an estimation of the total mass of PCE that was removed after each injection. The volume of effluent between each sub-sample was estimated knowing the time between samples and the measured flowrate. There were over 500 samples taken during each experiment therefore, from Brooks and Wise (2005) the coefficient of variation, defined as the ratio of standard deviation to measurement value, of the zeroth moment calculation was < 2%.

Estimating Flux Reduction (FR)

In most cases, given the available technologies, the contaminate mass can not be completely removed from the subsurface. But, there can be benefits of removing a portion of the mass. For these experiments, the contaminant mass flux ($M/T/L^2$) of the chamber effluent was measured during both aqueous dissolution and cosolvent dissolution. In a similar system utilizing aqueous dissolution, Fure et al. (2006) showed that the relationship between fractional MR and fractional flux reduction (FR) could be approximated by a 1:1 relationship, or $\beta = 1$.

In terms of aqueous flushing, the single-flushing experiments yield only one data point on a MR vs. FR graph: the post-flushing MR and FR as shown in Figure 3-15. Table 3-4 shows the aqueous based pre-flushing and post-flushing PCE concentrations, the cumulative MR, and the aqueous based post-flushing FR for the single-flushing experiments. However, it would be much more beneficial to know the path to that point that occurred during cosolvent flushing (i.e., $\beta = 1$, $\beta < 1$, or $\beta > 1$ as described in Chapter 1).

The multiple-flushing experiments were developed as a way to create the MR vs. FR relationship for cosolvents. The FR was based on the steady-state aqueous PCE concentrations measured after each flushing compared to the initial steady-state concentration. Table 3-5 shows

the aqueous based pre-flushing and post-flushing PCE concentrations and their standard deviations, the cumulative MR, and the aqueous-based post-flushing FR for the multiple-flushing experiments. The error associated with the flux reduction was based on error propagation for division with standard deviations (Lindberg, V., 2000).

The multiple flushes resulted in a total of 4 or 5 points on the MR vs. FR graph for each experiment, and the path could be estimated by connecting the points. Figure 3-16 shows the points obtained on the MR vs. FR graph for the multiple-flushing experiments. The repeating override and underride associated with multiple injections of 50% RA and 40% EL resulted in a lower than expected MR vs. FR (i.e., $\beta < 1$ rather than $\beta = 1$) after the first and second flushing of 50% RA and 40% EL up to approximately 0.6 fractional MR.

Multiple injections of the ND cosolvent were expected to show different results than the multiple injections of 50% RA or 40% EL. Because it has no override or underride, the MR vs. FR relationship in the ND-MF experiment was expected to more closely approximate the single-flushing experiment paths. However, the initial distribution of PCE in the ND-MF experiment differed from all of the other experiments so it could not be justified as the path of the single-flushing experiments. The different initial PCE distribution resulted in a unique MR vs. FR response as shown in Figure 3-16. In the ND-MF experiment, the FR increased greatly after about 0.2 fractional MR, but did not increase after about 0.6 fractional MR. Figure A-21, in the Appendix, shows that nearly all of the PCE mass other than that located in the large pool at the bottom of the chamber had been removed after the 4th flushing of ND cosolvent. After the 5th flushing, in which nearly 3 PVs of ND cosolvent was flushed through the chamber, there was less than 0.1 additional fractional MR and essentially no additional FR. This indicated that the

maximum benefits (i.e., maximum FR) that could be efficiently achieved using the ND cosolvent under these circumstances were reached after removing approximately 0.6 of the fractional mass.

Path Estimation by the Solubility Scaled Approach (SSA)

A second method was also utilized to estimate the MR vs. FR path based on the single-flushing experiments. It will be referred to as the solubility scaled approach (SSA). In the SSA, the FR for each sub-sample was based on the relative difference between the initial normalized PCE concentration during aqueous flushing and the normalized PCE concentration of each sub-sample during cosolvent flushing. The normalized PCE concentration (C_N) of any sub-sample was calculated from Equation 3-5:

$$C_N = \frac{C_{PCE}}{C_{MAX}} \tag{3-5}$$

where C_{PCE} is the PCE concentration of the sub-sample and C_{MAX} is the solubility of PCE at the measured cosolvent concentration of the sample. The FR was calculated from Equation 3-6:

$$FR = \frac{C_{No} - C_{Ni}}{C_{No}} \tag{3-6}$$

where C_{No} was the initial normalized PCE concentration during aqueous pre-flushing and C_{Ni} is the normalized PCE concentration a sub-sample, *i*, during cosolvent flushing.

For each cosolvent mixture, there is a unique relationship between the PCE solubility and the cosolvent concentration. Figure 3-10 shows the PCE solubility of ethanol (Van Valkenberg, 1999) and ethyl-lactate at different percentages. It was assumed that the RA solubility could be approximated by the ethanol solubility curve and the ethyl-lactate data was measured in the lab. The percent ethanol and ethyl-lactate PCE solubility curves were fit using a 2nd order polynomial for 0–20% cosolvent and a 3rd order polynomial for 20–50% cosolvent. The percent neutral density PCE solubility curve was measured in the laboratory and fit using a 2nd order polynomial

for 0–40% ND cosolvent and a 3rd order polynomial for 40–100% ND cosolvent. These curves are located in the Appendix as Figures A-22–A-27.

Figure 3-17 shows the MR vs. FR paths estimated by the SSA using the inline data of the single-injection experiments. The paths of the SSA did not lead directly to the values for aqueous based MR vs. FR end points which lie nearly on top of the 1:1 line; however, the paths end within approximately 10% of the aqueous FR. The paths do not end at the same MR because additional mass was removed while establishing steady-state aqueous dissolution after cosolvent flushing. The paths of the single-flushing experiments that were estimated by the SSA all follow the same favorable trend above the 1:1 line, indicating that there are benefits of partial source zone remediation using cosolvents in similar systems. For a given MR value, the FR calculated for all of the cosolvent mixtures are within 20% of one another. Also, this indicates that the override and underride associated with a single injection of cosolvent did not greatly influence the MR vs. FR relationship.

When the two data sets (single-flushing and multiple-flushing) of each cosolvent are overlaid as in Figure 3-18, the single-flushing curve lies above the multiple injection curve in the case of 50% RA and 40% EL. This is an indication that the increased override and underride of the multiple injections caused a less favorable flux reduction response. However, the ND-MF experiment favors the $\beta > 1$ side of the graph after 40% of the mass was removed and is relatively closer to the single-flushing paths than the other multiple-flushing experiments. A likely explanation for this goes back to the initial NAPL distribution. In all of the other experiments, the NAPL distributed over both ends of the top lens and there were more residual areas. In the case of the ND-MF experiment, the NAPL only went down one end of the top lens and created a larger pool of NAPL on the bottom layer of the chamber. Therefore there was less

residual PCE and it was removed more quickly and thus, reduced the integrated flux more quickly with less mass removal. The fact that the MR vs. FR relationship of the ND-MF experiment showed a different behavior than the other experiments and that the media heterogeneities were similar, indicate that the DNAPL distribution had a greater effect on the MR vs. FR response than the buoyancy or viscosity characteristics of the cosolvents.

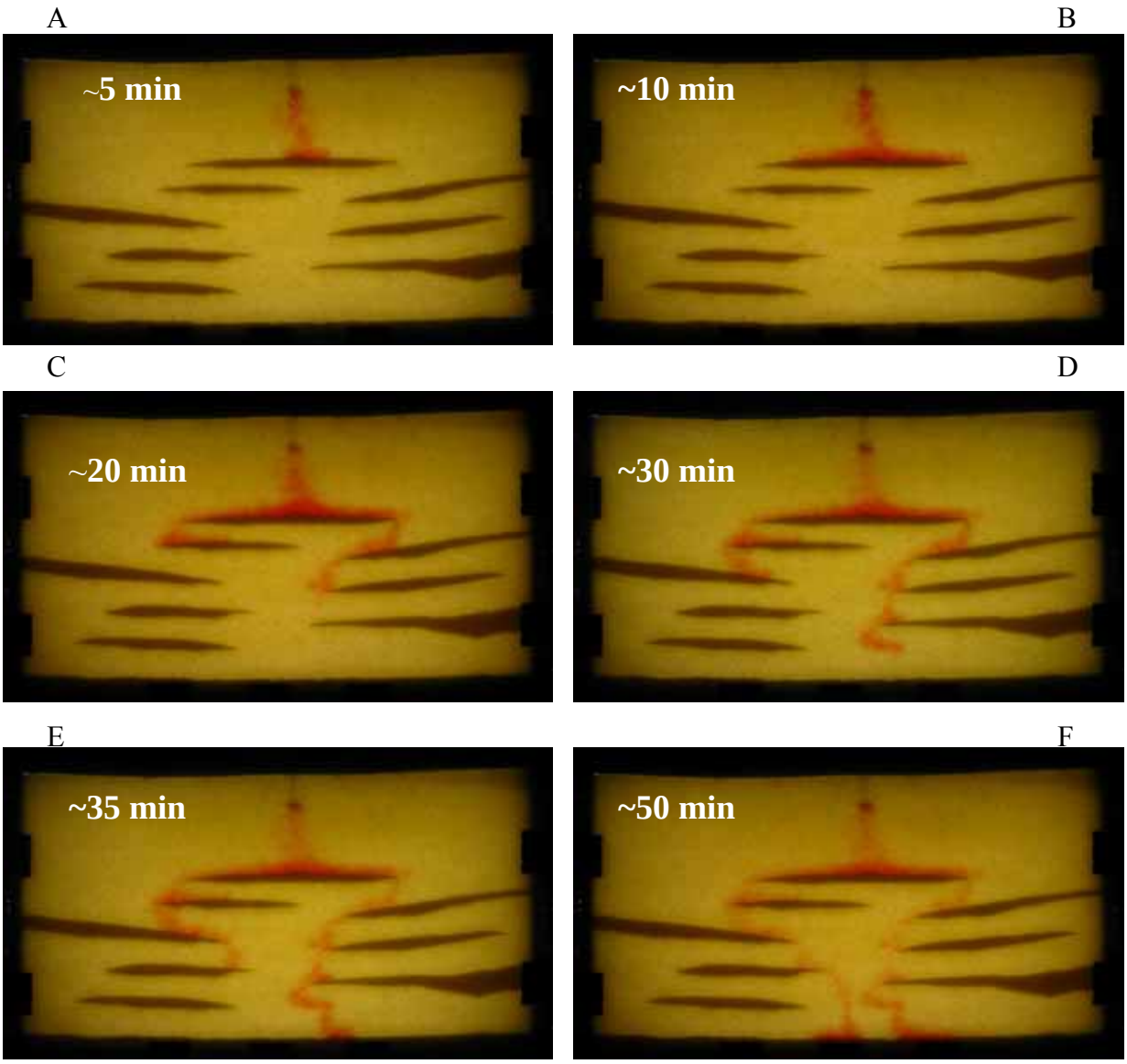

Figure 3-1. A typical PCE spill at several times after beginning PCE injection. A) 5 minutes. B) ~10 minutes. C) ~20 minutes. D) ~30 minutes. E) ~35 minutes. F) ~50 minutes. 10 mL of PCE was injected at a rate of 0.5 mL/min. Flow was from left to right at a Darcy velocity of approximately 1.5 m/d.

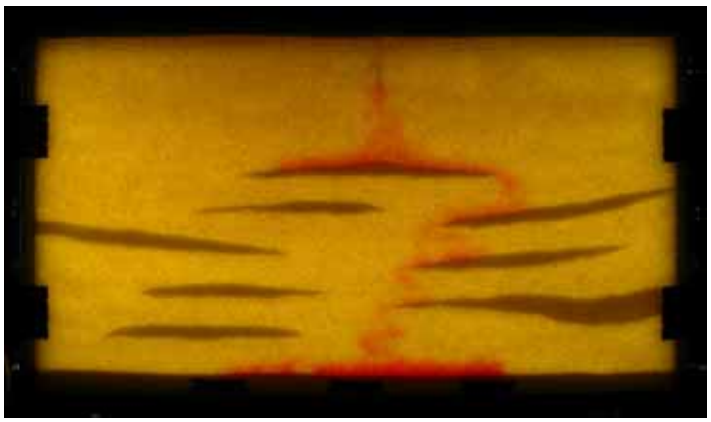

Figure 3-2. ND-MF PCE spill in which the PCE only flowed one side of the top lense. The direction of flow was from left to right at a Darcy velocity at approximately 1.5 m/d.

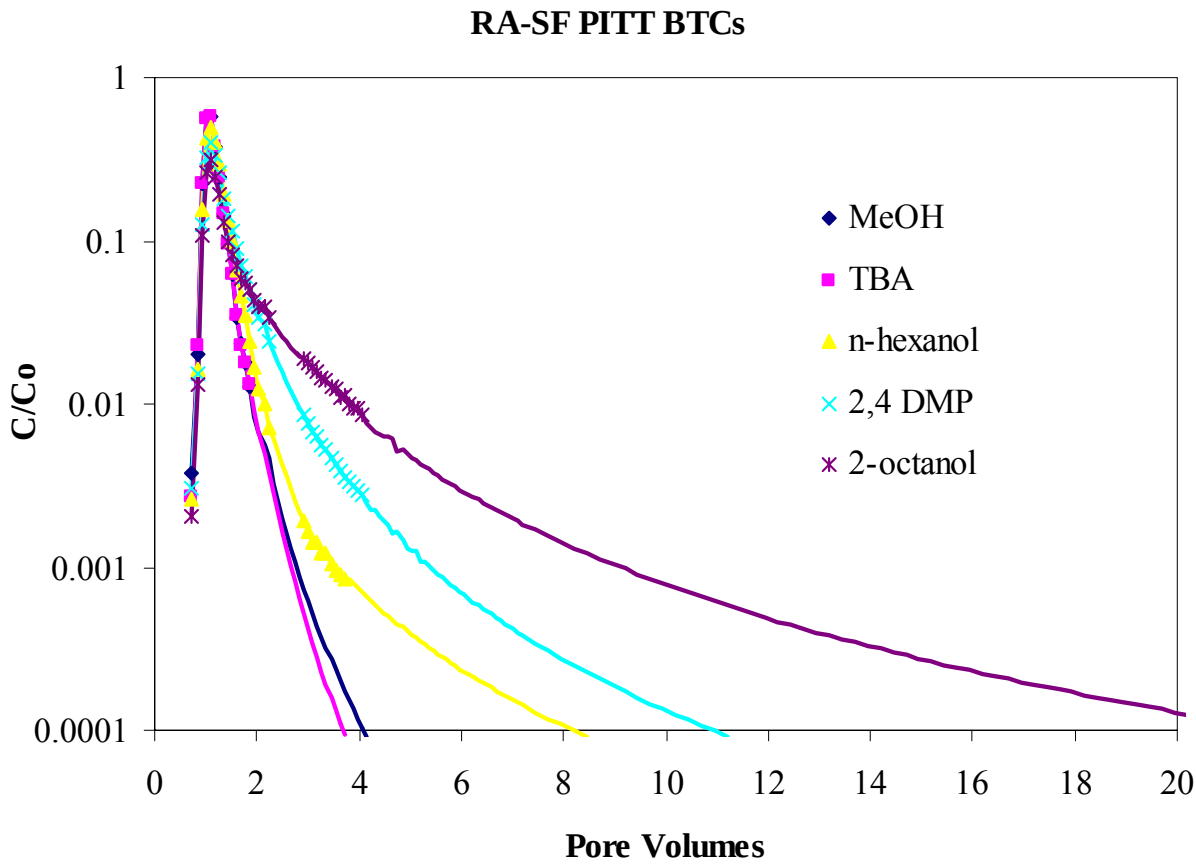

Figure 3-3. Tracer BTCs of the RA-SF experiment. Markers indicate the measured data and the lines represent the log-log extrapolated values.

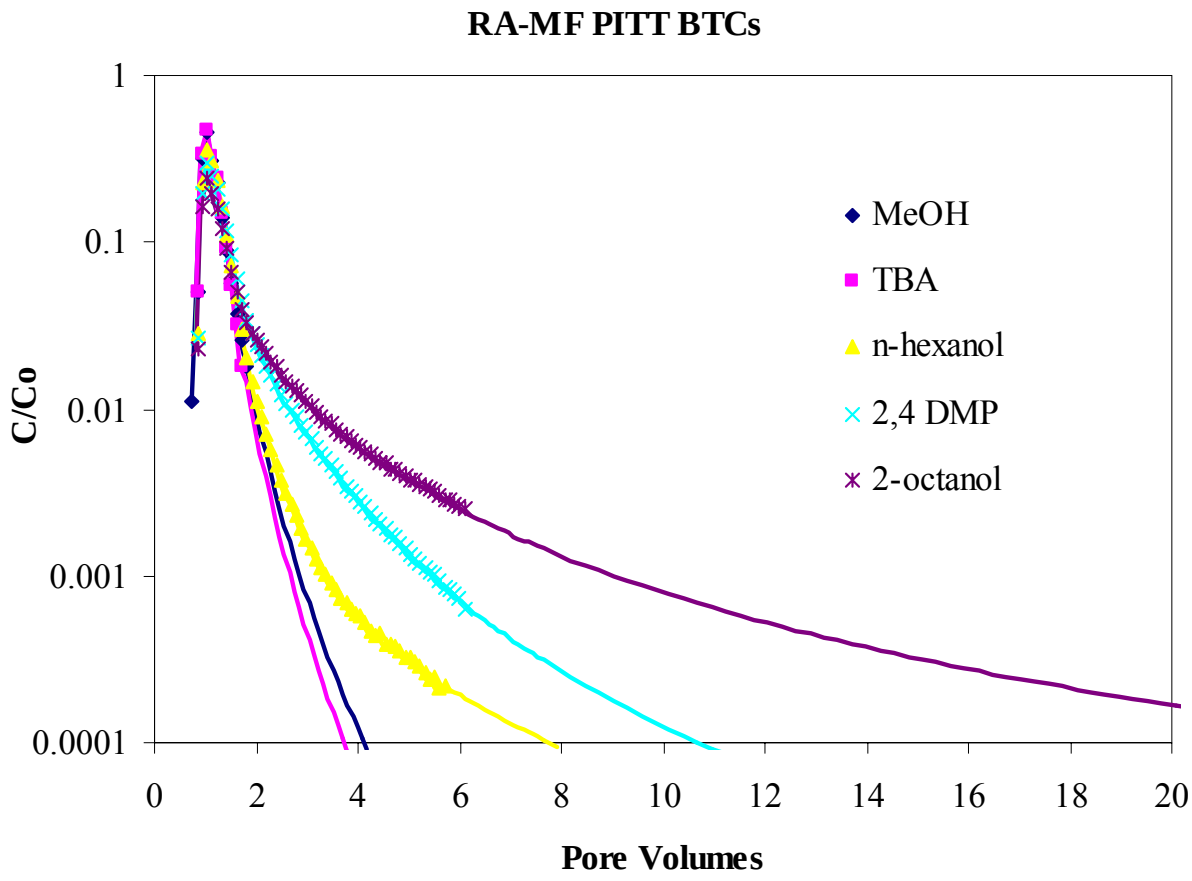

Figure 3-4. Tracer BTCs of the RA-MF experiment. Markers indicate the measured data and the lines represent the log-log extrapolated values.

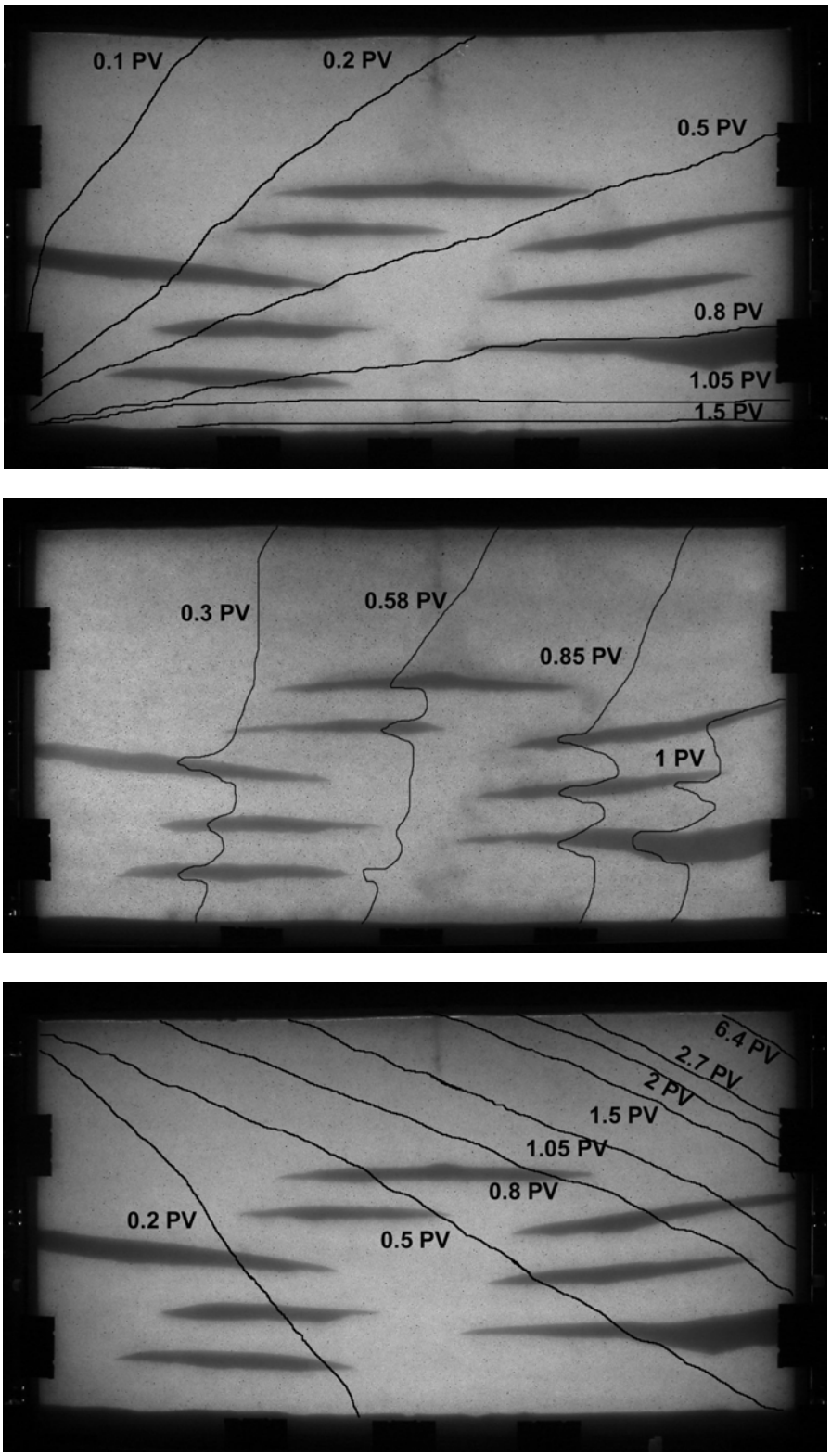

Figure 3-5. Displacement of resident water at different cosolvent injection volumes (PV). A) 50% RA, B) neutral density cosolvent, and C) 40% EL. The flow was from left to right at a Darcy velocity of approximately 1.3 m/d.

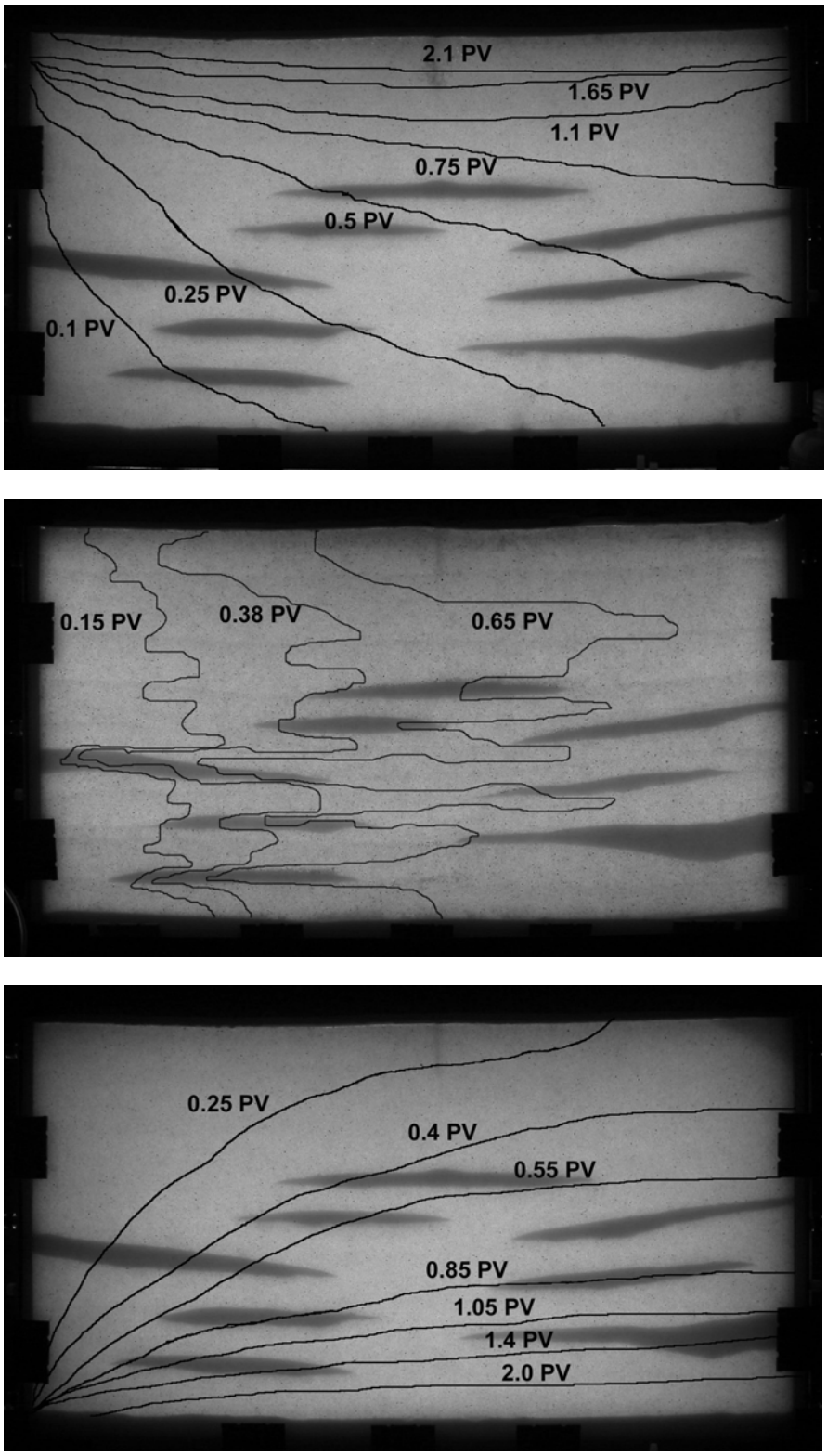

Figure 3-6. Displacement of resident cosolvent by water at different injection pore volumes (PV): A) 50% RA, B) neutral density cosolvent, and C) 40% EL. The flow was from left to right at a Darcy velocity of approximately 1.3 m/d.

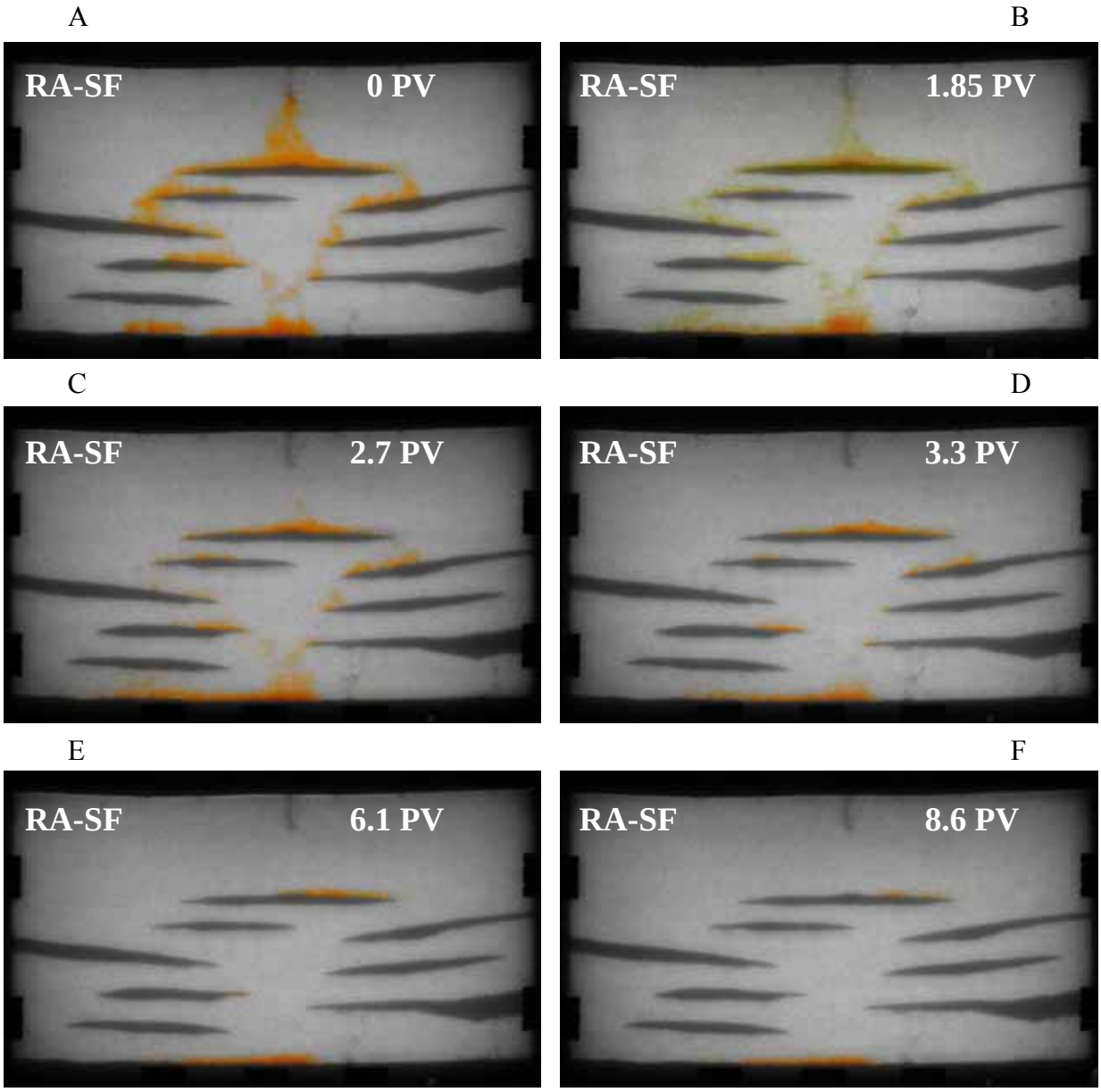

Figure 3-7. 50% RA single-flushing experiment at different cosolvent injection pore volumes (PVs). A) 0 PV. B) 1.85 PVs. C) 2.7 PVs. D) 3.3 PVs. E) 6.1 PVs. F) 8.6 PVs. Flow is from left to right and the Darcy velocity is approximately 1.3 m/d.

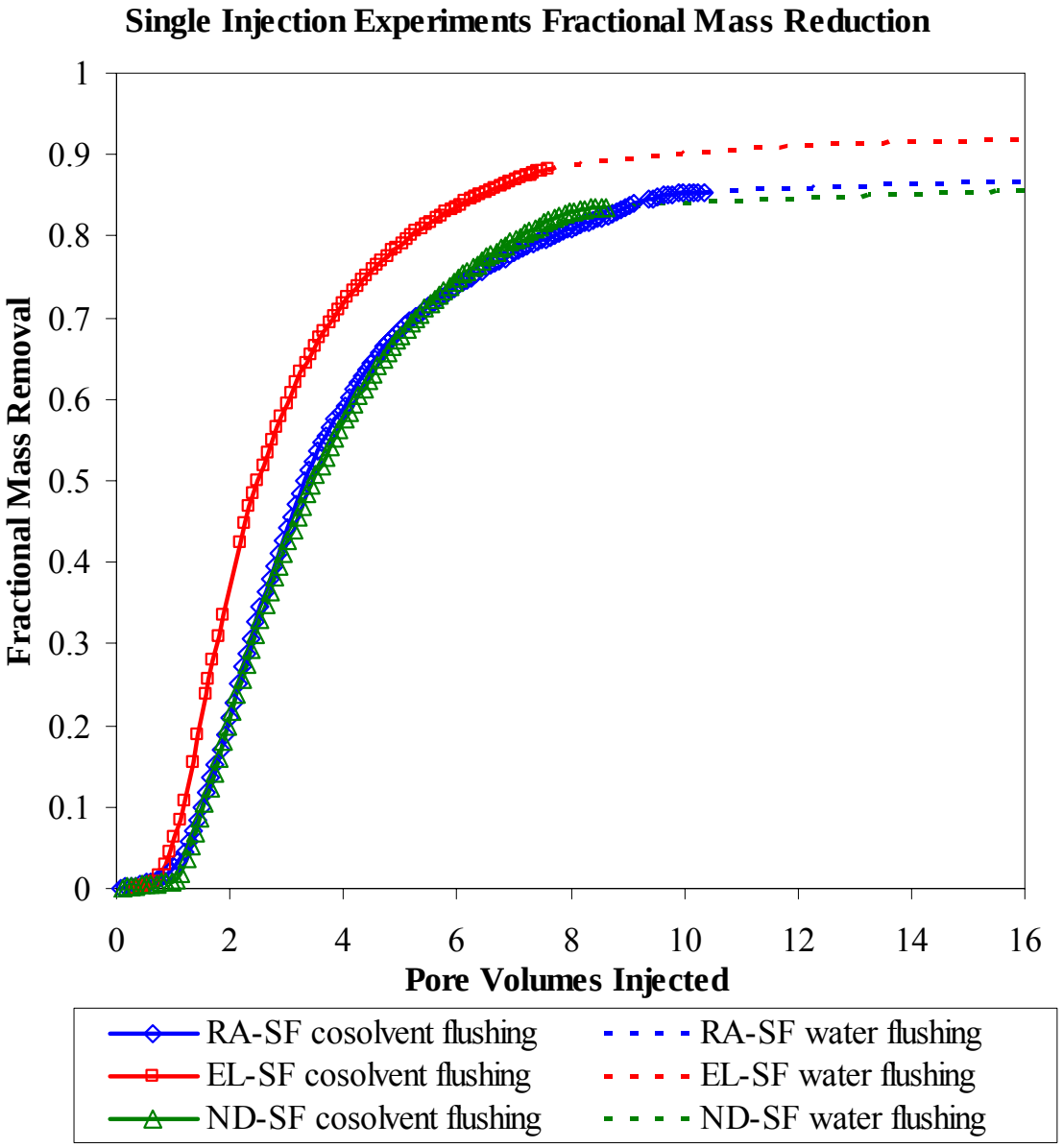

Figure 3-8. Fractional PCE mass removal as a function of pore volumes (PVs) of cosolvent injected during the single-flushing experiments. Solid lines with markers were during cosolvent flushing and the dashed lines were during aqueous flushing.

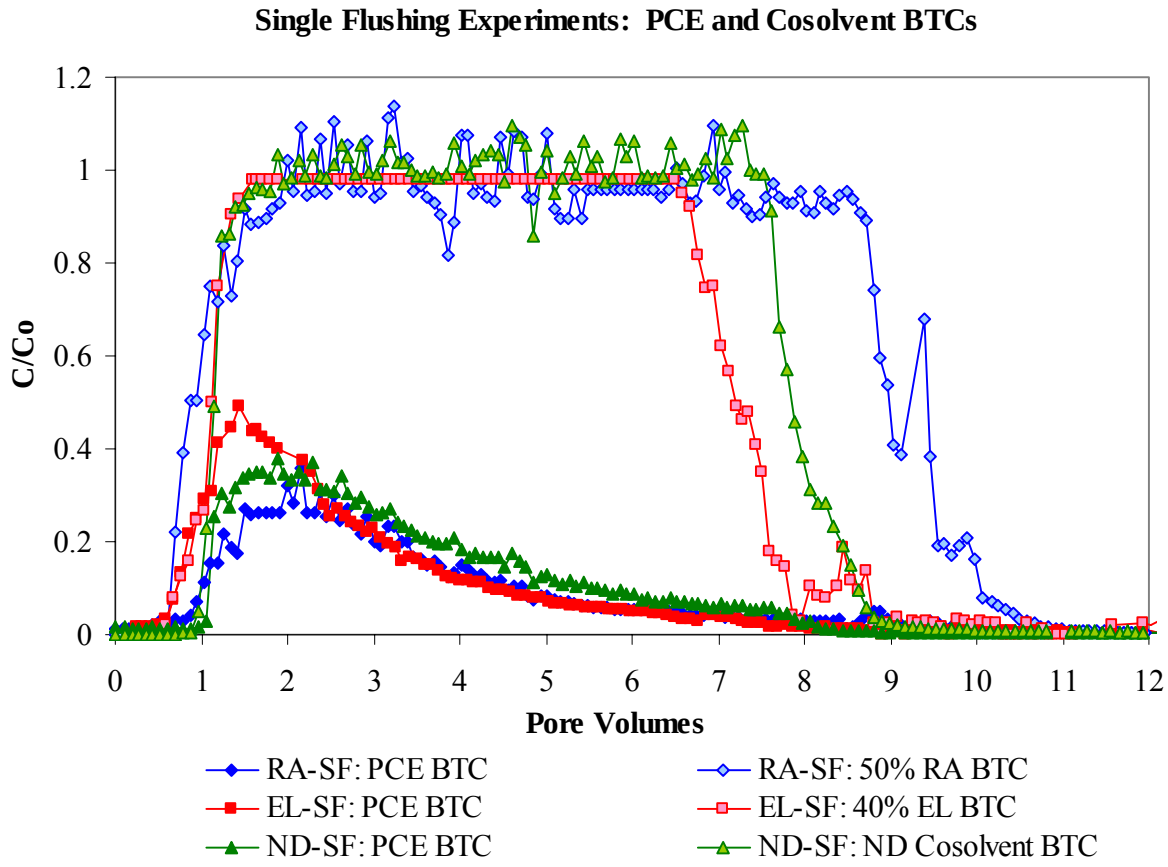

Figure 3-9. PCE and cosolvent breakthrough curves (BTCs) of the single-flushing experiments.

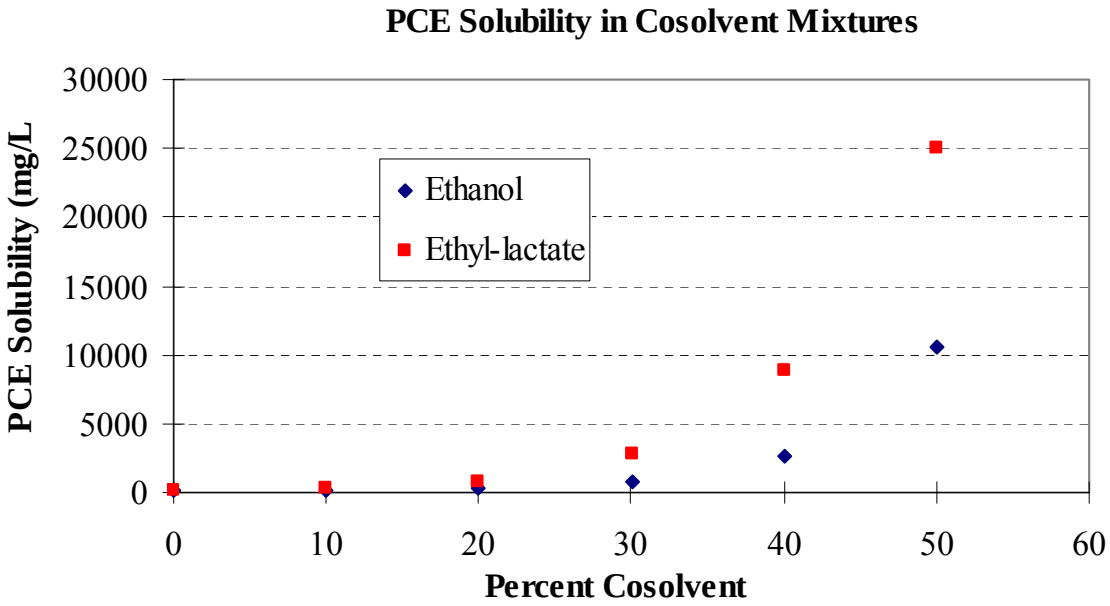

Figure 3-10. PCE solubility of different concentrations of ethanol and ethyl-lactate.

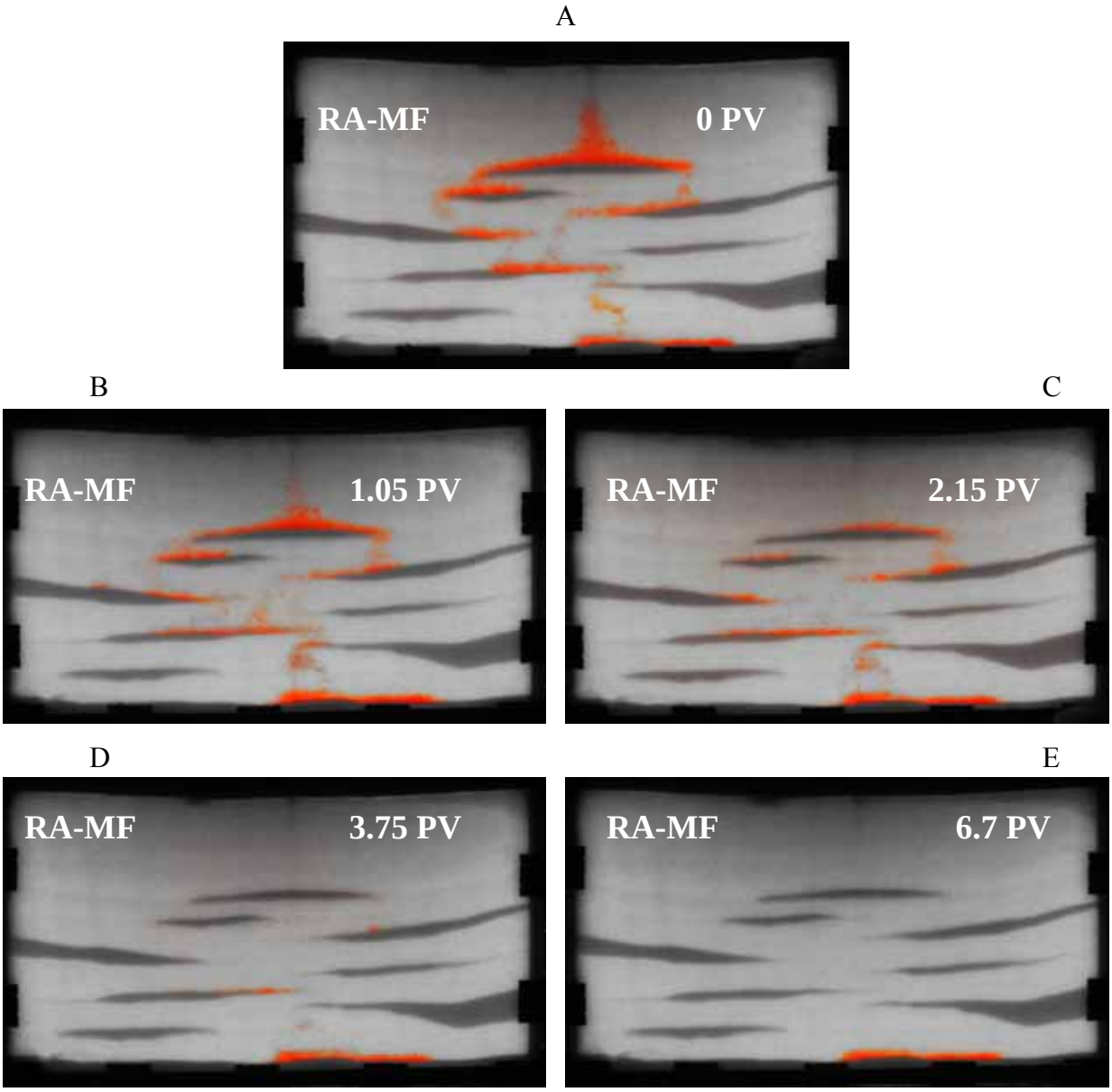

Figure 3-11. 50% reagent alcohol (RA) multiple-flushing experiment with total injected pore volumes (PV) of cosolvent in the top-right corner of each picture. A) Initial distribution. B) After 1st flushing. C) After 2nd flushing. D) After 3rd flushing. E) After 4th flushing. Flow was from left to right at a Darcy velocity of approximately 1.3 m/d.

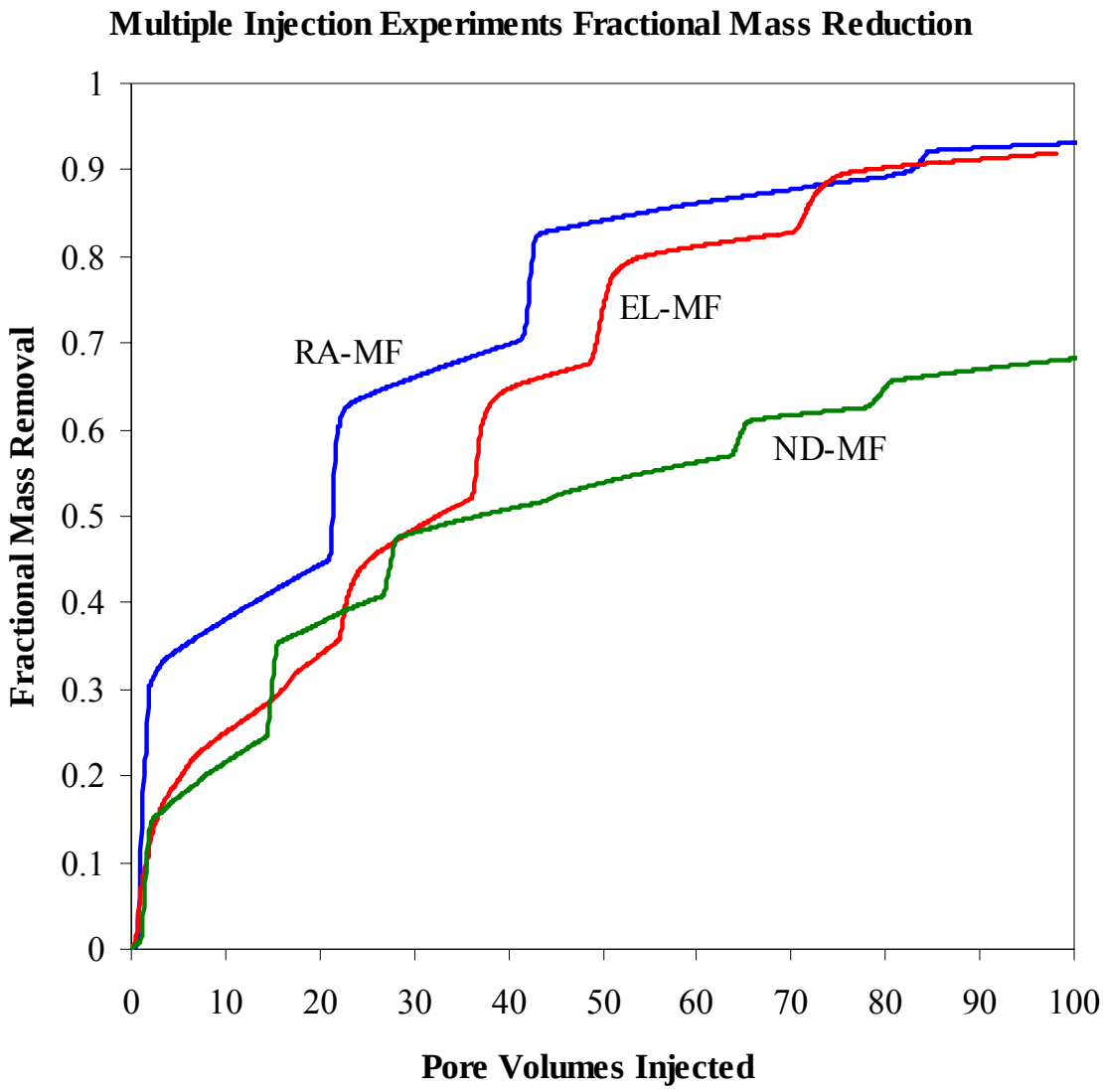

Figure 3-12. Fractional PCE mass removal as a function of pore volumes (PVs) of fluid injected, including both cosolvent and water, during the multiple-flushing experiments.

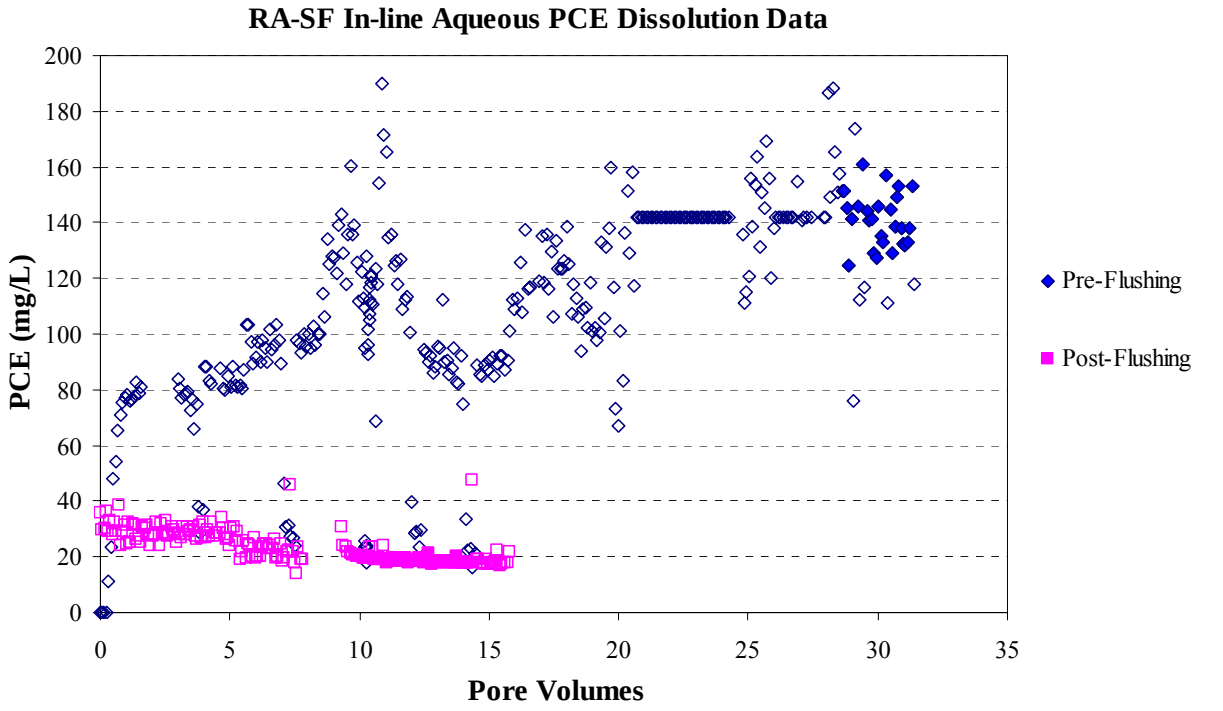

Figure 3-13. Inline aqueous PCE dissolution data for the single-flushing experiment RA-SF.

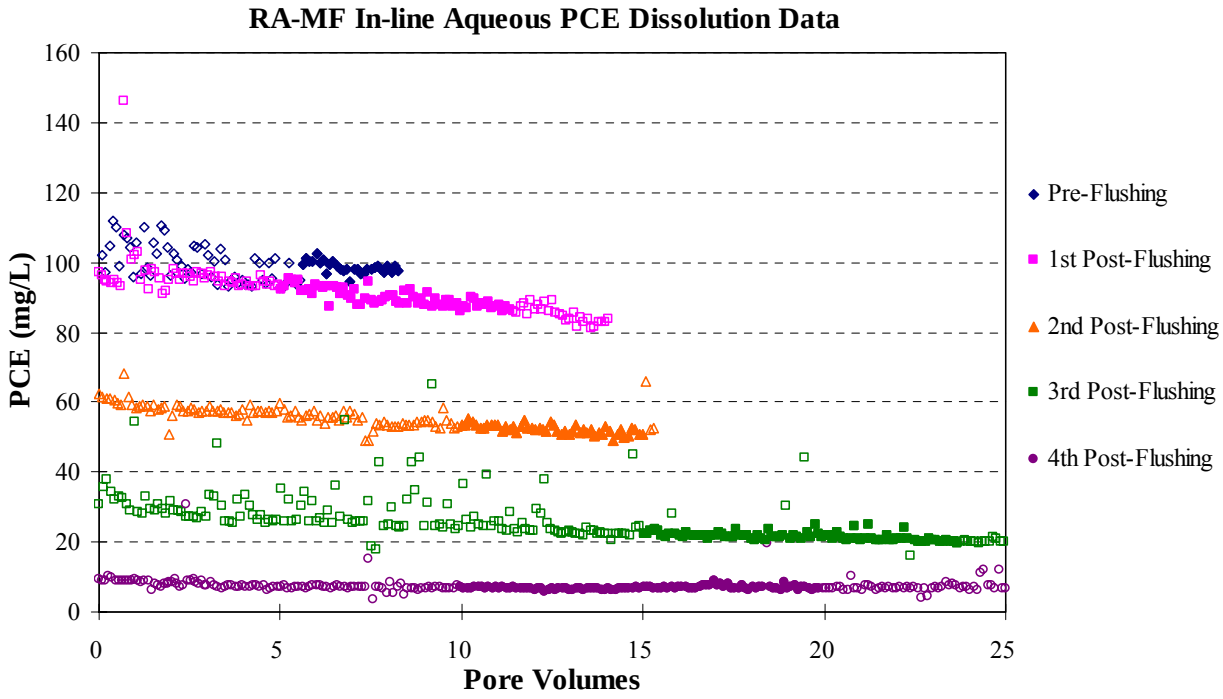

Figure 3-14. Inline aqueous PCE dissolution data for the multiple-flushing experiment RA-MF.

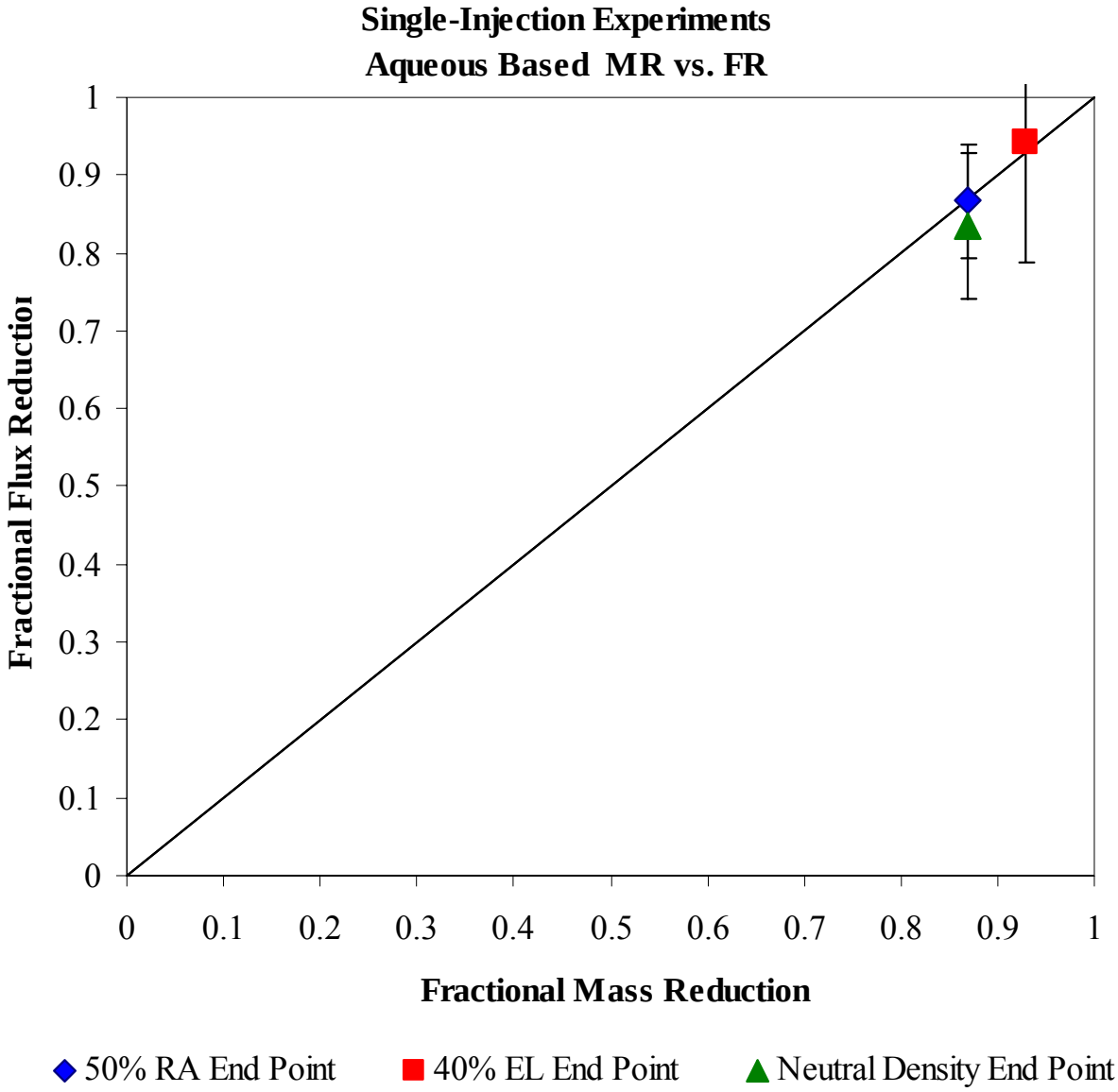

Figure 3-15. Aqueous based mass reduction (MR) versus flux reduction (FR) for the single-flushing experiments with 50% reagent alcohol (RA), 40% ethyl-lactate (EL), and neutral density cosolvent.

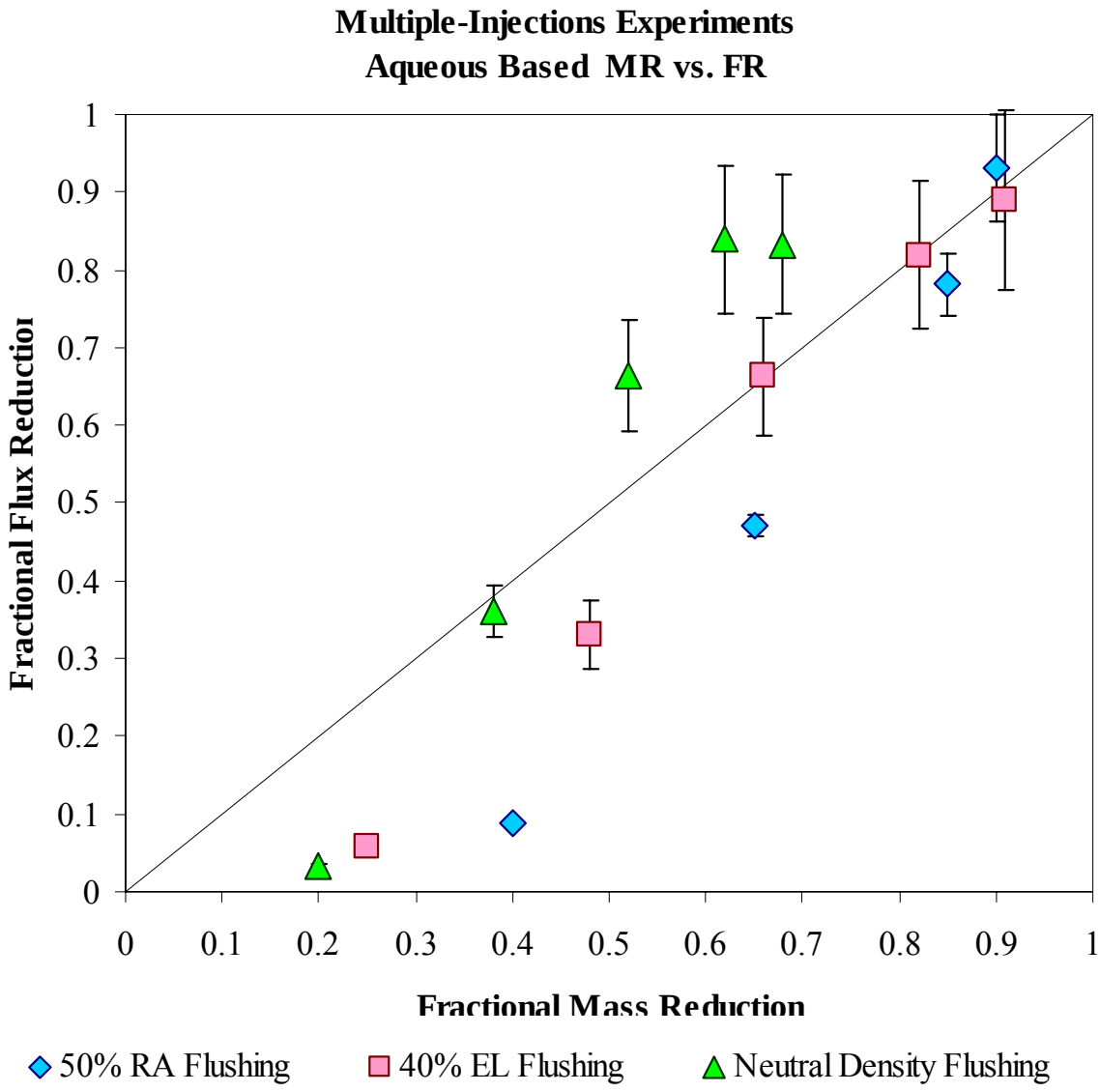

Figure 3-16. Aqueous based mass reduction (MR) versus flux reduction (FR) for the multiple-flushing experiments with 50% reagent alcohol (RA), 40% ethyl-lactate (EL), and neutral density cosolvent.

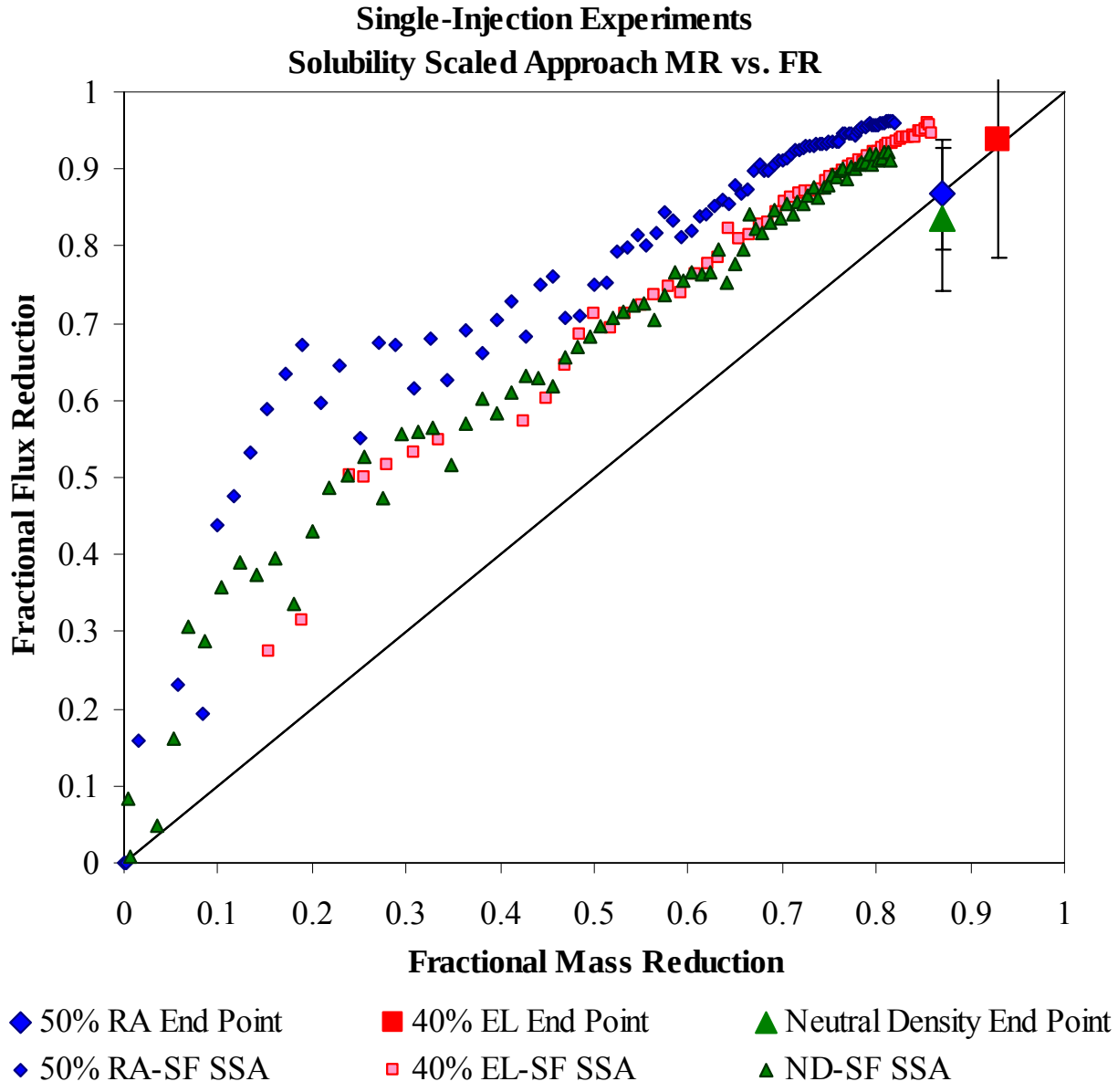

Figure 3-17. Solubility scaled approach (SSA) mass reduction (MR) versus flux reduction (FR) path estimation for the single-flushing experiments with 50% reagent alcohol (RA), 40% ethyl-lactate (EL), and neutral density cosolvent, including aqueous based end points.

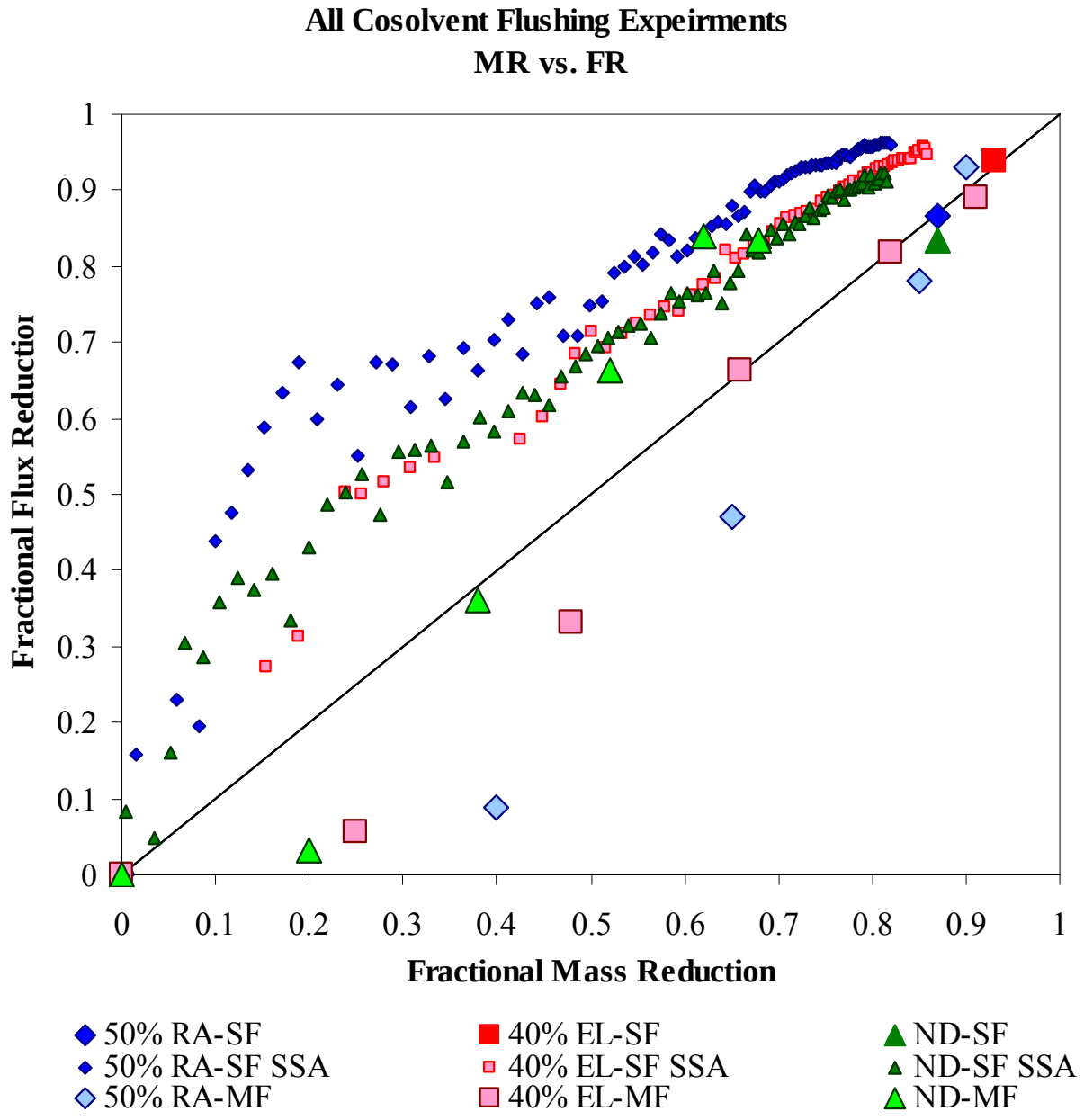

Figure 3-18. Aqueous based mass reduction (MR) versus flux reduction (FR) of the single and multiple-flushing experiments with the solubility scaled approach (SSA) path estimation of the single-flushing experiments.

Table 3-1. Tracer mass recovery for all experiments

Experiment ID	MEOH (mg)	TBA (mg)	n-hexanol (mg)	2,4 DMP (mg)	2-octanol (mg)
RA-SF					
Mass recovered	367	262	189	193	74.0
Mass injected	388	279	199	199	79.7
Recovery %	94.4	94.1	95.0	96.8	92.9
RA-MF					
Mass recovered	282	208	137	141	53.8
Mass injected	301	216	154	154	61.8
Recovery %	93.5	96.0	88.8	91.1	87.1
EL-SF					
Mass recovered	320	230	169	172	70.5
Mass injected	357	257	183	183	73.3
Recovery %	89.6	89.5	92.5	93.7	96.2
EL-MF					
Mass recovered	327	232	167	170	66.1
Mass injected	339	243	174	174	69.4
Recovery %	96.6	95.5	96.3	98.1	95.2
ND-SF					
Mass recovered	341	243	173	174	69.2
Mass injected	343	246	176	176	70.4
Recovery %	99.3	98.7	98.2	98.9	98.3
ND-MF					
Mass recovered	340	246	173	175	70.5
Mass injected	348	250	178	178	71.4
Recovery %	97.9	98.3	96.9	98.1	98.7

Table 3-2. Pore volume, S_N, and NAPL volume estimations of the tracer experiments.

	Estimated pore volume (mL)		Estimated S_n			Estimated NAPL volume (mL)		
	MeOH	TBA	n-hexanol	2,4 DMP	2-octanol	n-hexanol	2,4 DMP	2-octanol
RA-SF	1157	1154	0.0144	0.0115	0.0083	16.7	13.3	9.6
RA-MF	1126	1106	0.0119	0.0109	0.0071	13.4	12.3	8.0
EL-SF	1158	1150	0.0117	0.0092	0.0095	13.6	10.7	11.0
EL-MF	1190	1187	0.0111	0.0081	0.0061	13.1	9.7	7.3
ND-SF	1142	1135	0.0117	0.0101	0.0093	13.3	11.6	10.7
ND-MF*	1221	1215	0.0053	0.0059	0.0045	6.4	7.2	5.5
Average	1166	1158	0.0110	0.0093	0.0075	12.8	10.8	8.7
Avg (no *)	1155	1146	0.0122	0.0100	0.0081	14.0	11.5	9.3

Table 3-3. M, $R_{v/g}$ and β estimates based on Equations 3-3, 3-4, and 3-5.

Cosolvent displacing water	50% RA	40% EL	ND mixture
M	0.38	0.40	0.38
$R_{v/g}$	0.126	0.992	54
β (observed β)	6.5° (35°)	141° (130°)	88.8° (85°)
Water displacing cosolvent	**50% RA**	**40% EL**	**ND mixture**
M	2.7	2.5	2.6
$R_{v/g}$	0.335	2.48	142
β (observed β)	173.5° (155°)	38.8° (25°)	91.2° (95°)

Table 3-4. Cosolvent single injection summary

Experiment ID	Pore volumes injected	Average aqueous PCE concentration (mg/L)				Post flushing mass reduction (%)	Post flushing aqueous flux reduction (%)
		Pre-cosolvent flushing	STDEV	Post-cosolvent flushing	STDEV		
RA-SF	8.5	141.0	9.6	18.7	0.9	87 ± 1.7	86.7 ± 7.25
EL-SF	6.4	143.5	12.0	8.5	1.2	93 ± 1.9	94.1 ± 15.4
ND-SF	8.5	128.6	9.9	21.2	1.7	87 ± 1.7	83.5 ± 9.28

Table 3-5. Multiple cosolvent injection summary

Cosolvent mixture	Cumulative pore volumes injected	Aqueous PCE concentration (mg/L)		Post flushing mass reduction	Post flushing aqueous flux reduction
RA-MF		(mg/L)	STDEV	(%)	(%)
Initial	-	98.5	1.6	0	0
1st post flushing	1.1	89.9	2.4	40 ± 0.8	8.7 ± 0.27
2nd post flushing	2.2	52.3	1.3	65 ± 1.3	47.0 ± 1.4
3rd post flushing	3.8	21.6	1.1	85 ± 1.7	78.1 ± 4.1
4th post flushing	6.7	6.9	0.5	90 ± 1.8	93.0 ± 6.9
EL-MF					
Initial	-	116.8	12.1	0	0
1st post flushing	0.46	110.2	5.5	25 ± 0.5	5.7 ± 0.66
2nd post flushing	0.95	78.2	6.3	48 ± 1.0	33.1 ± 4.34
3rd post flushing	1.8	39.3	2.0	66 ± 1.3	66.3 ± 7.66
4th post flushing	3.4	21.2	1.1	82 ± 1.6	81.9 ± 9.49
5th post flushing	5	12.8	1.0	91 ± 1.8	89.0 ± 11.54
ND-MF					
Initial	-	81.1	5.6	0	0
1st post flushing	1	78.5	5.8	20 ± 0.4	3.2 ± 0.32
2nd post flushing	2.3	51.9	3.0	38 ± 0.8	36.1 ± 3.25
3rd post flushing	3.9	27.3	2.2	52 ± 1.0	66.4 ± 7.04
4th post flushing	5.9	13.1	1.2	62 ± 1.2	83.9 ± 9.62
5th post flushing	8.8	13.6	1.1	68 ± 1.4	83.3 ± 8.86

CHAPTER 4
SUMMARY, CONCLUSIONS, AND FUTURE WORK

Summary

There are hundreds of thousands of commercial, military, and industrial sites across the country where chemical wastes cause contamination to subsurface materials including groundwater (NRC, 2004). Some of the more challenging sites contain chlorinated solvents that are present as dense non-aqueous phase liquids (DNAPLs). Most often, plume management based approaches are implemented to reduce the risk of the receptors. However, due to the longevity of the DNAPL source, the cost of implementing these approaches can be tremendous. In terms of long-term environmental stewardship, DNAPL plume management approaches fail in the sense that the contaminant problem is being passed on to future generations.

An alternative approach is seeking the removal or destruction of the contaminant source. Unfortunately, it is very difficult or impossible to completely remove the NAPL mass from the source zone of the subsurface due to the complex NAPL entrapments conditions, specifically in the case of DNAPLs (Soga et al., 2004). However, several source zone remediation technologies that have shown the ability to remove a significant portion of the source zone, one of which is cosolvent flushing. But, there is currently no consensus in the academic, technical and regulatory communities on the ecological or environmental impacts of DNAPL source zone treatment (U.S. EPA, 2003).

To help characterize the functional relationship between DNAPL architecture, mass removal and contaminant mass flux, a series of experiments were conducted under well defined heterogeneous aquifer conditions in which the reduction in contaminant flux due to partial removal of DNAPL source zones by cosolvent flushing was quantified. The experiments were conducted using a 2-D aquifer model similar to those in other studies (Jawitz et al., 1998a, Fure

et al., 2006) in which discrete layers of less permeable porous media were placed into otherwise homogeneous porous media. A known amount of tetrachloroethylene (PCE) was released into the chamber and acted as the source of contamination to the down gradient well. The DNAPL source zone architecture was similar for all the experiments except for one where there was a relatively larger portion of the mass than the other experiments trapped in a pool at the bottom of the flow chamber. In six separate experiments, three unique cosolvent mixtures that had similar PCE solubility, but significantly different behaviors during miscible fluid displacement due to density and viscosity differences, were flushed through the source zone to remove a portion of the PCE mass. Each cosolvent mixture was used in two different experiments: a single-flushing experiment and a multiple-flushing experiment. To estimate the mass flux through the chamber both before and after remediation, steady-state aqueous conditions were measured. The PCE mass removed during cosolvent flushing was also measured. The relationship between fractional mass removal (MR) and fractional flux reduction (FR) was used to assess the performance of the cosolvent flushing.

The MR vs. FR relationship of all of the single-flushing experiments was nearly identical, and in all of these experiments the initial DNAPL distribution was similar. Together, these observations indicate that the override and underride effects associated with the 50% RA and the 40% EL during miscible fluid displacement did not significantly effect the remediation performance of the cosolvents during the single-flushing experiments. The MR vs. FR relationship of the multiple injection experiments with both the 50% RA and the 40% EL tended to be less desirable in the sense that there was less FR for a given MR than in the MR vs. FR relationship of the single injection experiments with the same cosolvent mixtures. It can be

concluded that this was caused by the increased override and underride of fluid associated with the multiple flushing procedure.

In the experiment where the initial PCE distribution was different from that of the other experiments, the MR vs. FR relationship tended to differ as well. The fact that the MR vs. FR relationship of the ND-MF experiment showed a different behavior than the other experiments and that the media heterogeneities were similar, indicate that the DNAPL distribution had a greater effect on the MR vs. FR response than the buoyancy or viscosity characteristics of the cosolvents.

Conclusions

- The MR vs. FR relationships of all the single-flushing experiments were favorable as they were above the 1:1 line. This indicates that a model with $\beta > 1$ may be a good approximation of the MR vs. FR relationship using enhanced dissolution by the cosolvents in similar systems.
- The override and underride effects associated with the 50% RA and the 40% EL during miscible fluid displacement did not significantly effect their remediation performance during the single-flushing experiments.
- The increased override and underride of fluid associated with the multiple-flushing experiments resulted in a less desirable MR vs. FR. relationship for 50% RA and 40% EL.
- In the system studied, the DNAPL architecture had a greater effect on the MR vs. FR response than the buoyancy or viscosity characteristics of the cosolvents.

Future Work

The laboratory experiments provide high quality data sets that could be useful to a studies to further investigate the benefits of different partial source zone removal:

- Estimate the MR vs. FR from the tracers based on higher moment techniques (Jawitz et al., 2003).
- The processes used in the laboratory could be modeled using a multiphase flow and transport code such as UTCHEM. Parameters necessary for accurate simulation could be estimated by matching the results of simulations to the laboratory experiments.

- Different NAPL architectures could be assessed more easily once an accurate simulation of the laboratory conditions was created.
- NAPLs with different densities or different wetting properties could also be evaluated.
- Image analysis software (e.g., Optimus, Media Cybernetics) could be utilized to analyze the color images.

APPENDIX
ADDITIONAL EXPERIMENTAL FIGURES

The Appendix contains figures that are referred to throughout the document.

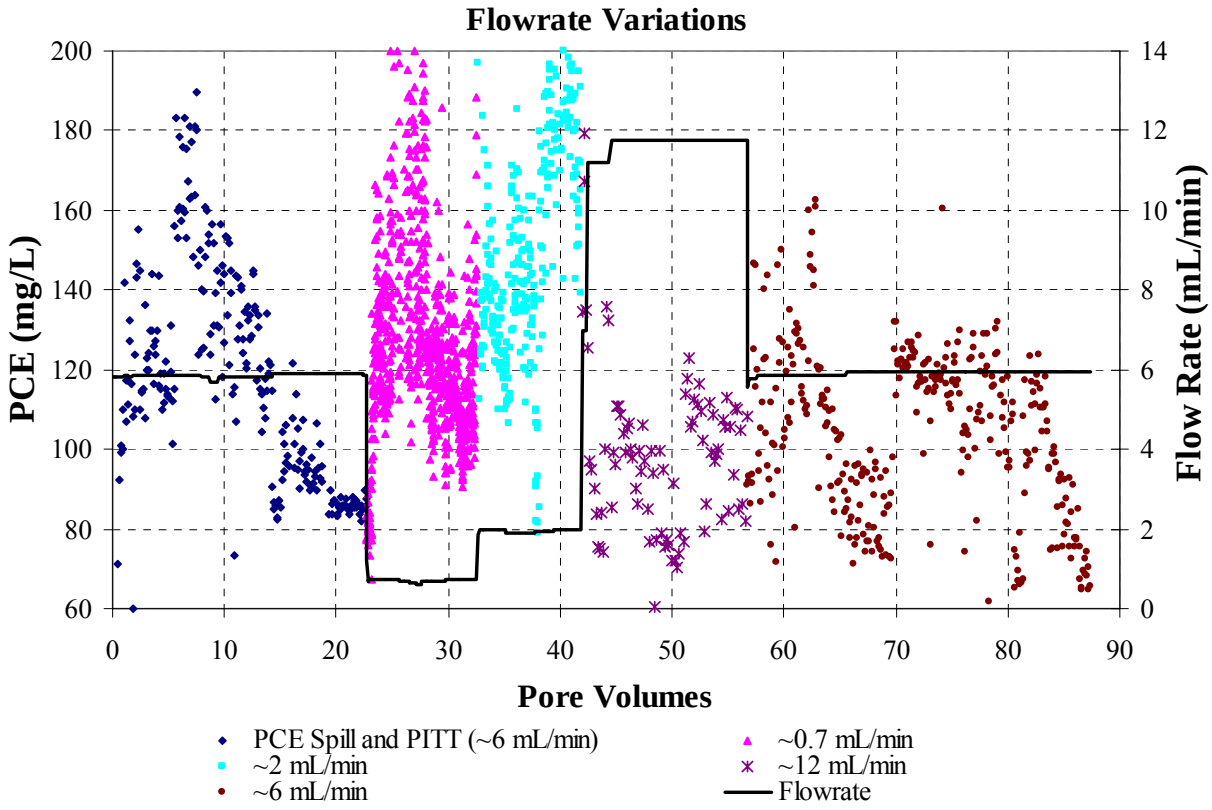

Figure A-1. Investigation of the effects of variations of flowrate on PCE concentrations. PCE concentrations were measured for 10 pore volumes (PVs) at each flowrate.

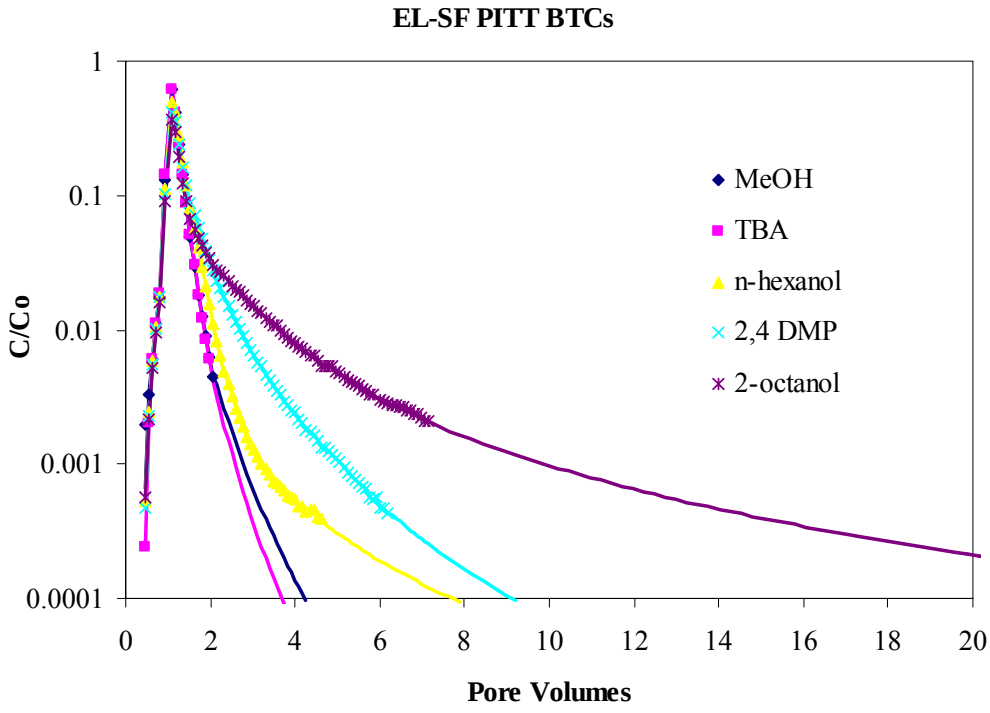

Figure A-2. Tracer breakthough curves (BTCs) of the EL-SF experiment. Markers indicate the measured data and the lines represent the log-log extrapolations.

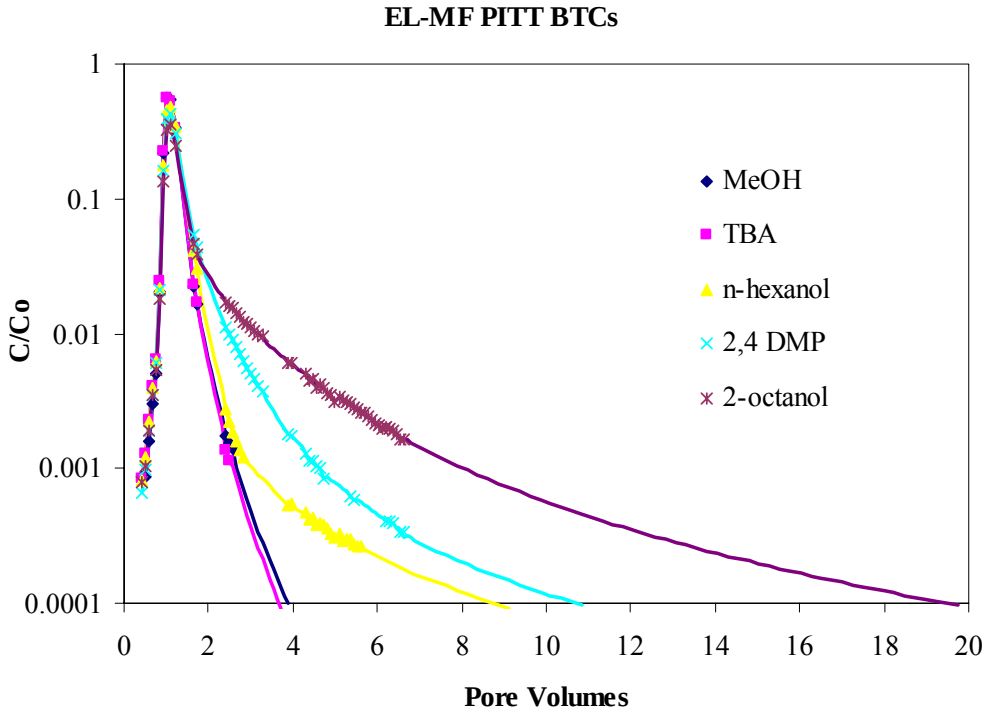

Figure A-3. Tracer BTCs of the EL-MF experiment. Markers indicate the measured data and the lines represent the log-log extrapolations.

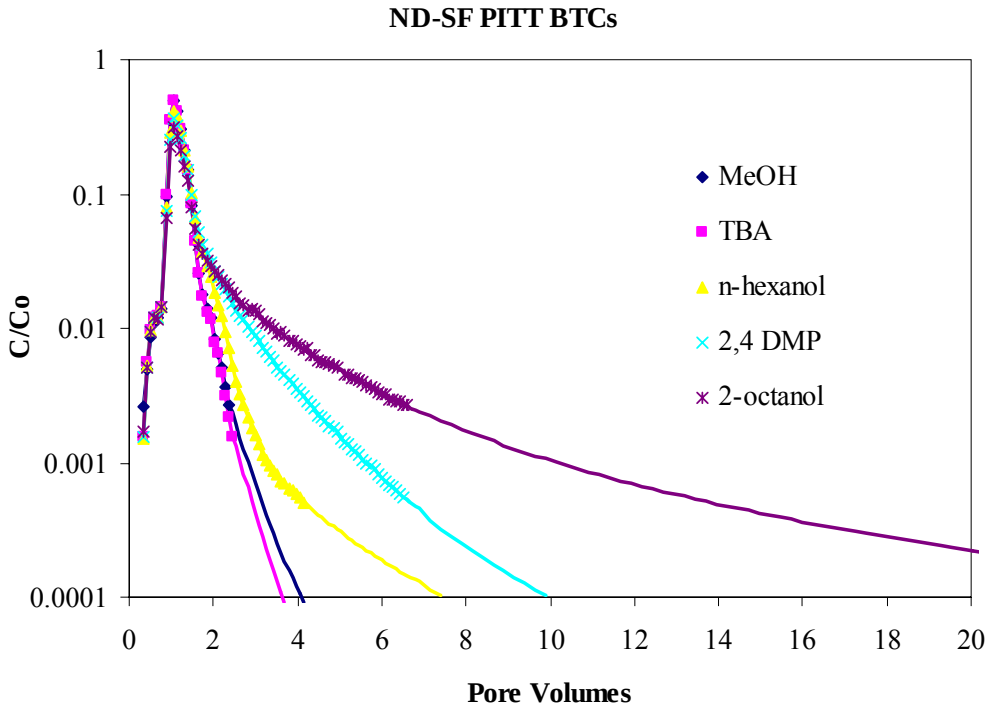

Figure A-4. Tracer BTCs of the ND-SF experiment. Markers indicate the measured data and the lines represent the log-log extrapolations.

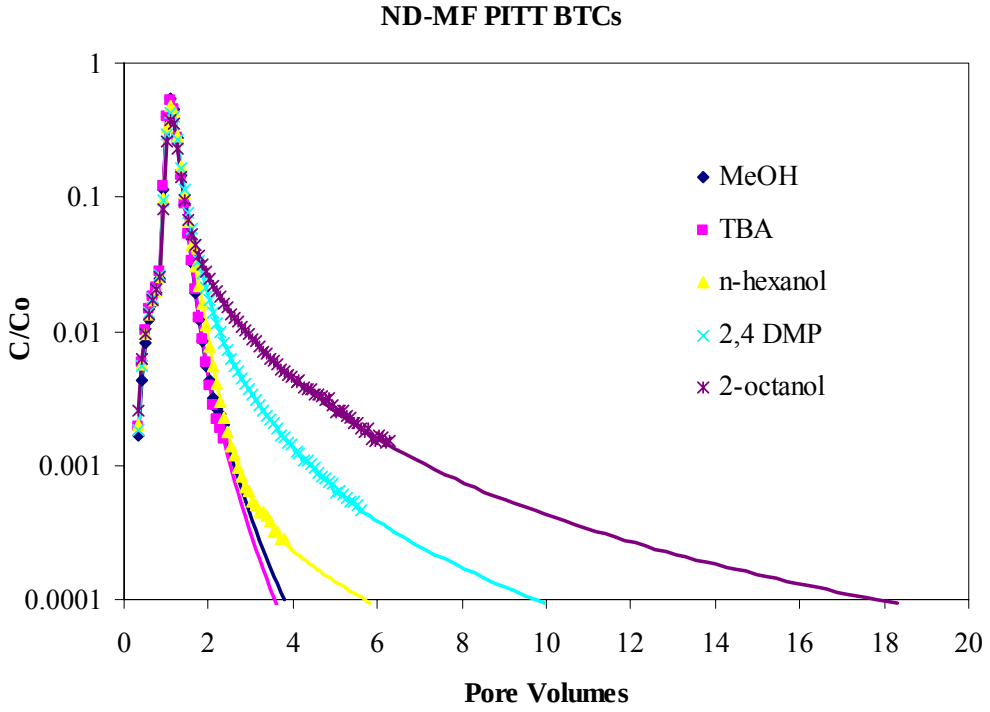

Figure A-5. Tracer BTCs of the ND-MF experiment. Markers indicate the measured data and the lines represent the log-log extrapolations.

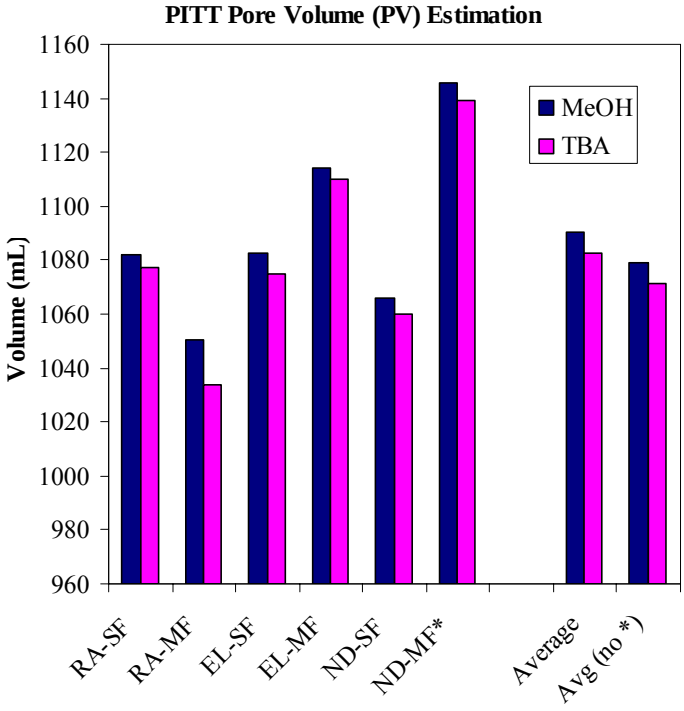

Figure A-6. Pore volume (PV) estimates and averages by the non-partitioning tracers methanol (MeOH) and tert-butyl alcohol (TBA) for the six experiments.

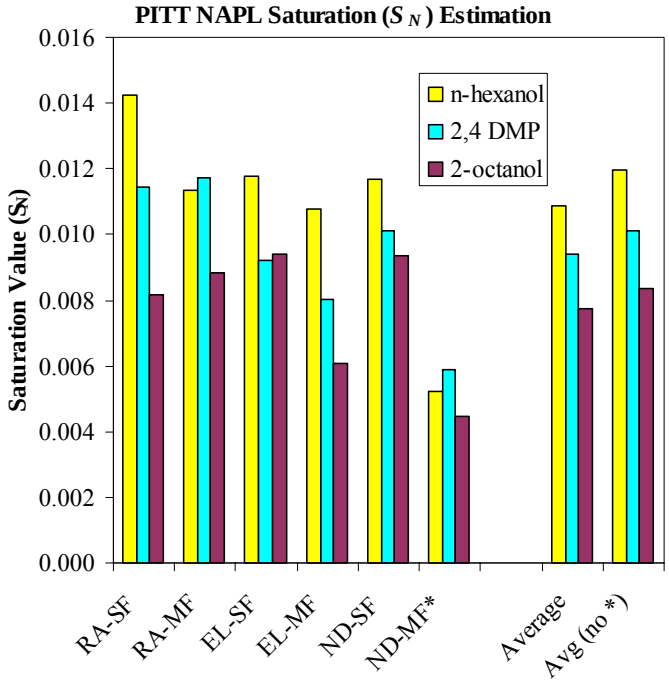

Figure A-7. NAPL saturation (S_N) estimates and averages by the partitioning tracers n-hexanol, 2,4 dimethyl 3 pentanol (2,4 DMP) and 2-octanol for the six experiments.

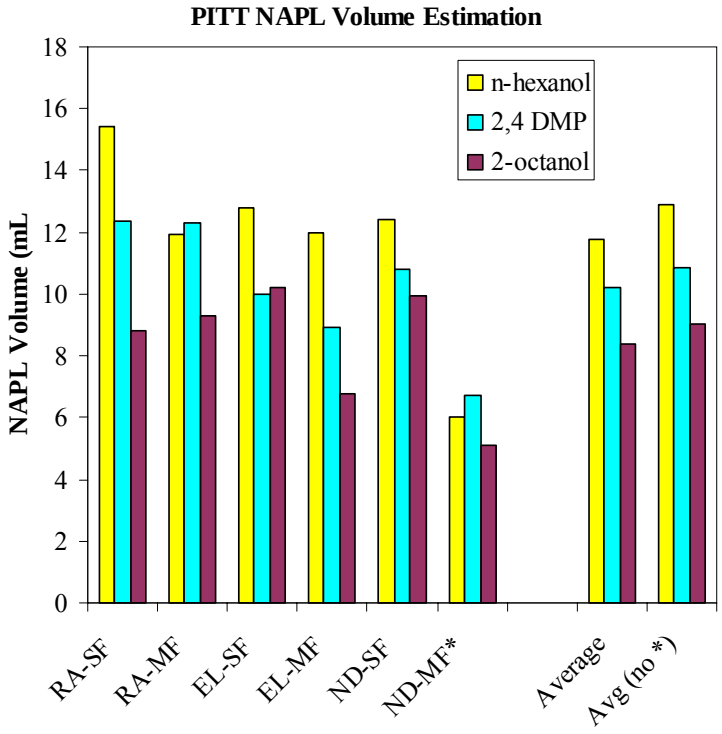

Figure A-8. NAPL volume estimates and averages by the partitioning tracers n-hexanol, 2,4 dimethyl 3 pentanol (2,4 DMP) and 2-octanol for the six experiments.

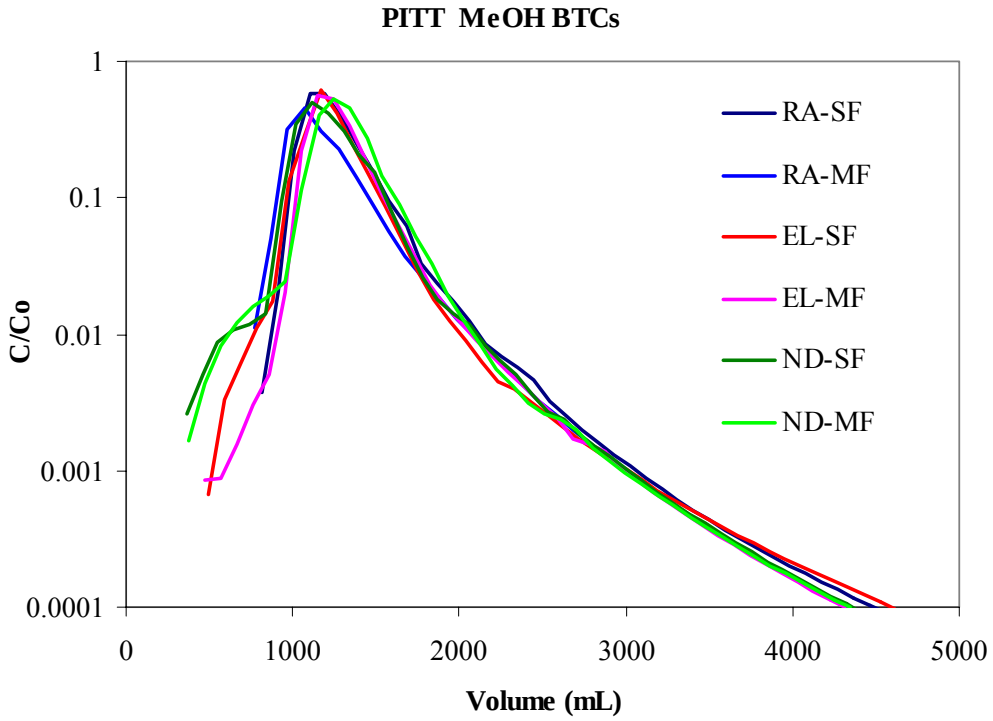

Figure A-9. MEOH tracer BTCs for all of the experiments.

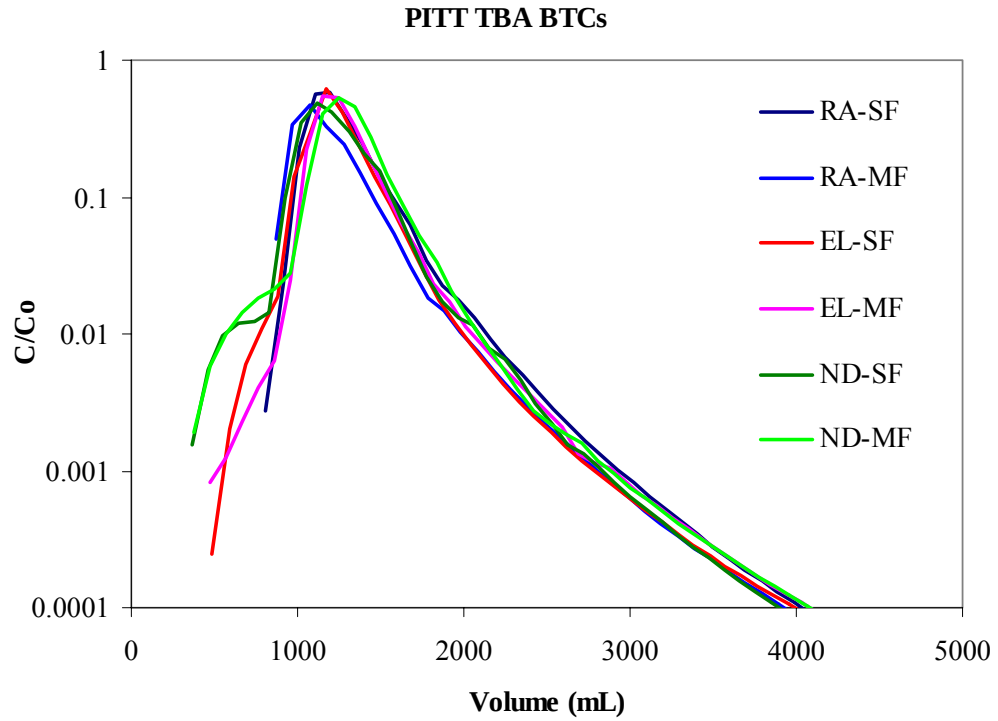

Figure A-10. The TBA tracer BTCs for all of the experiments.

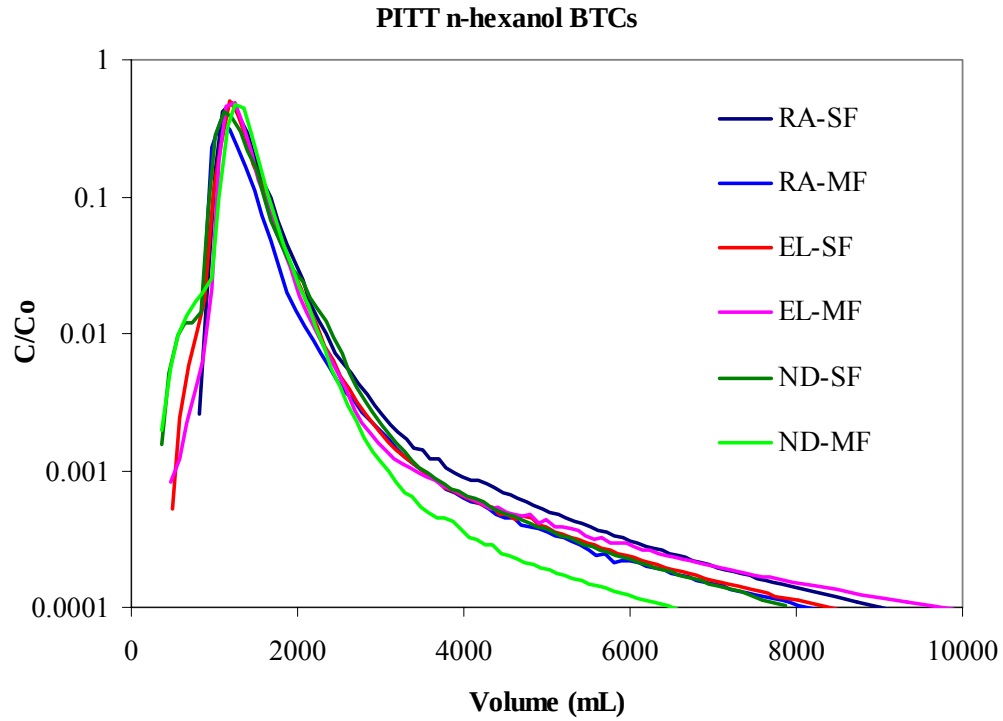

Figure A-11. The n-hexanol tracer BTCs for all of the experiments.

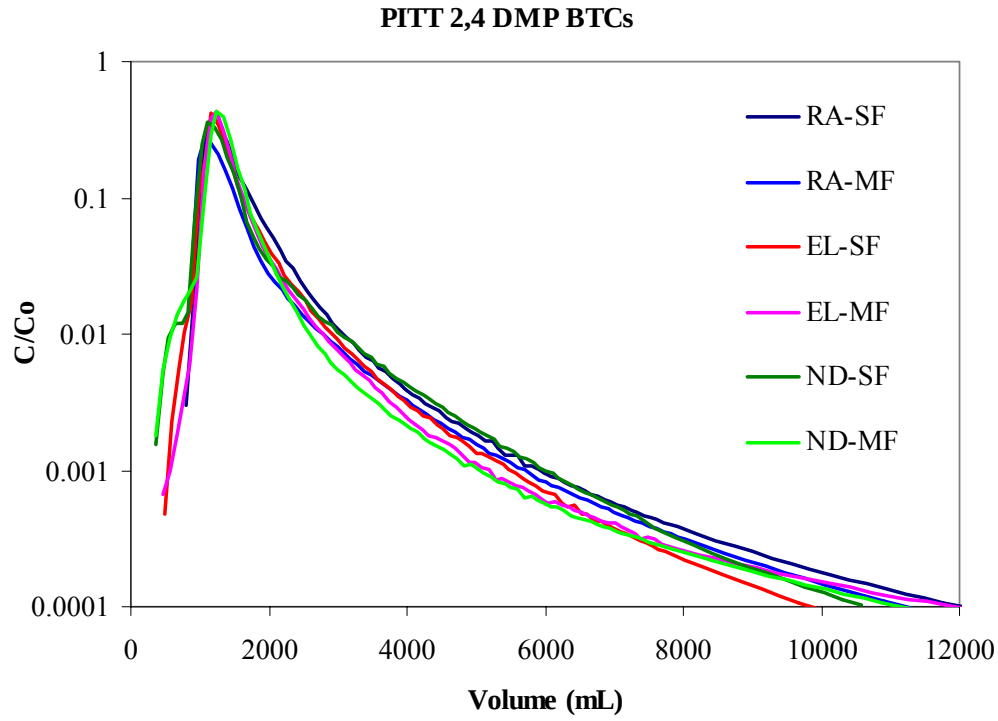

Figure A-12. The 2,4 DMP tracer BTCs for all of the experiments.

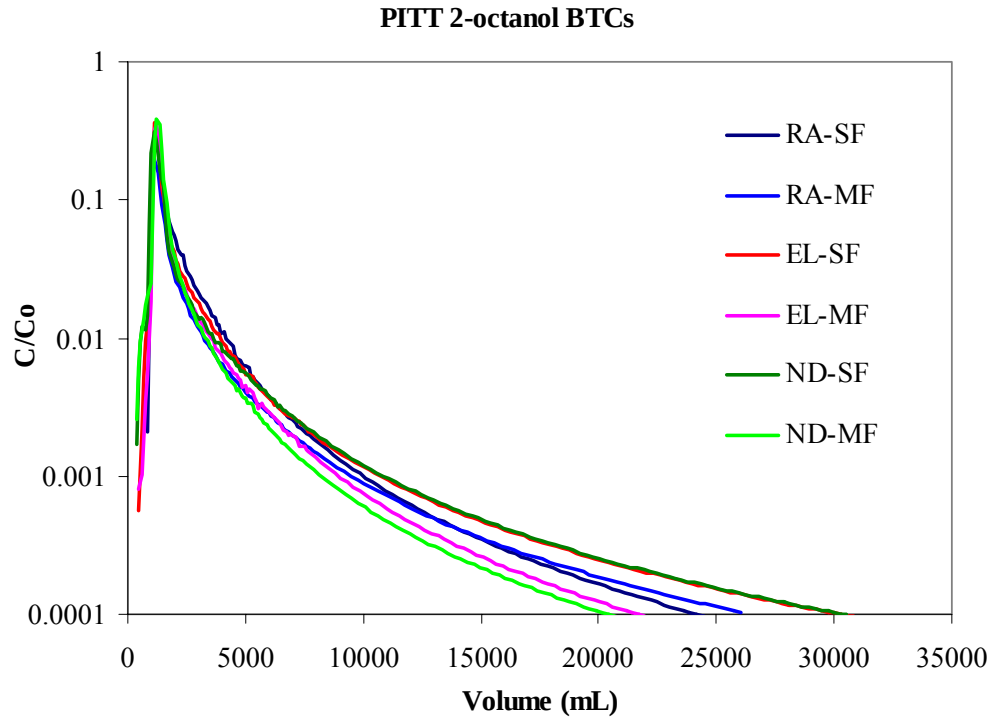

Figure A-13. The 2-octanol tracer BTCs for all of the experiments.

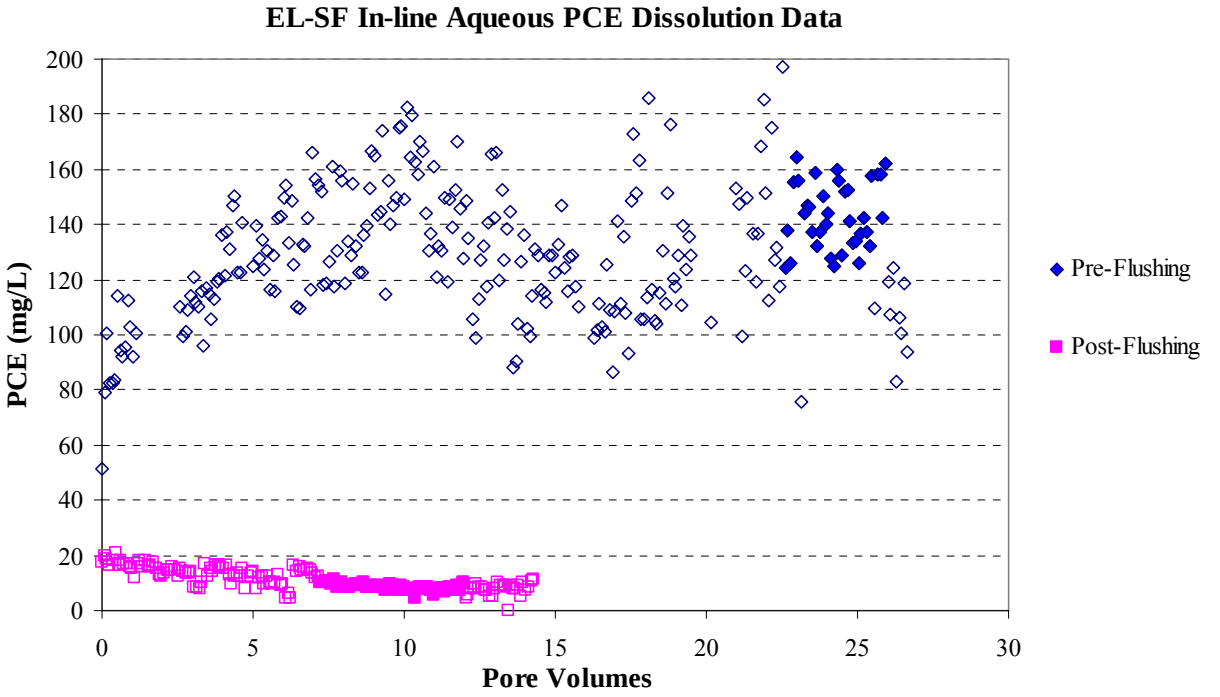

Figure A-14. In-line aqueous PCE dissolution data for EL-SF.

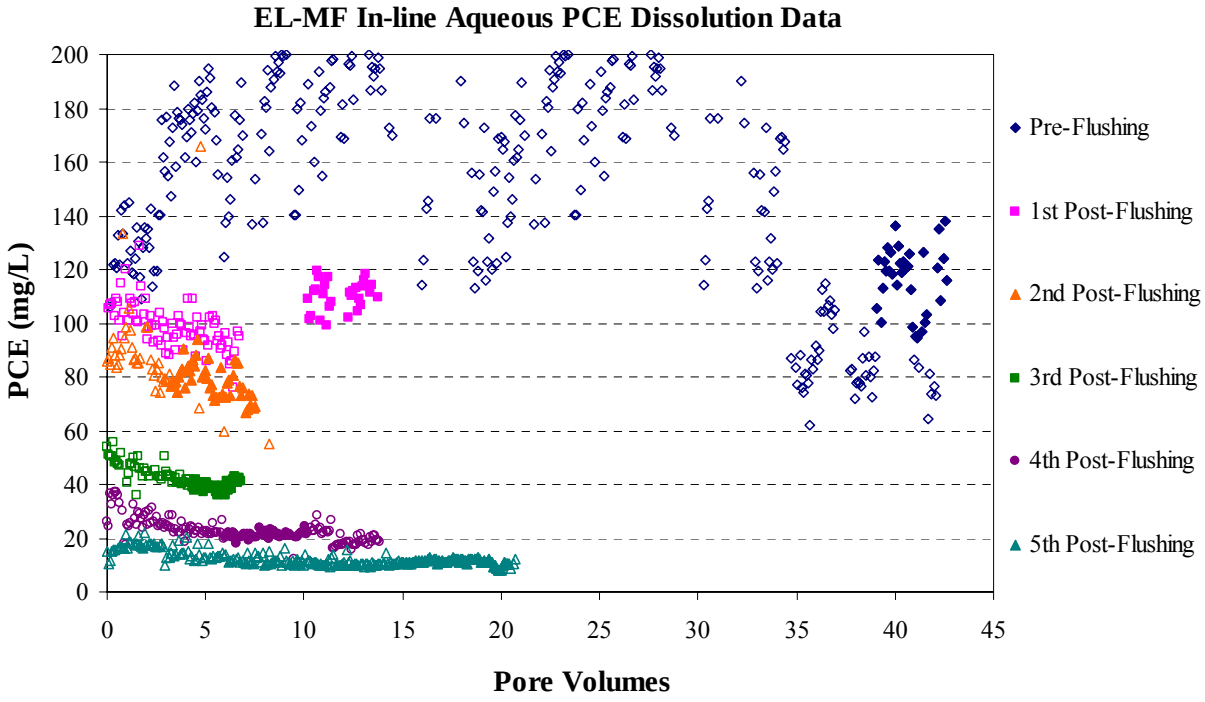

Figure A-15. In-line aqueous PCE dissolution data for EL-MF.

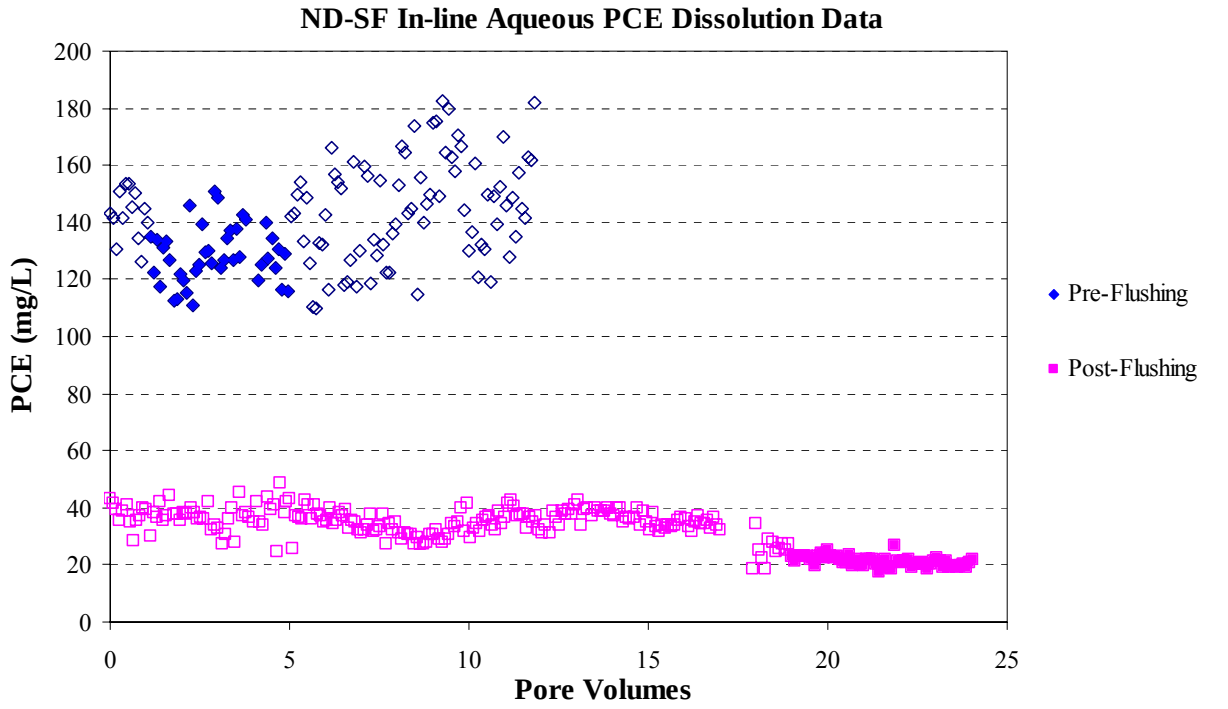

Figure A-16. In-line aqueous PCE dissolution data for ND-SF.

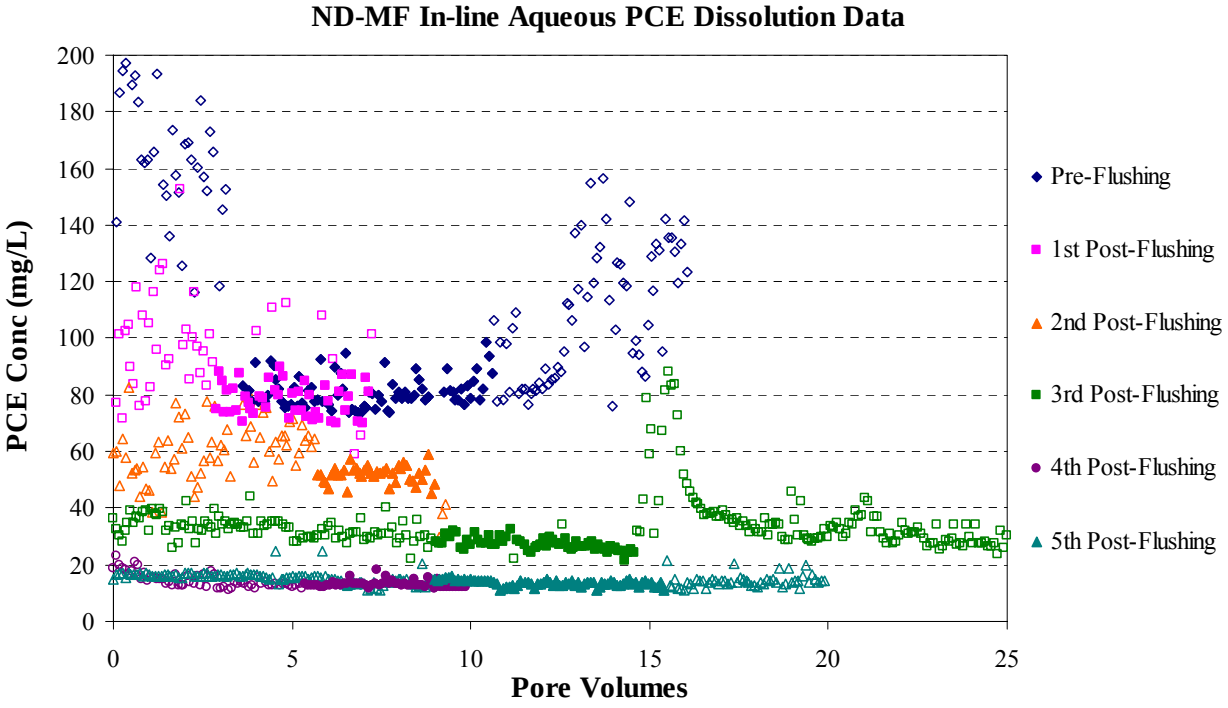

Figure A-17. In-line aqueous PCE dissolution data for ND-MF.

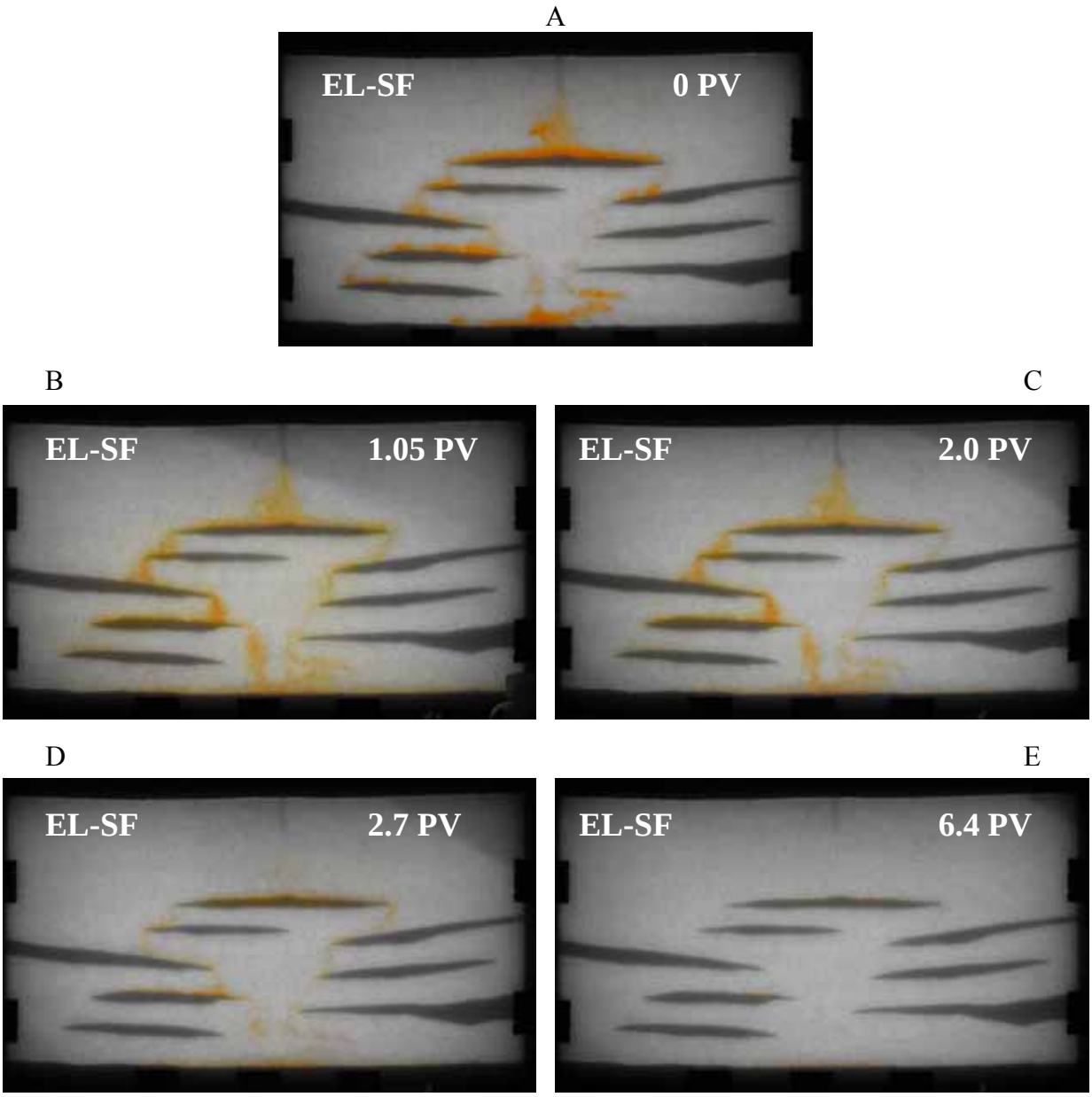

Figure A-18. 40% ethyl-lactate (EL) single-flushing experiment at different cosolvent injection pore volumes(PVs). A) 0 PV. B) 1.05 PVs. C) 2.0 PVs. D) 2.7 PVs. E) 6.4 PVs. Flow is from left to right and the Darcy velocity is approximately 1.3 m/d.

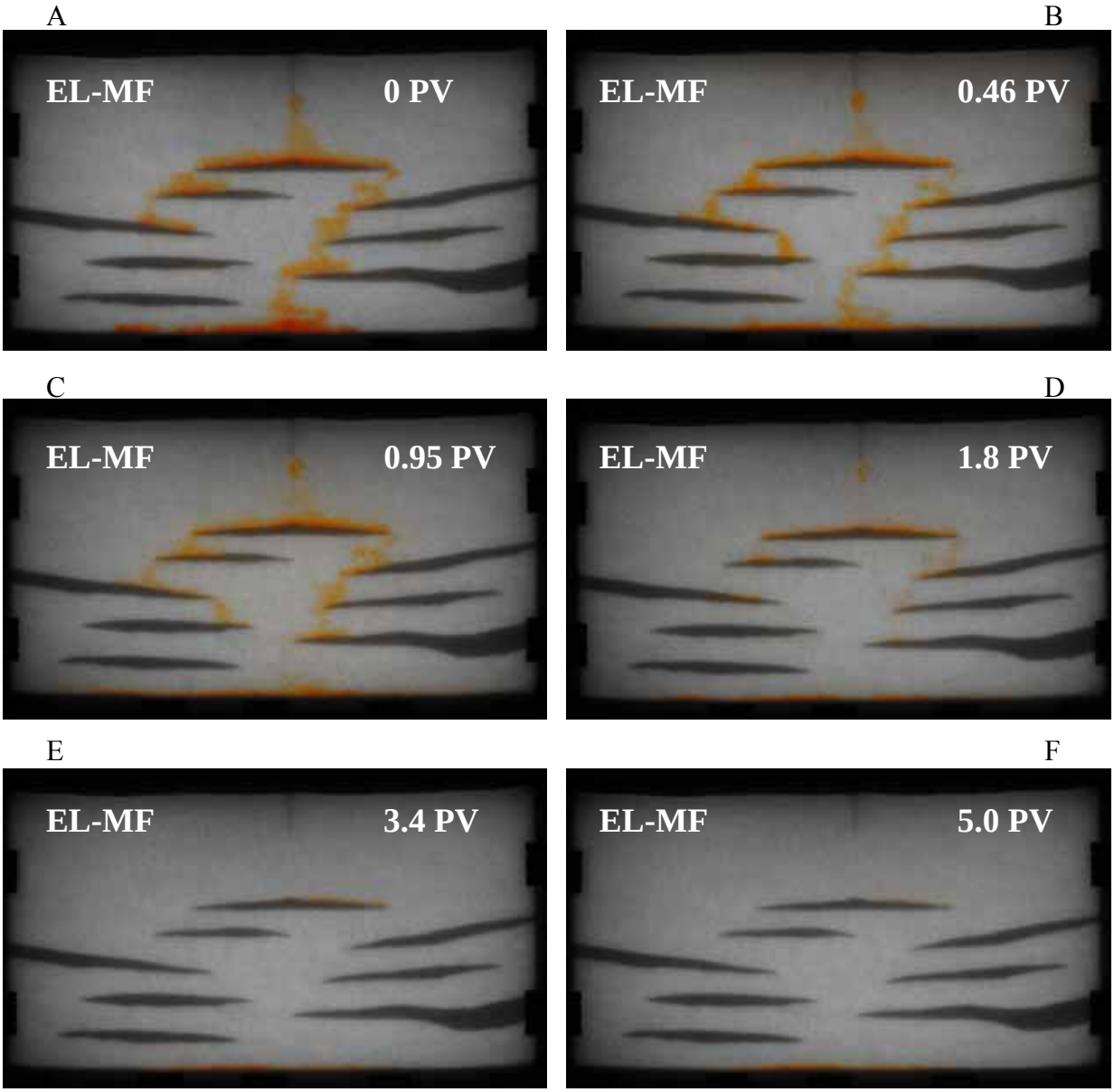

Figure A-19. 40% ethyl-lactate (EL) multiple-flushing experiment with total injected pore volumes (PV) of cosolvent in the top-right corner of each picture. A) Initial distribution. B) After 1st flushing. C) After 2nd flushing. D) After 3rd flushing. E) After 4th flushing. F) After 5th flushing. Flow was from left to right at a Darcy velocity of approximately 1.3 m/d.

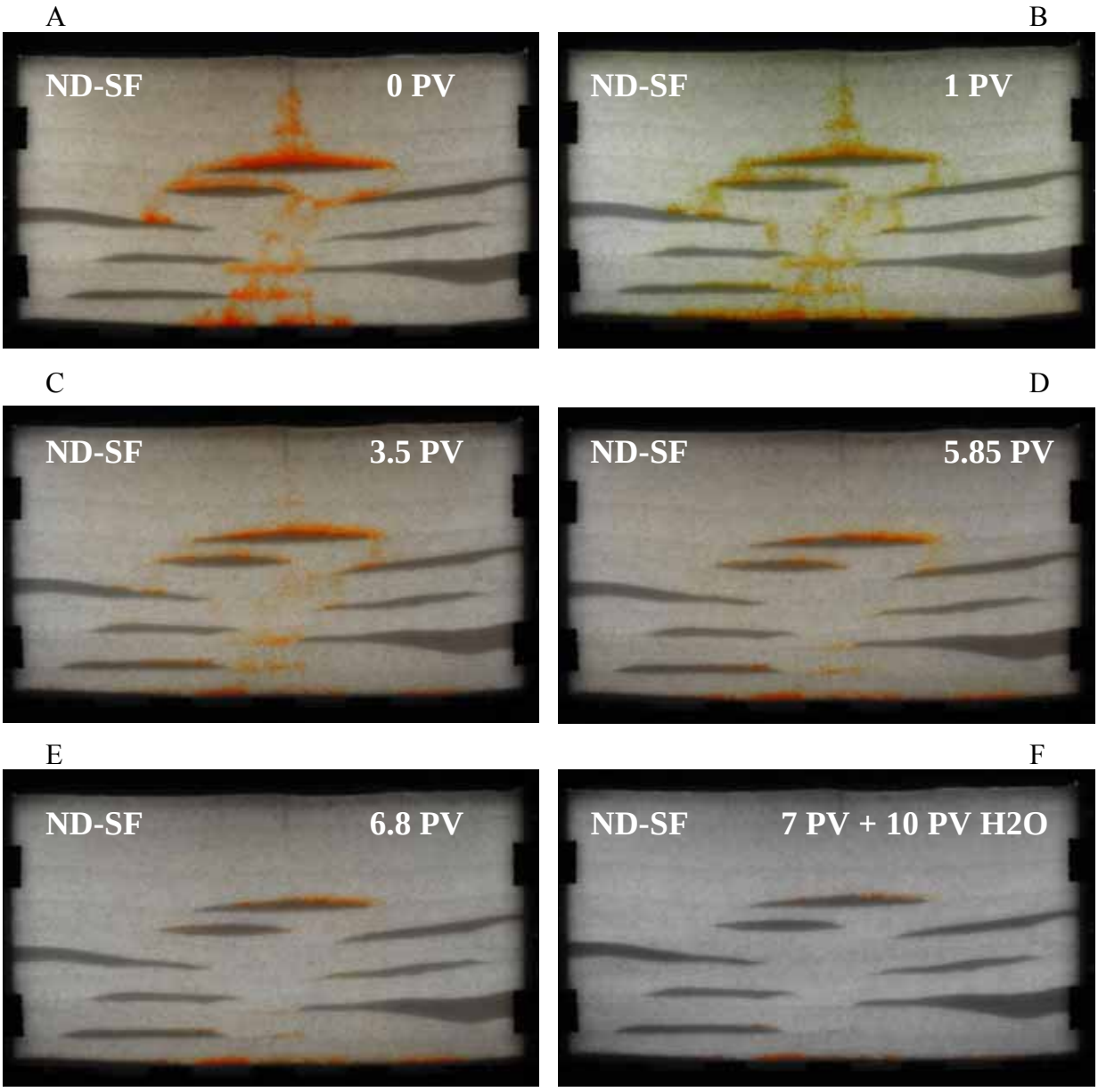

Figure A-20. Neutral density (ND) cosolvent single-flushing experiment at different cosolvent injection pore volumes (PVs). A) 0 PV. B) 1 PV. C) 3.5 PVs. D) 5.85 PVs. E) 6.8 PVs. F) 7 PVs. Flow is from left to right and the Darcy velocity is approximately 1.3 m/d.

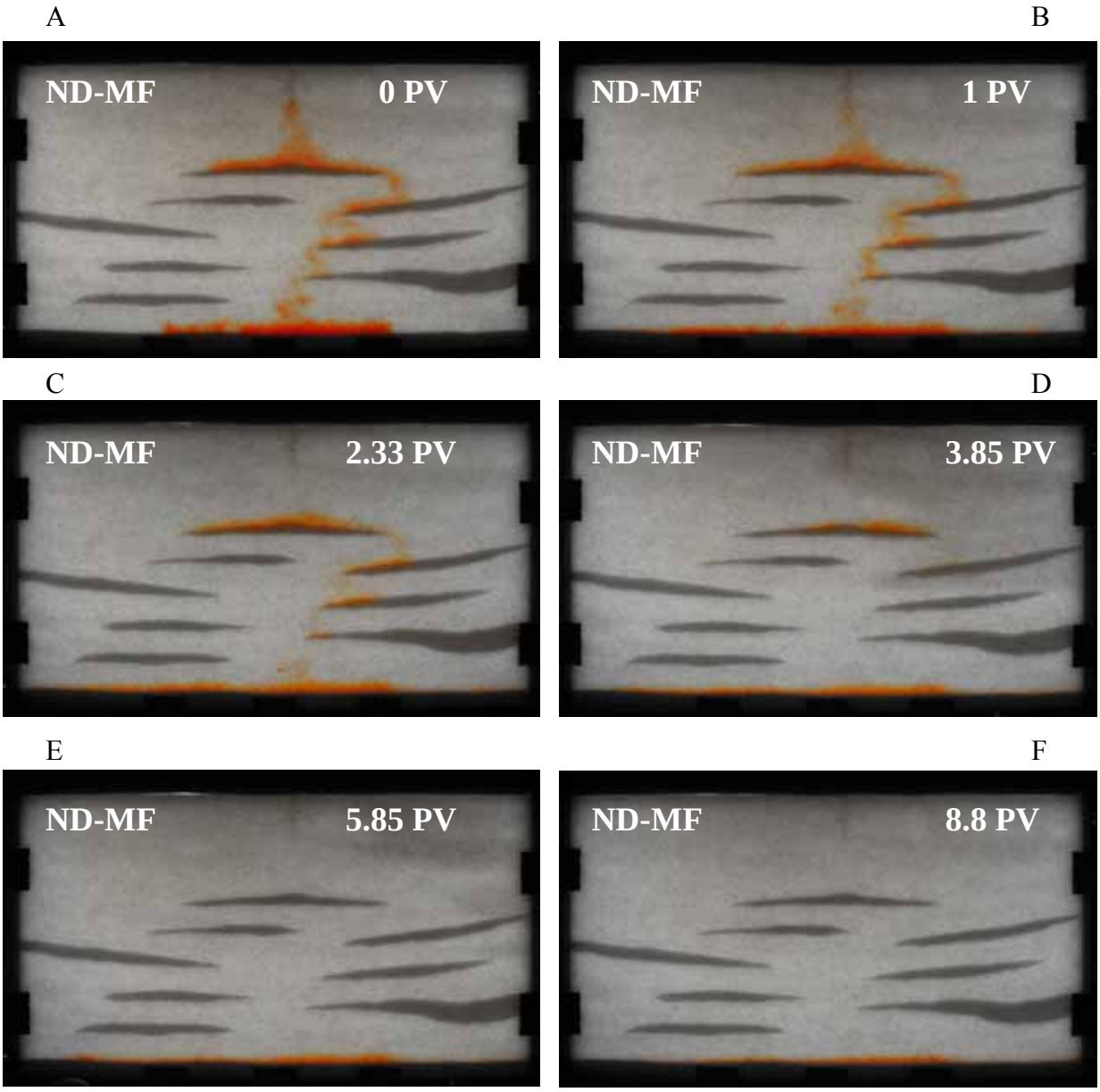

Figure A-21. Neutral density (ND) cosolvent multiple-flushing experiment with total injected pore volumes (PV) of cosolvent in the top-right corner of each picture. A) Initial distribution. B) After 1st flushing. C) After 2nd flushing. D) After 3rd flushing. E) After 4th flushing. F) After 5th flushing. Flow was from left to right at a Darcy velocity of approximately 1.3 m/d.

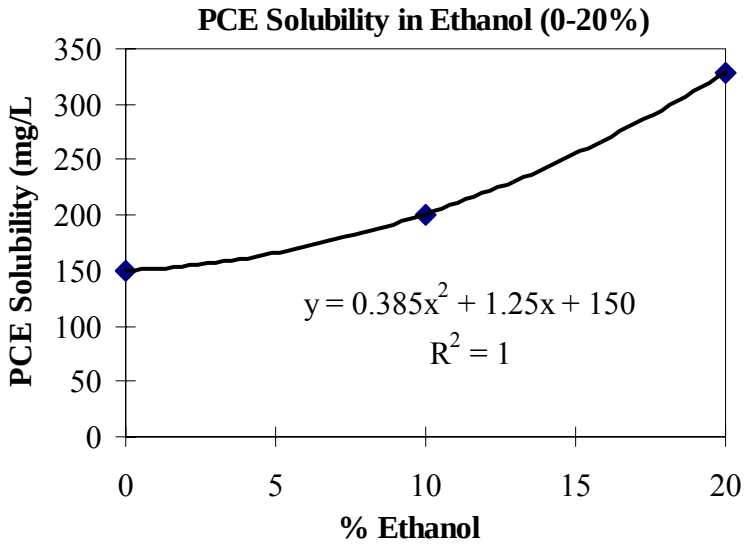

Figure A-22. PCE solubility in ethanol (0–20%). (Van Valkenberg, 1999)

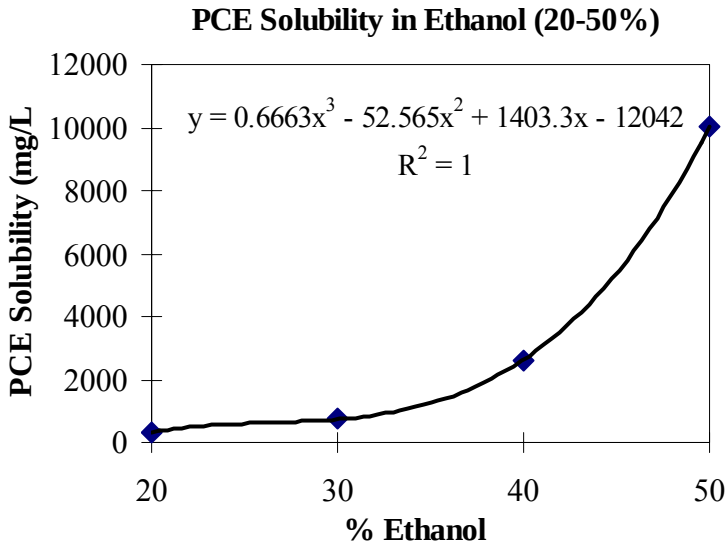

Figure A-23. PCE solubility in ethanol (20–50%). (Van Valkenberg, 1999)

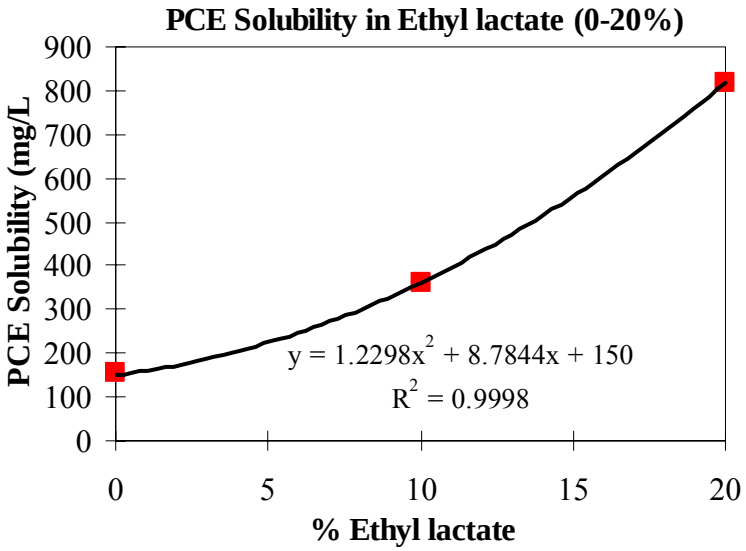

Figure A-24. PCE solubility in ethyl-lactate (0–20%). These values were obtained from laboratory experiments.

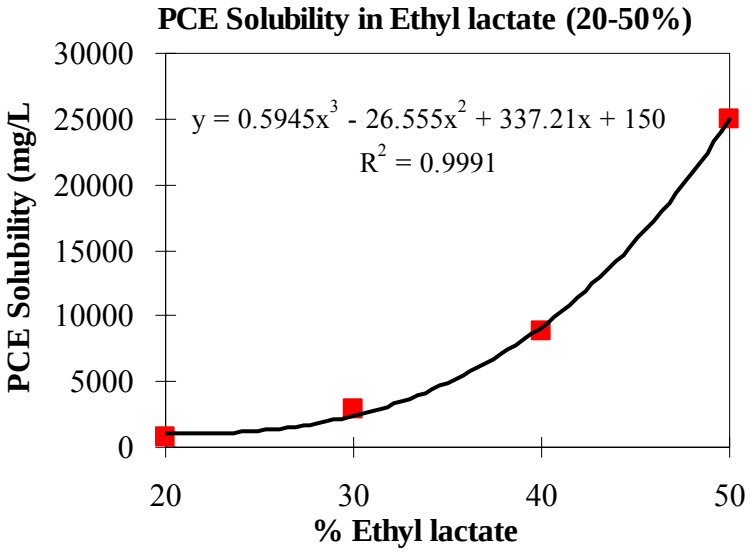

Figure A-25. PCE solubility in ethyl-lactate (20–50%). These values were obtained from laboratory experiments.

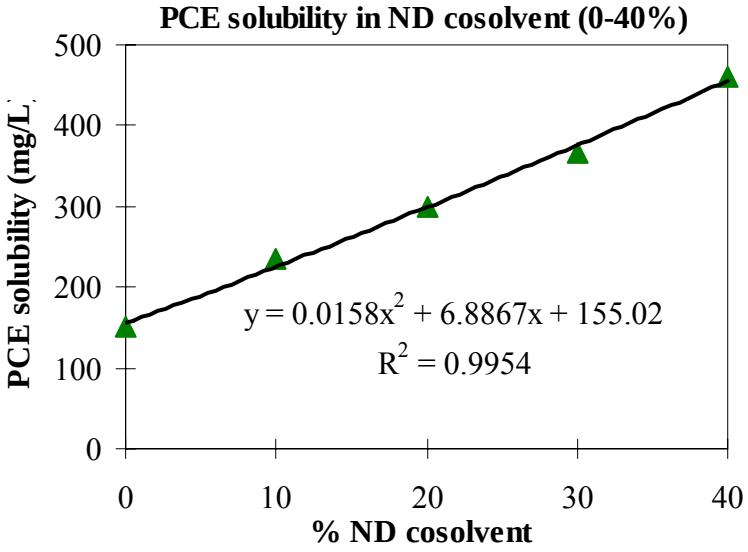

Figure A-26. PCE solubility in neutral density cosolvent (0–40%). These values were obtained from laboratory experiments.

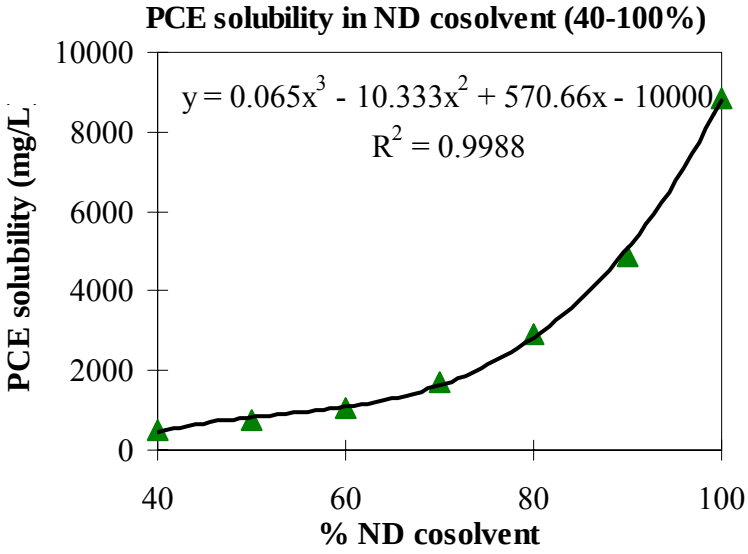

Figure A-27. PCE solubility in neutral density cosolvent (40–100%). These values were obtained from laboratory experiments.

LIST OF REFERENCES

Annable, M.D., Rao, P.S.C., Hatfield, K., Graham, W.D., Wood, A.L., Enfield, C.G., 1998. Partitioning tracers for measuring residual NAPL: field-scale test results. J. Environ. Eng. 124(6), 498–503.

Annable, M. D., Hatfield, K., Cho, J., Klammer, H., Parker, B.L., Cherry, J.A., Rao, P.S.C., 2005. Field-scale evaluation of the passive flux meter for simultaneous measurement of groundwater and contaminant fluxes. Environ. Sci. Technol. 39(18), 7194–7201.

Basu, N.B., Rao, P.S.C., Poyer, I.C., Annable, M.D., Hatfield, K., 2006. Flux-based assessment at a manufacturing site contaminated with trichloroethylene. J. Contam. Hydrol. 86(1–2), 105–127.

Bockelmann, A., Ptak, T., Teutsch, G., 2001. An analytical quantificationof mass fluxes and natural attenuation rate constants at a former gasworks site. J. Contam. Hydrol. 53 (3–4), 429–453.

Bradford, S.A., Abriola, L.M., Rathfelder, K.M., 1998. Flow and entrapment of dense nonaqueous phase liquids in physically and chemically heterogeneous aquifer formations. Adv. Water Resour. 22 (2), 117–132.

Bradford, S.A., Rathfelder, K.M., Lang, J., Abrioal, L.M., 2003. Entrapment and dissolution of DNAPLs in heterogeneous porous media. J. Contam. Hydrol. 67 (1–4), 133–157.

Brooks, M.C., Annable, M.D., Rao, P.S.C., Hatfield, K., Jawitz, J.W., Wise, W.R., Wood, A.L., Enfield, C.G., 2002. Controlled release, blind test of DNAPL characterization using partitioning tracers. J. Contam. Hydrol. 59 (3–4), 187–210.

Brooks, M.C., Annable, M.D., Rao, P.S.C., Hatfield, K., Jawitz, J.W., Wise, W.R., Wood, A.L., Enfield, C.G., 2004. Controlled release, blind test of DNAPL remediation by ethanol flushing. J. Contam. Hydrol. 69 (3–4), 281–297.

Brooks, M.C., Wise, W.R., 2005. Quantifying uncertainty due to random errors for moment analyses of breakthrough curves. J. Hydrol. 303 (1–4) 165–175.

Brusseau, M.L., Nelson, N.T., Costanza-Robinson, M.S., 2003. Partitioning tracer tests for characterizing immiscible-fluid saturations and interfacial areas in the vadose zone. Vadose Zone J. 2 (2), 138–147.

Crane, F.E., Kendall, H.A., Gardner, G.H.F., 1963. Some experiments on the flow of miscible fluids of unequal density through porous media. Soc. Pet. Eng. J. 3 (4), 277–280.

Enfield, C.G., Wood, A.L., Espinoza, F.P., Brooks, M.C., Annable, M., Rao, P.S.C., 2005. Design of aquifer remediation systems: (1) Describing hydraulic structure and NAPL architecture using tracers. J. Contam. Hydrol. 81 (1–4), 125–147.

Falta, R.W., Lee, C.M., Brame, S.E., Roeder, E., Coates, J.T., Wright, C., Wood, A.L., Enfield, C.G., 1999. Field test of high molecular weight alcohol flushing for subsurface nonaqueous phase liquid remediation. Water Resour. Res. 35 (7), 2095–2108.

Falta, R.W., Rao, P.S., Basu, N., 2005a. Assessing the impacts of partial mass depletion in DNAPL source zones I. Analytical modeling of source strength functions and plume response. J. Contam. Hydrol. 78 (4), 259–280.

Falta, R.W., Basu, N., Rao, P.S., 2005b. Assessing the impacts of partial mass depletion in DNAPL source zones II. Coupling source strength functions to plume evolution. J. Contam. Hydrol. 79 (1–2), 45–66.

Feenstra, S., Cherry, J.A., Parker, B.L., (1996). Conceptual models for the behavior of dense nonaqueous-phase liquids (DNAPLs) in the subsurface. In Pankow, J.F., Cherry, J.A. (Eds.) Chlorinated Solvents and Other DNAPLs in Groundwater; Waterloo Press: Portland, OR.

Fetter, C.W., 2001. Applied Hydrogeology – Fourth Edition. Prentice-Hall, Inc. Upper Saddle River, New Jersey.

Fure, A.D., Jawitz, J.W., Annable, M.D., 2006. DNAPL source depletion: Linking architecture and flux response. J. Contam. Hydrol. 85 (3–4), 118–140.

Hatfield, K., Annable, M., Cho, J.H., Rao, P.S.C., Klammler, H., 2004. A direct passive method for measuring water and contaminant fluxes in porous media. J. Contam. Hydrol. 75 (3–4), 155–181.

Jalbert, M., Dane, J.H., Bahaminyakamwe, L., 2003. Influence of porous medium and NAPL distribution heterogeneities on partitioning inter-well tracer tests: a laboratory investigation. J. Hydrol. 272 (1–4), 79–94.

Jawitz, J.W., Annable, M.D., Rao, P.S.C., 1998a. Miscible fluid displacement stability in unconfined porous media: two dimensional flow experiments and simulations. J. Contam. Hydrol. 31 (3–4), 211–230.

Jawitz, J.W., Annable, M.D., Rao, P.S.C., Rhue, R.D., 1998b. Field implementation of a Winsor Type I surfactant/alcohol mixture for in situ solubilization of a complex LNAPL as a single-phase microemulsion. Environ. Sci. Technol. 32 (4), 523–530.

Jawitz, J.W., Sillan, R.K., Annable, M.D., Rao, P.S.C., Warner, K., 2000. In situ alcohol flushing of a DNAPL source zone at a dry cleaner site. Environ. Sci. Technol. 34 (17), 3722–3729.

Jawitz, J.W., Annable, M.D., Clark, C.J., Puranik, S. 2002. Inline gas chromatographic tracer analysis: An alternative to conventional sampling and laboratory analysis for partitioning tracer tests. Instrumen. Scien. Technol. 30 (4), 415–426.

Jawitz, J.W., Annable, M.D., Demmy, G.G., Rao, P.S.C., 2003. Estimating non-aqueous phase liquid spatial variability using partitioning tracer higher temporal moments, Water Resour. Res. 39 (7), 1192.

Jawitz, J.W., Fure, A.D., Demmy, G.G., Berglund, S., Rao, P.S.C., 2005. Groundwater contaminant flux reduction resulting from nonaqueous phase liquid mass reduction. Water Resour. Res. 41 (10), W10408.

Jin, M., Delshand, M., Dwarakanath, V., McKinney, D.C., Pope, G.A., Sepehrnoori, K., Tilburg, C.E., 1995. Partitiong tracer test for detection, estimation, and remediation performance assessment of subsurface nonaqueous phase liquids. Water Resour. Res. 31 (5), 1201–1211.

Lide, D.R., Frederikse, H.P.R., 1996. CRC Handbook of Chemistry and Physics. CRC Press Inc., Boca Raton, FL.

Lindberg, V. Uncertainties and Error Propagation Part 1 of a manual on Uncertainties, Graphing, and the Vernier Caliper. [updated 1 July 2000; cited 1 December 2006]. Available from http://www.rit.edu/~uphysics/uncertainties/Uncertaintiespart2.html#muldiv .

MacKay, D.M., Cherry, J.A., 1989. Groundwater contamination: Pump-and-treat remediation, Environ. Sci. Technol. 23 (6), 630–636.

National Research Council, 2004. Contaminants in the Subsurface: Source Zone Assessment and Remediation. The National Academies Press, Washington, D.C.

Niemet, M.R., Selker, J.S., 2001. A new method for quantification of liquid saturation in 2D translucent porous media systems using light transmission. Adv. Water Resour. 24 (6), 651–666.

Oostrom, M., Hofstee, C., Walker, R.C., Dane, J.H., 1999. Movement and remediation of trichloroethylene in a saturated heterogeneous porous medium: 1. Spill behavior and initial dissolution. J. Contam. Hydrol. 37 (1–2), 159–178.

Parker, J. C., Park, E., 2004. Modeling field-scale dense nonaqueous phase liquid dissolution kinetics in heterogeneous aquifers, Water Resour. Res. 40 (5), 1–12.

Pope, G.A., Jin, M., Varadarajan, D.; Rouse, B.; Sepehrnoori, K., 1994. Partitioning Tracer Tests to Characterize Organic Contaminants. 2nd Tracer Workshop. University of Texas at Austin. November 14 & 15, 1994.

Rao, P.S.C., Annable, M.D., Sillan, R.K., Dai, D.P., Hatfield, K., Graham, W.D., Wood, A.L., Enfield, C.G., 1997. Field-scale evaluation of in situ cosolvent flushing for enhanced aquifer remediation, Water Resour. Res. 33 (12), 2673–2686.

Rao, P.S.C., Jawitz, J.W., 2003. Comment on ‘‘Steady-state mass transfer from single-component dense non-aqueous phase liquids in uniform flow fields’’ by T.C. Sale and D. B. McWhorter, Water Resour. Res. 39 (3), 1068.

Sale, T.C., McWhorter, D.B., 2001. Steady state mass transfer from single-component dense nonaqueous phase liquids in uniform flow fields. Water Resour. Res. 37 (2), 393–404.

Schroth, M.H., Ahearn, S.J., Sekler, J.S., Istok, J.D., 1996. Characterization of miller-similar silica sands for laboratory hydrologic studies. Soil Sci. Soc. Am. J. 60 (5), 1331–1339.

Slobod, R.L., Lestz, S.J., 1960. Use of a graded viscosity zone to reduce fingering in miscible phase displacements. Producers Monthly 24 (10), 12–19.

Soga, K., Page, J.W.E., Illangasekare, T.H., 2004. A review of NAPL source zone remediation efficiency and the mass flux approach. J. Hazardous Mat. 110 (1–3), 13–27.

Stroo, H.F., Unger, M., Ward, C.H., Kavanaugh, M.C., Vogel, K., Leeson, A., Marqusee, J.A., Smith, B.P., 2003. Chlorinated solvent source zones. Envir. Sci. and Technol. 37 (11), 225A–230A.

Taylor, T.P., Pennell, K.D., Abriola, L.M., Dane, J.H., 2001. Surfactant enhanced recovery of tetrachloroethylene from a porous medium containing low permeability lenses – 1. Experimental studies. J. Contam. Hydrol. 48 (3–4), 325–350.

Totten, C.T., 2005. Effect of Porous Media and Fluid Properties on Dense Non-Aqueous Phase Liquid Migration and Dilution Mass Flux. Ph.D Dissertation,University of Florida, Gainesville, FL.

U.S. Environmental Protection Agency, 1997. Cleanup of the Nation’s Waste Sites: Markets and Technology Trends. EPA 542-R-96-005. U.S. Government Printing Office: Washington, DC.

U.S. Environmental Protection Agency, 2003. The DNAPL remediation challenge: Is there a case for source depletion? Rep. EPA/600/R-03/143, Natl. Risk Manage. Res. Lab., Cincinnati, Ohio.

Van Valkenberg, M.E., 1999. Solubilization and Mobilization of Perchloroethylene by Cosolvents in Porous Media. Ph.D. Dissertation, University of Florida, Gainesville, FL.

Wood, A.L., Enfield, C.G., Espinoza, F.P., Annable, M.D., Brooks, M.C., Rao, P.S.C., Sabatini, D., Knox, R., 2005. Design of aquifer remediation systems: (2) Estimating site-specific performance and benefits of partial source removal. J. Contam. Hydrol. 81 (1–4), 148–166.

BIOGRAPHICAL SKETCH

Andrew Kaye grew up in South Lyon, Michigan, a relatively rural area outside of Ann Arbor. He began his college career as a no-preference engineering student at Michigan State University (MSU), where he celebrated his school's Citrus Bowl victory and a men's basketball national championship victory over the University of Florida in 2000. When the time came to officially declare a major at MSU, his appreciation, enjoyment, and concern for the outdoors and the environment in general influenced his decision to study Biosystems Engineering with a focus on natural resources and the environment. While an undergraduate, he took the opportunity to participate in summer study abroad programs in both Hawai'i and Australia, the two places he had always wanted to visit. During another summer, he was accepted to a research internship program through the College of Engineering at MSU in which he worked with Dr. Ted Loudon and found an appreciation for graduate level research. After this internship and continued work with Dr. Loudon, he decided he would attend graduate school. He found an escape from the harsh Michigan winters by accepting a graduate assistantship with Dr. Mike Annable, a fellow MSU alumnus, at the University of Florida to pursue a master's degree in environmental engineering. The contagious enthusiasm of the Gator Nation in the Swamp and in the O'Dome proved to Andrew that it was, in fact, great to be a Florida Gator; and, he once again celebrated his school's men's basketball national championship in 2006. Still, he remains a loyal fan to MSU and to his hometown teams including the Detroit Tigers, Pistons, Red Wings and Lions.